UNIVERSIDADE FEDERAL DE MINAS GERAIS

Programa de Pós-Graduação em Engenharia Metalúrgica, Materiais e de Minas

Tese de Doutorado

Utilização de Radiação Micro-ondas para Melhoria do Controle de Umidade de Pelotas de Minério de Ferro

Autor: Maycon Athayde

Orientador: Prof. Dr. Maurício Covcevich Bagatini

Fevereiro/2019

Athayde, Maycon.
A865u Utilização de radiação micro-ondas para melhoria do controle de umidade de pelotas de minério de ferro [manuscrito] Maycon Athayde. - 2019.
128 f., enc.: il.

Orientador: Maurício Covcevich Bagatini.

Tese (doutorado) - Universidade Federal de Minas Gerais, Escola de Engenharia.

1. Engenharia metalúrgica - Teses. 2. Metalurgia extrativa - Teses. 3. Pelotização (Beneficiamento de minério) - Teses. 4. Minérios de ferro - Teses. 5. Microondas - Teses. I. Bagatini, Maurício Covcevich. II. Universidade Federal de Minas Gerais. Escola de Engenharia. III. Título.

CDU: 669(043)

Maycon Athayde

Utilização de Radiação Micro-ondas para Melhoria do Controle de Umidade de Pelotas de Minério de Ferro

Tese de Doutorado apresentada ao Curso de Pós-Graduação em Engenharia Metalúrgica, Materiais e de Minas da Universidade Federal de Minas Gerais.

Área de Concentração: Metalurgia Extrativa

Orientador: Prof. Dr. Maurício Covcevich Bagatini

Belo Horizonte

Universidade Federal de Minas Gerais

Escola de Engenharia

AGRADECIMENTO

Desejo exprimir os meus agradecimentos a todos aqueles que, de alguma forma, permitiram que esta tese se concretizasse.

De forma especial, agradeço:

Ao meu orientador Professor Dr. Maurício Bagatini, pela confiança e suporte ao longo dessa trajetória e pelas valiosas orientações e discussões, sem as quais não seria possível atingir tão alto nível técnico. Ainda, aos Professores Dr. Roberto Tavares, Dr. Antonio Peres e Dr. Luiz Fernando de Castro, por todo apoio.

A todos que direta ou indiretamente apoiaram a realização deste trabalho, em especial aos especialistas Maurício Cota e Sérgio Nunes pela sempre disposição a ensinar e apoiar em todos esses anos. E ainda aos colegas Alexandre Anacleto, Heidy Simões, Alaécio Meschiatti, Adalberto Calazans, Anderson Pedruzzi por todo cuidado e apoio para realização dos experimentos e discussões que trouxeram importante resultados práticos.

Aos engenheiros Alysson Werneck e Thiago Marchezi por acreditar no tema desde o início e o apoio para que esta tese tenha virado realidade. Aos engenheiros Luiz Claudio Cotta e Alexandre Gonçalves pela ajuda nas inúmeras revisões dos artigos.

A minha família, pela paciência pelas incontáveis horas dedicadas a atingir o objetivo deste trabalho.

SUMÁRIO

RESUMO

O empobrecimento das reservas mundiais de minério de ferro tem levado à maior necessidade de beneficiamento e a tecnologia mais eficiente para a aglomeração destes minérios para aplicação siderúrgica é a pelotização. No entanto, o controle da umidade é crítico para o processo. A presente tese investigou o uso da tecnologia micro-ondas para o controle da umidade de aglomerados, através do estudo cinético da secagem em bancada e piloto, e ainda o efeito no prensamento do minério, pois a granulometria do concentrado impacta diretamente a etapa anterior de filtragem.

No presente estudo foi apresentado o mecanismo cinético para a secagem das pelotas através de micro-ondas, baseado em ensaios de bancada. A secagem completa ocorreu em 150 s, sendo que o método convencional remove apenas 60 % da umidade do aglomerado neste período. Ainda, os fenômenos cinéticos de secagem em escala piloto foram investigados. O novo processo acoplando aquecimento convectivo com micro-ondas apresentou melhor secagem que o processo convencional, já que as regiões de condensação no interior do leito foram completamente mitigadas. Adicionalmente, o processo de cominuição por prensamento foi otimizado pela utilização de micro-ondas. A aplicação inovadora para a operação de prensamento de pellet feed elevou a superfície específica com a exposição a micro-ondas, devido ao micro-trincamento e secagem dos minerais. A partir da microscopia ótica e de varredura foram demostrados estes ganhos.

Portanto, de maneira holística o estudo contribuiu para uma inovação na rota de processo com uso da tecnologia micro-ondas controlando a umidade, aumentando a eficiência no prensamento dos minerais e secagem dos aglomerados.

ABSTRACT

The depleting of the world's iron ore reserves has increased the upgrading need. Currently, the most efficient agglomeration technology to enable the use of fine ore in the ironmaking is the pelletizing. However, moisture control is key to the process. The present thesis investigated the use of microwave technology for the agglomerate moisture control, through the kinetic study in bench and pilot scale drying, as well as the effect on the ore pressing process, due the strong impact of the ore particle size on the filtration.

The present thesis proposes a novel kinetic mechanism for the pellets drying by means of microwaves, in bench scale. The complete drying occurred in 150 s, and the conventional method removes only 60% of the agglomerate moisture in this period. The kinetic drying phenomena at pilot scale was investigated. The new process coupling convective microwave heating had better drying than the conventional process, since the condensation regions inside the bed were completely mitigated. Additionally, the crushing by pressing was optimized using microwaves. The innovative application for the pellet feed operation increased the specific surface area with microwave exposure due to micro-cracking and drying of the minerals. Optical and scanning microscopy were used in this characterization. Therefore, holistic the study contributed to an innovation in the process route with the use of microwave technology controlling the humidity, increasing the efficiency in pressing and drying the iron ore.

Capítulo 1. Considerações Iniciais

1.1. Desafio da aglomeração de finos de minérios de ferro

A escassez de reservas de minério com alto teor de ferro tem aumentado a disponibilidade de concentrados de baixa granulometria (ultrafinos). Estes são considerados inviáveis para aplicação direta nos atuais processos de redução, onde o fluxo gasoso é necessário. Adicionalmente, o aumento do grau de hidratação dos minerais e a maior presença de ultrafinos (gerados por moagem para liberação dos minerais e ainda para melhorar a aglomeração) prejudica a eficiência do desaguamento dos minérios. O processo típico de filtragem a vácuo depende da permeabilidade da camada de minério sob o meio filtrante para a extração da fase líquida.

O cenário de aumento na geração de finos aumenta a relevância da pelotização como processo para geração de insumo para a produção de ferro primário, já que aglomeração ocorre devido às partículas finas com grande superfície específica apresentarem forças de coesão nos capilares formados entre os finos e a umidade residual. Tradicionalmente, a mistura de concentrado desaguado e prensado, aglomerantes e fundentes necessita de um processamento térmico em fluxo contracorrente para que o aglomerado possa adquirir as propriedades mecânicas adequadas para resistir ao transporte até os reatores de redução.

Para a resistência mecânica, o endurecimento a quente é obtido através do processamento em fornos divididos em etapas de secagem, queima e resfriamento. A secagem das pelotas de minério de ferro ocorre através da convecção de calor, recuperando esta energia de etapas subsequentes do forno. Portanto, o processo tem forte dependência do rendimento térmico das etapas posteriores.

O processo de secagem é o primeiro afetado pela variação de umidade. Com base na literatura publicada, a pelota deve permitir a difusão de calor para o interior desta, enquanto

a umidade flui do interior para a atmosfera, garantindo que elas não colapsem devido às taxas de aquecimento da região de queima. No caso de excesso de umidade, o processo de transferência de calor torna-se limitador da produtividade dos fornos, devido ao choque térmico causado pela maior geração de gases no interior da pelota. Atualmente, uma solução encontrada em plantas modernas para o controle da umidade foi a inclusão da etapa de prensamento do concentrado após a filtragem, visando sua cominuição do concentrado apenas para a liberação dos minerais e não para a geração de superfície adicional desejada pela etapa de pelotização. Esta mudança de fluxograma proporciona uma menor quantidade de ultrafinos para a filtragem do concentrado, com melhor permeabilidade da camada de minério e menor obstrução do meio filtrante. No entanto, o prensamento do concentrado entre rolos (*HPGR – High Pressure Griding Rolls*) também é um processo sensível ao aumento da umidade do concentrado, devido ao escorregamento entre as partículas. Portanto, não somente a etapa de secagem das pelotas, mas também o processo de cominiução deve ser otimizado para garantir a ótima umidade dos aglomerados.

Estudos recentes demonstram que a cinética dos processos térmicos e de cominuição é favorecida pela aplicação da irradiação de micro-ondas em minérios e na metalurgia extrativa. Em geral, essa tecnologia já é utilizada em diversos processos industriais como aquecimento, secagem, calcinação, redução carbotérmica de óxidos metálicos, lixiviação e fundição (Haque, 1999; Kingman *et al.*, 1998; Chen *et al.*, 2012a). As micro-ondas são ondas eletromagnéticas com frequências entre 300 MHz e 300 GHz, ou seja, possuem comprimentos de onda de 1 a 300 mm. Huang *et al.* (2012) afirmaram que o método de secagem do minério de ferro com micro-ondas em termos de eficiência energética é superior aos métodos convencionais.

O processo de pelotização de minério de ferro utiliza energia de forma intensiva e o fato da tecnologia micro-ondas não utilizar a queima de hidrocarbonetos para seu funcionamento

torna-se uma vantagem considerável na redução de gases poluentes, minizando a geração de gases de efeito estufa pelo potencial de menor utilização de combustíveis sólidos (Saito *et al.*, 2011; Chen *et al.*, 2012a; Huang *et al.*, 2012; Zhao *et al.*, 2014). As micro-ondas são geradas por energia elétrica e possuem uma eficiência de conversão termoelétrica de aproximadamente 50% para frequências de 2450 MHz e 85% para a frequência de 915 MHz, segundo HAQUE, 1999. Embora alguns autores decrevam o uso para secagem de minério, a literatura é bastante escassa quanto aos fenômenos cinéticos e efeito do uso de micro-ondas.

O comportamento dos diferentes minerais em relação às micro-ondas ocorre de três maneiras distintas, podendo não sofrer qualquer influência (transparente às micro-ondas, como a sílica), refletir (como ocorre com os metais) e absorver essas ondas (água ou hematita).

O presente estudo investigou o comportamento dos aglomerados e minérios submetidos a esta tecnologia, com objetivos descritos no capítulo seguinte.

1.2. Objetivos

O presente trabalho teve como objetivo central investigar e caracterizar a hipótese tecnológica de controle da umidade de pelotas de minério de ferro através do uso de micro-ondas, em forno de grelha móvel (*travelling grate*). Adicionalmente ao objetivo geral, a presente tese busca contribuir para o conhecimento dos fenômenos de secagem e a interação do minério de ferro com as micro-ondas, de acordo com os seguintes objetivos específicos:

- Avaliar o estado-da-arte da tecnologia de micro-ondas na indústria mineral e o processo de aglomeração de pelotas de uma operação industrial no estado-da-arte atual;
- Investigar o efeito das micro-ondas na secagem de um leito de pelotas;
- Investigar a cinética da secagem de pelotas submetidas à ação de micro-ondas.
- Avaliar modificações estruturais e fenômenos que afetam a qualidade física da pelota de minério de ferro durante a secagem;
- Avaliar o comportamento do concentrado de minério de ferro prensado após ser submetido a exposição em um forno micro-ondas.

1.3. Estrutura da Tese e Descrição dos Artigos

A presente tese foi redigida a partir de cinco artigos publicados em periódicos relevantes nacionais e internacionais que seguem o cronograma de desenvolvimento da pesquisa. Além dos artigos apresentados, o último capítulo deste documento foi destinado às considerações finais que entrelaçam as informações obtidas em todas as etapas do desenvolvimento da tese, sendo possível destacar a contribuição científica de cada capítulo de forma individualizada. A seguir são citados os artigos que se referem aos capítulos da presente tese e a contribuição de cada um deles no desenvolvimento dessa pesquisa:

- Artigo A - *Aplicação de Micro-ondas como Alternativa ao Desafio do Processamento de Minérios e Metais*: análise do estado-da-arte da aplicação das micro-ondas na indústria extrativa, na área de aglomeração e cominuição de minérios;
- Artigo B - *A Case Study of Pellet Size Fractions Influence on Pelletizing Operation:* caracterização de uma operação industrial de pelotização com fornos convencionais onde a transferência de calor predominantemente ocorre por convecção;
- Artigo C - *Iron Ore Pellet Drying Assisted by Microwave: A Kinetic Evaluation:* o artigo propôs o mecanismo cinético do processo, inédito na literatura, de secagem de pelotas de minério de ferro através de micro-ondas, através de estudos em bancada;
- *Artigo D - Novel Drying Process Assisted by Microwave to Iron Ore Pelletizing:* Após a investigação da secagem de pelotas individuais, foi investigada a condição inovadora em ambiente similar ao processo industrial, em leito de pelotas;
- *Artigo E - Iron Ore Concentrate Particle Size Controlling Through Application of Microwave at the HPGR Feed:* Investigação do efeito da secagem do minério de

ferro e geração de micro-trincamento induzido nas partículas através do uso de micro-ondas e sua relação com a eficiência de prensagem.

Capítulo 2. Artigo A - Aplicação de Micro-ondas como Alternativa ao Desafio do Processamento de Minérios e Metais

Maycon Athayde and Maurício Covcevich Bagatini

Artigo publicado em 15 de junho de 2017 *na revista Brasil Mineral*, n 372, pp 24 – 29. ISSN 0102 - 4728

Sumário

Nos últimos 20 anos várias investigações sobre os efeitos da aplicação de irradiação de micro-ondas em minérios e na metalurgia extrativa têm sido realizadas e essa técnica vem sendo utilizada em vários processos industriais como aquecimento, secagem, calcinação, redução carbotérmica de óxidos metálicos, lixiviação e fusão (Haque, 1999; Kingman et al., 1998; Lovás et al., 2010; Xiu-jing et al., 2010; Koleini et al., 2012). Além das aplicações citadas, Jones et al. (2002) inclui ainda nas aplicações o processamento de alimentos, secagem de madeira, tratamento de plástico e borrachas e cura e pré-tratamento de materiais cerâmicos. A evolução da tecnologia nos processos industriais é de grande interesse em todos os ramos das indústrias, principalmente no que se refere aos resíduos de processo (Lovás et al., 2003). Este trabalho apresenta uma revisão acerta do uso da tecnologia de micro-ondas no setor industrial.

2.1. Comportamento dos materiais frente às irradiações de micro-ondas

Não apenas a água reage às micro-ondas. Segundo HAQUE (1999), CLARK et al. (2000), USLU et al.(2003), WATERS et al. (2007) e SAHOO et al.(2011a), os materiais comportam se de três maneiras frente à radiação de micro-ondas, podendo não sofrer qualquer influência, sendo transparentes às micro-ondas, como os silicatos, carbonatos e sulfatos (KINGMAN et al., 2000), refletir, como ocorre com os metais, ou absorver essas ondas, caso dos alimentos, sulfitos, arsenietos, sulfossais (KINGMAN et al., 2000; KINGMAN et al., 2004). CLARK et al. (2000) cita um quarto tipo de comportamento de materiais frente a tais radiações, que seriam absorvedores mistos. Esse comportamento é observado em compósitos ou em materiais multifásicos em que uma ou mais fases apresentam altas perdas dielétricas enquanto outras apresentam baixas perdas dielétricas (propriedade fundamental para absorção das ondas). De fato, o incremento de temperatura surge devido ao aquecimento pelo atrito dos dipolos em rotação ou por causa da migração de componentes iônicos (materiais condutores) conforme ilustrado pela Figura 2.1-1.

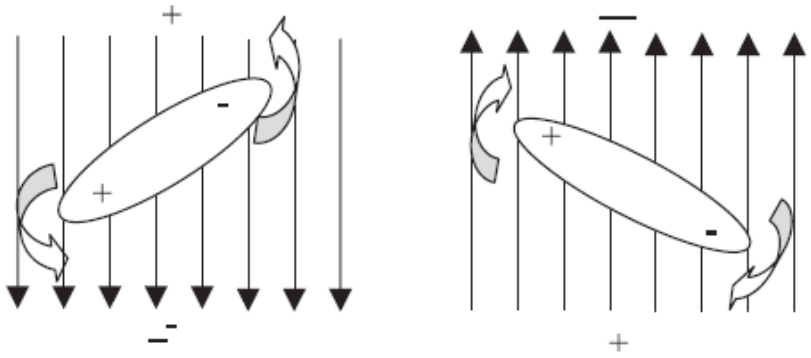

Figura 2.1-1 Realinhamento de dipolos em função do campo eletromagnético.

Tal aquecimento depende da taxa do fator de perda (relação entre a perda dielétrica com a constante dielétrica do material), sendo que, quanto maior for esse fator, mais facilmente ocorrerá o aquecimento. Adicionalmente, a distorção da nuvem de elétrons ao redor de moléculas ou átomos apolares devido à presença de um campo elétrico externo pode gerar

dipolos induzidos de forma que o movimento desses elétrons resulta em fricção no interior do dielétrico, sendo que a energia dissipada por essa fricção surge na forma de calor (JONES et al., 2002; MAKUL et al., 2014). A Figura 2.1-2 ilustra o comportamento e a penetração de micro-ondas através dos três tipos de materiais.

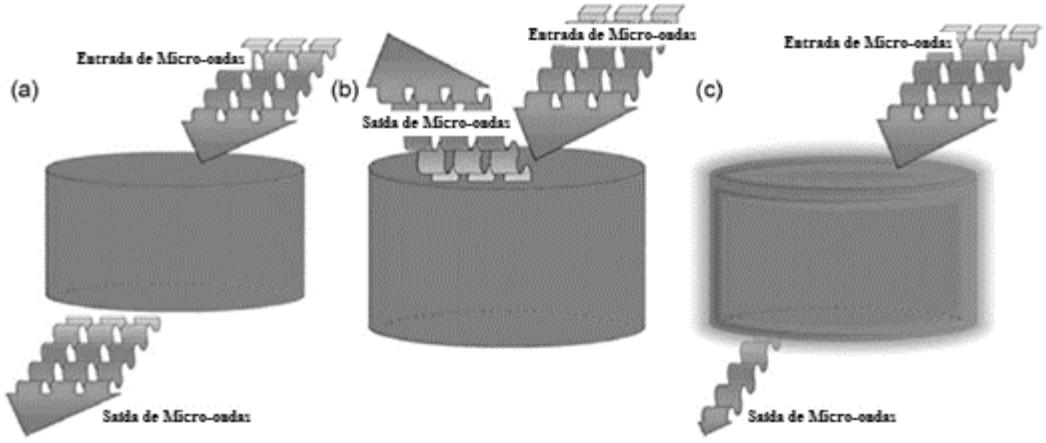

Figura 2.1-2 - Comportamento dos três tipos de materiais frente à irradiação de micro-ondas (OGHBAEI *et al.*, 2010).

2.2. Consolidação da Utilização de Micro-Ondas em Processos Industriais

O aquecimento via micro-ondas se diferencia do convencional devido às micro-ondas serem uma forma eletromagnética de energia e poderem penetrar profundamente na amostra, o que permite que o aquecimento ocorra volumetricamente (SAHOO et al., 2011a; CHANDRA-SEKARAN et al., 2011; MAKUL et al., 2014). O aquecimento convencional aquece o material de fora para dentro através dos mecanismos de transferência de calor: convecção, condução e radiação (SAHOO et al., 2011a; CHANDRASEKARAN et al., 2011). As maiores vantagens de se usar micro-ondas no processo industrial são a velocidade da transferência de calor, o aquecimento direcional, o menor tamanho do equipamento, a agilidade na comutação e a ausência de produtos de combustão que contribui para a redução de resíduos de processo. Além destas vantagens, o equipamento permite um bom controle do aquecimento, não necessitando

de contato direto com os materiais. Importante incentivo ao uso da tecnologia micro-ondas é não fazer uso da queima de hidrocarbonetos para o seu funcionamento implicando na redução de emissão de gases poluentes (PICKLES, 2009; SAITO et al., 2011; HUANG et al., 2012; ZHAO et al., 2014). A redução volumétrica de gases com o uso de micro-ondas é alcançada através da pirólise ao invés da incineração dos resíduos para prevenir a formação de dioxinas, furanos e NO_x (JONES et al., 2002). Segundo CHA (1993), o carvão ativado é um excelente absorvedor de micro-ondas e também um ótimo agente redutor. Quando o carbono é colocado em um campo de energia de micro-ondas ele atinge altas temperaturas rapidamente e, com isso, um alto gradiente de temperatura é estabelecido entre o ar e as partículas de carbono. Caso o ar contenha NO_x e SO_2, o carvão ativado irá capturar o oxigênio desses óxidos a uma taxa muito mais alta do que quando não há a energia do campo de micro-ondas.

2.3. Tratamento de Resíduos Industriais

LAM *et al.* (2012) realizaram estudos acerca do aproveitamento de óleo de motor automotivo através da pirólise em um reator (de quartzo em forma de sino) que utiliza a energia de micro-ondas como fonte de calor. Os produtos da pirólise consistiam em uma mistura de líquidos e gases hidrocarbonetos e sólidos em suspensão existente numa fase vapor. Esses produtos são valiosos para a utilização como combustíveis. Dessa forma, produtos prejudiciais ao meio ambiente podem ser transformados em produtos úteis, servindo como fonte alternativa de energia de hidrogênio ou de hidrocarbonetos. JONES *et* al. (2002) realizaram estudos acerca de escórias infiltradas em refratários de magnésia e cromo, onde o aquecimento convencional em conjunto com o micro-ondas é uma alternativa devido à capacidade de temperar os materiais, ao fácil manuseio e ao baixo custo. A cada ano, na Europa, veículos automotivos fora de circulação geram de 8 a 9 milhões de toneladas de sucata (FERRÃO et al., 2004), que é constituída de materiais plásticos (19%), borrachas (20%), materiais têxteis e fibras (10%),

madeira (2%), metais (8%), óleos (5%) e outros materiais (36%). DONAJ *et al.* (2010) estudaram a reciclagem de retalhamentos automotivos com a pirólise via micro-ondas combinado com gaseificação de vapor a alta temperatura. A conversão atingiu 99% dos líquidos e 45-55% dos sólidos de acordo com a fração de tamanho. Esse conceito mostrou que é possível gerar produtos com valor de mercado (por exemplo, gasosos), preservando a integridade dos metais em cada etapa do processo (que podem ser reutilizados posteriormente). Nesse desenvolvimento, todos os sólidos orgânicos foram convertidos em combustíveis.

2.4. Pré-tratamento de Minérios para Processamento Metalúrgico e Cominuição

Quanto aos tratamentos preliminares do minério ilmenítico, estudos realizados por NURI *et al.* (2014) através de XPS (X-ray Photoelectron Spectroscope) mostraram que a quantidade de Fe^{3+} na Ilmenita aumentou de 48,5% para 66,0% após 2,5 minutos de irradiação de micro-ondas. O uso de aquecimento via micro-ondas é vantajoso na modificação de propriedades químicas e físicas dos minérios de cobre (LOVÁS *et al.*, 2003). LOVÁS *et al.* (2003) realizaram experimentos sobre a decomposição da tetraedrita via micro-ondas utilizando carvão ativado. Durante a referida decomposição houve liberação das substâncias voláteis Hg, Sb e As. Após a irradiação, a tetraedrita tornou-se fortemente magnética e foi separada a partir do carvão ativado. O melhor resultado da diminuição da quantidade de Sb foi de 14,3% para 0,8% e da quantidade de Hg de 0,8% para 0,1% com relação mássica entre tetraedrita e carvão ativado de 1:1.

Segundo KINGMAN *et al.*(1998), os minérios são constituídos de materiais com propriedades mecânicas e térmicas muito distintas. Quando a energia de micro-ondas atinge esse minério, ocorrem, em seu interior, tensões de várias magnitudes que se devem aos processos de aquecimento e resfriamento do corpo. Como os coeficientes de expansão térmicos dos constituintes desse minério são diferentes, as tensões geradas causam fraturas

de naturezas inter e/ou transgranulares (KINGMAN *et al.*, 1998; KINGMAN *et al.*, 2000). Da mesma forma, ocorre o fenômeno conhecido como fuga térmica, pois os materiais heterogêneos não apresentam um aquecimento uniforme de seus constituintes (HAQUE, 1999). Obviamente, as fraturas ocorrem preferencialmente em minérios que contêm bons absorvedores de radiação de micro-ondas em uma matriz de material de pouca absorção (KINGMAN *et al.*, 2000; KOLEINI *et al.*, 2012). KINGMAN *et al.* (2000), também afirmam que o efeito da radiação de micro-ondas é mais significante se a amostra for mais consistente em vez de finamente disseminada.

Observa-se que, em geral, os minérios são os responsáveis pela absorção das micro-ondas e a ganga é transparente ao referido tratamento com exceção, por exemplo, da pirita, principal ganga do minério de sulfeto maciço, que se comporta absorvendo as micro-ondas (KINGMAN *et al.*, 2000). O mesmo autor afirma que os minerais que apresentam aumento significante da temperatura quando da exposição à radiação de micro-ondas são considerados como os responsáveis pela absorção dessas ondas, enquanto os que têm pequenas variações de temperatura são transparentes para a radiação.

KUMAR *et al.* (2010) mostram que o minério de ferro, quando exposto a um tratamento com irradiação de micro-ondas, sofre fissuras. A Figura 2.4-1 ilustra o minério antes e após o tratamento de micro-ondas. Tais fissuras proporcionam uma maior eficiência na posterior moagem do minério.

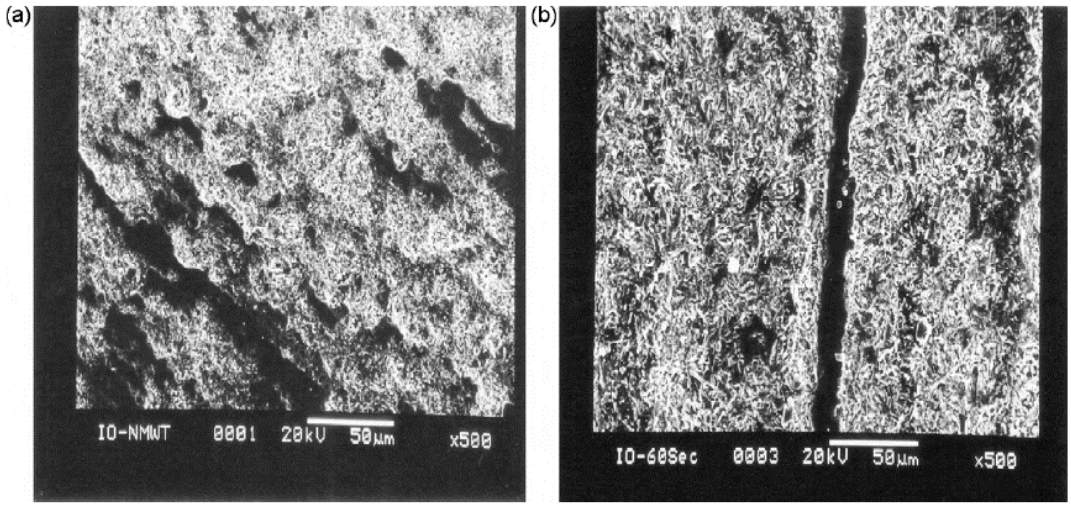

Figura 2.4-1 - Amostra de minério de ferro antes (a) e depois (b) da exposição de micro-ondas (KUMAR *et al.*, 2010).

Segundo ALI *et al.* (2010), a tensão térmica causada pela aplicação de micro-ondas na galena-calcita é maximizada quando há altas taxas de dissipação dessa energia. Ainda os mesmos autores afirmam que as micro-trincas que surgem da aplicação de micro-ondas são orientadas radialmente a partir dos contornos de grão da fase absorvente. O aumento do tempo de exposição às micro-ondas aumenta consideravelmente o número de micro trincas. A energia requerida (absorvida) aumenta linearmente com o tempo. O tempo de exposição (0,1 s) as energias requeridas são as mesmas (E_{in} = 0,868 kWh/t), porém o número de trincas da granulometria grosseira é 71,2 vezes o da granulometria fina. KINGMAN *et al.* (2000) investigaram também a influência da irradiação de micro-ondas no BWI (Bond Work Index) de várias amostras utilizando uma potência de 2,6 kW como mostra a figura 2.4-2. É possível observar claramente que o método apresenta efeito significante sobre os minérios de ilmenita e carbonato. O minério de sulfeto maciço também apresenta redução significativa de BWI com o tempo de exposição. Já o minério refratário de ouro sofre pouco ou nenhum efeito sob a irradiação. No estudo de KINGMAN et al (2000) o minério de ilmenita possuía mineralogia grossa e sua estrutura continha magnetita (excelente absorvedor de micro-ondas), ilmenita (bom absorvedor de micro-ondas) e matriz de plagioclásio (mal absorvedor

de micro-ondas), ou seja, trata-se de um material com grande potencial de apresentar microfissuras como foi constatado e ilustrado na Figura 2.4-2.

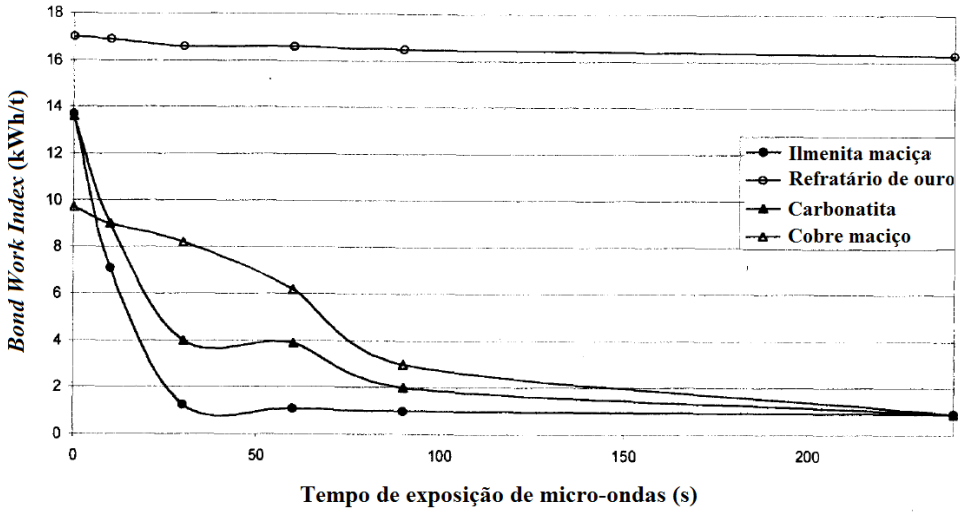

Figura 2.4-2 - BWI versus tempo de exposição às micro-ondas para diferentes minérios (KINGMAN *et al.*, 2000).

Estudos de KINGMAN *et al.*(2004) indicam que amostras de minério de chumbo-zinco tratadas com micro-ondas a 15 kW apresentaram menos que 55% de sua resistência original após 1 segundo de exposição. Ainda segundo os mesmos autores, para amostras tratadas com potência de 5 kW ocorre uma queda significante da resistência após exposição de 5 segundos. Estudos de KOLEINI *et al.*(2012) mostram a variação da taxa específica de quebra quando do tratamento de micro-ondas de 1100 W e 2,45 GHz durante 3 minutos. Para cada tamanho de partícula foram utilizadas duas amostras de 300g para medir a taxa específica de quebra. Tais amostras foram analisadas com e sem o tratamento de micro-ondas. Os valores das taxas são mostrados na

Tabela 2.4-1 percebe-se que, após o tratamento com micro-ondas, a taxa de quebra aumenta, sobretudo para as amostras com partículas maiores (aproximadamente 12 % entre 2,00 mm e 2,36 mm e 8 % entre 0,300 mm e 0,355 mm).

Tabela 2.4-1 - Taxa específica de quebra (min^{-1}) (KOLEINI *et al.*, 2012).

Estado da Amostra	Tamanho das Partículas (mm)			
	-2,36 + 2,00	-1,4 + 1,18	-1 + 0,850	-0,355 + 0,300
Sem tratamento	0,4318	0,9542	0,7876	0,5572
Tratada com micro-ondas	0,485	1,0588	0,8582	0,6013

XIU-JING *et al.* (2010) estudaram os efeitos da potência das micro-ondas sobre a taxa de lixiviação de laterita contendo limonita. A melhora de até 30 % na taxa de lixiviação do níquel pelo aumento de 300 W no tratamento com micro-ondas é explicada pela migração de espécies iônicas e/ou rotação de espécies dipolares que promovem o processo de reação líquido/sólido devido ao incremento de superfície de contato entre os reagentes. Quando a potência do forno de micro-ondas é de 800 W (potência ótima de operação) a taxa de lixiviação alcança o valor de 92 % (XIU-JING *et al.*, 2010).

Ainda, XIU-JING *et al.*(2010) investigaram o tempo ótimo de exposição de micro-ondas para a lixiviação de níquel. Pode-se observar que com uma exposição de 6 minutos, a taxa de lixiviação sobe para cerca de 92 %. É possível notar que exposições maiores que o referido intervalo de tempo não alteram consideravelmente a lixiviação, visto que a diferença ocorrida entre 6 e 8 minutos é muito pequena (92,76 % para 6 minutos e 92,97 % para 8 minutos). Assim, conclui-se que o tempo ótimo de exposição é de 6 minutos apenas (XIU-JING *et al.*, 2010. OLUBAMBI (2009) verificou que é possível extrair uma maior quantidade de metais através de biolixiviação de minérios sulfetados complexos com o uso preliminar de micro-ondas. Os experimentos de OLUBAMBI (2009) foram procedidos à temperaturas entre 32 e 35 °C com velocidade de agitação constante igual a 150 rpm, densidade de polpa igual a 10 % e inóculo a 12 $\%_{v/v}$. Estudos de CASTRO *et al.* (2014)

mostram a redução carbotérmica de 20 g de pelotas autorredutora por meio de um micro-ondas que opera com 2,45 GHz e 4,5 kW.

2.5. Melhoria de Eficiência Energética de Processos Industriais a partir do uso de Micro-ondas

PICKLES (2009) apresentou a calcinação e sinterização de carbonato de manganês pelo método convencional e por meio de micro-ondas (Figura 2.5-1). Após os minutos iniciais, a taxa de calcinação no forno de micro-ondas aumenta repentinamente ultrapassando a do forno tradicional. Ao final o processo com micro-ondas termina o processo de calcinação alcançando uma perda de massa superior e tempo de processamento 10 minutos inferior.

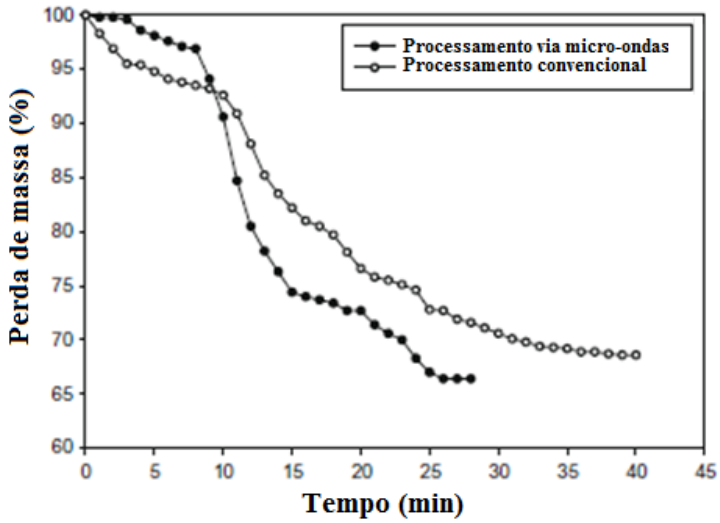

Figura 2.5-1 - Perda de massa no minério de manganês em função do tempo de processamento para a técnica convencional e por micro-ondas (PICKLES, 2009).

A Figura 2.5-2 ilustra a diferença estrutural entre a amostra operada na forma tradicional e com micro-ondas. É notável que o forno convencional (Figura 2.5-2 a) gerou muitas fraturas no material, porém para o tratamento com micro-ondas (Figura 2.5-2b) as trincas são muito mais pronunciadas.

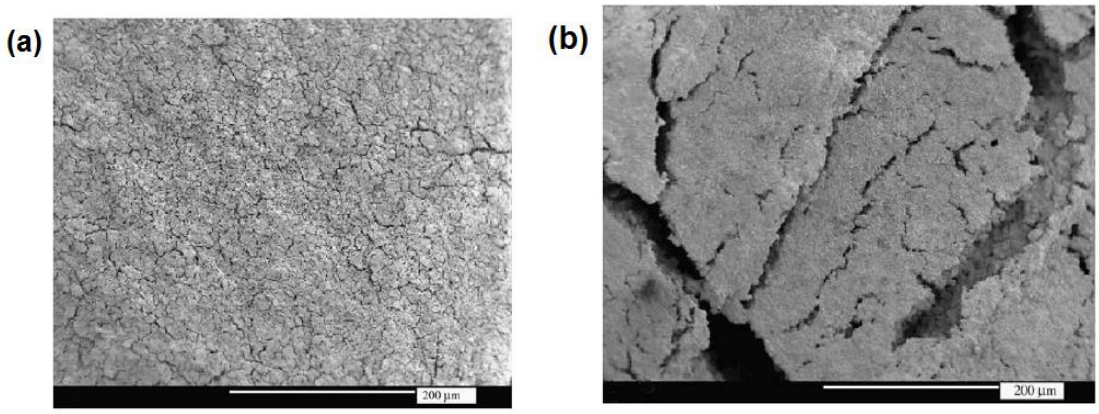

Figura 2.5-2 – Microscopia eletrônica de varredura de carbonato de manganês tratado via forno convencional (a) e via forno micro-ondas (b) (PICKLES 2009).

2.6. Redução de Minérios e Fusão de metais

Ainda de forma a otimizar o processo de ignição no processo de sinterização de minérios de ferro, HUANG *et al.* (2012) considerou o MHI (Microwave Heating Ignition) onde a temperatura atingida para a sinterização foi menor, como também a energia consumida. As velocidades de sinterização são praticamente iguais e os valores de rendimento, tamboramento e produtividade foram maiores. Essas informações são mostradas na Tabela 2.6-1. Além disso, a energia consumida na ignição é muito menor para o MHI (43,77 MJ/m² contra 185,13 MJ/m² do CGI (Coal Gas Ignition)).

Tabela 2.6-1 - Comparação entre MHI e CGI no processo de sinterização (HUANG *et al.*, 2012).

Ignição	Temperatura (°C)	IEC (MJ/m²)	VSS (mm/min)	TI (%)	Rendimento (%)	Produtividade (t/(m².h))
MHI	660	43,77	24,23	59,50	76,60	1,83
CGI	1050	185,13	24,89	58,78	76,13	1,76

O maior volume de oxigênio no MHI reduz a temperatura de ignição como também permite gerar calor suficiente para o processo de sinterização. Além disso, as quantidades de SO_2 e NO_x no processo utilizando MHI são muito inferiores às quantias no que usa CGI (HUANG *et al.*, 2012). Essas informações são ilustradas na Figura 2.6-1.

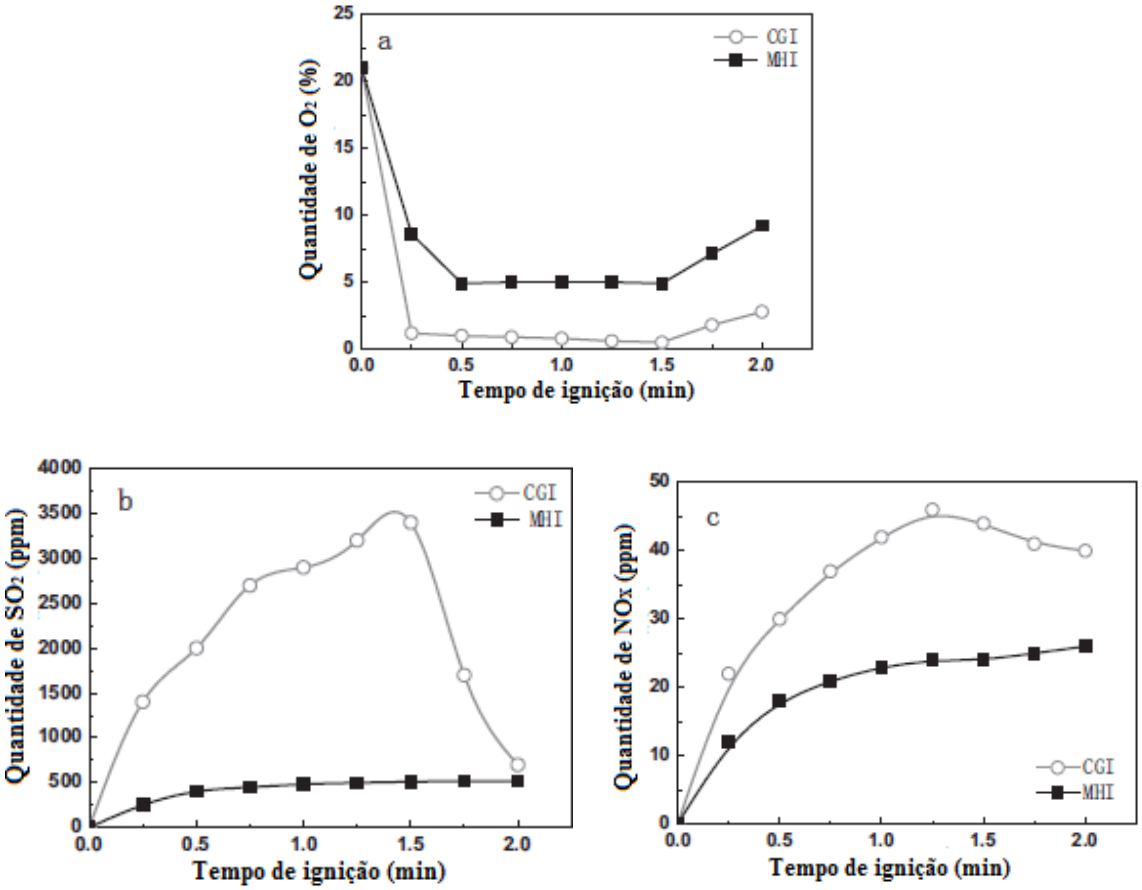

Figura 2.6-1 - Quantidades de O_2, SO_2 e NO_x no gás de combustão durante a ignição (HUANG *et al.*, 2012).

Em termos financeiros, para o cenário de preços atuais, isto representa uma redução de 57% no custo energético. Mesmo para processos ainda mais tradicionais como a geração de ferro gusa a partir de minério de ferro, segundo HARA *et al.* (2011), é possível com 30 minutos utilizando um forno de micro-ondas de 60 kW para produzir 1 tonelada por dia. Sabendo que a energia para o aquecimento e reação é em torno de 48 kW, a perda energética nesse procedimento é de 12 kW (HARA *et al.*, 2011). Dessa forma, os autores afirmam que a

eficiência energética do forno de micro-ondas é 80% superior à do alto-forno. Devido ao fato de as reações ocorrerem rapidamente, o tamanho do forno pode ser diminuído, reduzindo os custos de construção (HARA *et al.*, 2011).

Ainda na área de fusão de metais, pesquisas de CHANDRASEKARAN *et al.*(2011) revelam que a fusão de estanho, chumbo, alumínio e cobre via micro-ondas é realizada rapidamente num processo de produção limpo e controlado. Nota-se que, com o aumento da potência do micro-ondas, o tempo para a fusão diminui. Ainda CHANDRASEKARAN *et al.* (2011) compararam o tempo de fusão de amostras de estanho, chumbo e alumínio via forno de micro-ondas (1300 W) e via forno convencional (mufla de 2500 W), mostrando ser possível obter aumento de produtividade e melhoria energética do processo, conforme Figura 2.6-2. Fica claro no estudo que as condições variam para cada material estudado.

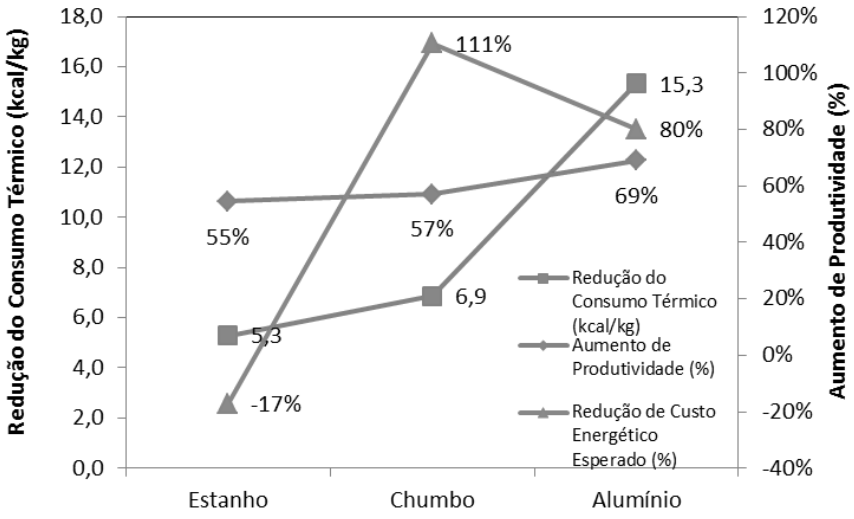

Figura 2.6-2 - Avaliação de eficiência do estudo apresentado por CHANDRASEKARAN *et al.*, 2011.

2.7. Conclusão

Aplicação de micro-ondas em processos Minero-Metalúrgicos é ampla e representa um deslocamento do padrão atual de produtividade e processo. Análise de custo-benefício

devem ser realizadas para cada aplicação, porém pode representar investimento em plantas existente competitivo em relação a novas operações.

2.8. Referências

AKPINAR, E., MIDILLI, A., BICER, Y. Single layer drying behaviour of potato slices in a convective cyclone dryer and mathematical modeling, Energy Conversion and Management, Elazig, v.44, p.1689–1705, 2003.

Ali, A.Y., Bradshaw, S.M. Bonded-particle modelling of microwave-induced damage in ore particles, Minerals Engineering, Matieland, v.23, p780-p790, 2010.

Barani, K., Koleini, S.M.J., Rezaei, B. Magnetic Properties of an Iron Ore Sample after Microwave Heating, Separation and Purification Technology, Tehran, v.76, p331-p336, 2011.

Castro, E.R., Jermolovicius, L.A., Mourão, M.B., Pouzada, E.V., Nascimento, R.B., Takano, C., Senise, J.T. Processo e forno para a produção de ferro gusa utilizando micro-ondas, Redução de Minério de Ferro & Tecnologia Mineral, Belo Horizonte, 2014.

Cha, C.-Y. Microwave induced reactions of SO2 and NOx decomposition in the char-bed, Res. Chem. lntermed., Laramie, v.20, n.1, p13-p28, 1994.

Chandrasekaran, S., Basak, T., Ramanathan, S. Experimental and theoretical investigation on microwave melting of metals, Journal of Materials Processing Technology, Chennai, v.211, p482–p487, 2011.

Chandrasekaran, S., Ramanathan S., Basak T. Microwave food processing -A review, Chennai, v.52, p243–p261, 2013.

Chang, Y., Zhai, X., Fu, Y., Ma, L., Li, B., Zhang, T. Phase transformation in reductive roasting of laterite ore with microwave heating, Transaction of Nonferrous Metal Society of China, Shenyang, v.18, p969-p973, mar. 2008.

Chen, G., Chen, J., Guo, S., Li, J., Srinivasakannanc, C., Peng, J. Dissociation behavior and structural of ilmenite ore by microwave irradiation, Applied Surface Science, Abu Dhabi, v.258, p4826-p4829, 2012a.

Chen, G., Chen, J., Li, J., Guo, S., Srinivasakannan, C., Peng, J. Optimization of combined microwave pretreatment–magnetic separation parameters of ilmenite using response surface methodology, Powder Technology, Kunming, v.232, p58-p63, aug. 2012b.

Clark, D. E., Folz, D. C., West, J. K. Processing materials with microwave energy, Materials Science and Engineering, Gainesville, v.A287, p153–p158, 2000.

Cutmore, N., Evans, T., Cronokrak, D., Middleton, A., Stoddard, S. Microwave Technique for Analysis of Mineral Sands, Minerals Engineering, Menai, v.13, n.7, p729-p736, 2000.

Feng, H., Tang, J. Microwave Finish Drying of Diced Apples in a Spouted Bed, Journal of Food Science, Whashington, v.63, n.4, 1998.

Flamant, G.F., Fatah N., Flitris Y., Wall-to-bed heat transfer in gas-solid fluidized beds: prediction of heat transfer regimes, Powder Technology, Vol 69, p.223-230, Janeiro 1992.

Guo, S., Chen, G., Peng, J., Chen, J., Li, D., Liu, L., Microwave assisted grinding of ilmenite ore, Trans. Nonferrous Met. Soc. China, Kunming, v.21, p2122-p2126, aug. 2010.

Guo, S., Li, W., Peng, J., Niu, H., Huang, M., Zhang, L., Zhang, S., Huang, M. Microwave-absorbing characteristics of mixtures of different carbonaceous reducing agents and oxidized ilmenite, International Journal of Mineral Processing, Kunming, v.93, p289-p293, sep. 2009.

Haque, K. E., Microwave energy for mineral treatment processes - a brief review, Int. J. Miner. Process, Ontario, v.57, p1-p24, 1999.

Hara, K., Hayashi, M., Sato, M., Nagata, K. Continuous Pig Iron Making by Microwave Heating with 12.5 kW at 2.45 GHz, Journal of Microwave Power and Electromagnetic Energy, Tokyo, v.45, p137-p147, 2011.

Huang, Z., Yl, L., Jiang, T., Zhang, Y. Hot Airflow Ignition with Microwave Heating for Iron Ore Sintering, ISIJ International, China, v.52, n.10, p1750-p1756, may. 2012.

Jones, D.A., Lelyveld, T.P., Mavrofidis. S.D., Kingman, S.W., Miles, N.J. Microwave heating applications in environmental engineering - a review, Resources, Conservation and Recycling, Nottingham, v.34, p75–p90, 2002.

Jones, P.T., Vlegeus, J., Volders, I., Blanpain, B., Van der Biest, O., Wollants, P. A study of slag-infiltrated magnesia-cromite refractories using hybrid microwave heating, Journal of European Ceramic Society, Leuven, v.22, p903-p916, 2002.

Khalil R.H., Sakhrieh A., Hamdan M., Asfar J., Effect of Pressure and Inlet Velocity on the Adiabatic Flame.Jordan Journal of Mechanical and Industrial Engineering, Vol 4, p.21-28, Janeiro 2010.

Kingman, S.W., Jackson, K., Bradshaw, S.M., Rowson, N.A., Greenwood, R. An investigation into the influence of microwave treatment on mineral ore comminution, Powder Technology, Nottingham, v.146, p176-p184, sep. 2004.

Kingman, S.W., Rowson, N.A., Microwave treatment of minerals – a review, Minerals Enginering, Birmingham, v.11, n.11, p1081-p1087, jul. 1998.

Kingman, S.W., Vorster, W.,Rowson, N.A. The Influence of Mineralogy on Microwave Assisted Grinding, Minerals Engineering, Birmingham, v.13, n.13, p313-p327, 2000.

Koleini, S. M. J., Barani, K., Rezaei, B. The effect of microwave treatment on dry grinding kinetics of iron ore, Mineral Processing & Extractive Metall., Tehran, v.33, p159–p169, 2012.

Kumar, P., Sahoo, B.K., Dea, S., Kar, D.D., Chakraborty, S., Meikap, B.C. Iron ore grindability improvement by microwave pre-treatment, Journal of Industrial and Engineering Chemistry, West Bengal, v.16, p805-p812, 2010.

Lam, S. S., Russell, A. D., Lee, C. L., Lam, S. K., Chase, H. A. Production of hydrogen and light hydrocarbons as a potential gaseous fuel from microwave-heated pyrolysis of waste automotive engine oil, International Journal of Hydrogen Energy, Cambridge, v.37,p5011-p5021, 2012.

Liu, C., Zhang, L., Peng, J., Liu, B., Xia, H., Gu, X., Shi, Y. Effect of temperature on dielectric property and microwave heating behavior of low grade Panzhihua ilmenite ore, Trans. Nonferrous Met. Soc. China, Kunming, v.23, p3462-p3469, aug. 2013.

Lovás, M., Kováčová, M., Dimitrakis, G., Čuvanová, S., Znamenáčková, I., Jakabsky, Š. , International Journal of Heat and Mass Transfer, Košice, v.53, p3387-p3393, 2010.

Lovás, M., Murová, I., Mockovciaková, A., Rowson, N., Jakabsky, Š. Intensification of magnetic separation and leaching of Cu-ores by microwave radiation, Separation and Purification Technology, Birmingham, v.31, p291-p299, 2003.

Ma, S.J., Zhou, X.W., Su, X.J., Mo, W., Yang, J.L., Liu, P. A new practical method to determine the microwave energy absorption ability of materials, Minerals Engineering, Nanning, v.22, p1154-p1159, 2009.

Maeda, T., Nishioka, K., Shimizu, M. Effect of Granulation Condition and Property of Raw Material on Strength of Granulated Particle by Tumbling Granulation, ISIJ International, Fukuoka, v.49, n.5, p625-p630, jan. 2009.

Makul, N., Rattanadecho, P., Agrawal, D. K. Applications of microwave energy in cement and concrete – A review, Renewable and Sustainable Energy Reviews, Bangkok, v.37, p715-p733, 2014.

Martinazzo, A. P., Corrêa, P. C., Resende, O., Melo, E. C. Análise e descrição matemática da cinética de secagem de folhas de capim-limão, Revista Brasileira de Engenharia Agrícola e Ambiental, Campina Grande, v.11, n.3, p.301–306, 2007.

Matos, A.P., Influência da temperatura, pressão, produção e granulometria no processo de secagem das pelotas cruas, Ouro Preto: REDEMAT-UFOP, 2007, 150p (Dissertação, Mestrado em Engenharia Metalúrgica).

Menéndez, J.A., Arenillas, A., Fidalgo, B., Fernández, Y., Zubizarreta, L., Calvo, E.G., Bermúdez, J.M. Microwave heating processes involving carbon materials, Fuel Processing Technology, Oviedo, v.91, p1-p8, 2010.

Nuri, O.S., Mehdilo, A., Irannajad, M., Influence of microwave irradiation on ilmenite surface properties, Applied Surface Science, Tehran, v.311, p27-p32, may. 2014.

Oghbaei, M., Mirzaee, O. Microwave versus conventional sintering: A review of fundamentals, advantages and applications, Journal of Alloys and Compounds, Semnan, v.494, p175–p189, 2010.

Park, K. J., Vohnikova, Z., Brod, F. P. R. Evaluation of drying parameters and desorption isotherms of garden mint leaves (Mentha crispa L.), Journal of Food Engineering, Prague, v.51, p.193-199, 2002.

Pickles, C.A. Microwaves in extractive metallurgy: Part 2 – A review of applications, Minerals Engineering, Ontario, v.22, p1112-p1118, 2009.

Sahoo, B.K., De, S., Carsky, M., Meikap, B.C. Rheological characteristics of coal–water slurry Chemistry, West Bengal, v.17, p62-p70, 2011.

Sahoo, B.K., De, S., Meikap, B.C. Improvement of grinding characteristics of Indian coal by microwave pre-treatment, Fuel Processing Technology, West Bengal, v.92, p1920–p1928, 2011.

Saito, Y., Kawahira, K., Yoshikawa, N., Todoroki, H., Taniguchi, S. Dehydration Behavior of Goethite Blended with Graphite by Microwave Heating, ISIJ International, v. 51, n.6, p878-p883, mar. 2011.

Standish N., Huang, W. Microwave Application in Carbothermic Reduction of lron Ores, ISIJ International, Beijing, v.31, p241-p245, 1991.

Uslu, T., Atalay, U ., Arol, A.I. Effect of microwave heating on magnetic separation of pyrite, Colloids and Surfaces A: Physicochem. Eng. Aspects, Ankara, v.225, p161-p167, jun. 2003.

Waters, K.E., Rowson, N.A., Greenwood, R.W., Williams, A.J. Characterising the effect of microwave radiation on the magnetic properties of pyrite, Separation and Purification Technology, Birmingham, v.56, p9-p17, jan. 2007.

Xiu-jing, Z., Qiang, W., Yan F., Lin-zhi, M., Chuan-lin, F., Nai-jun, L. Leaching of nickel laterite ore assisted by microwave technique, Trans. Nonferrous Met. Soc. Shenyang, v.20, p77-p81, 2010.

Zhang M., Tang J., Mujumdarc, A.S., Wang S. Trends in microwave related drying of fruits and vegetables, Jiangsu, v.17, p524-p534, 2006.

Zhao W., Chen J., Chang X., Guo S., Srinivasakannan C., Chen G., Peng J.Effect of microwave irradiation on selective heating behavior and magnetic separation characteristics of Panzhihua ilmenite, Applied Surface Science, Abu Dhabi, v.300, p171-p177, 2014.

Znamenáčková, I., Lovás, M., Mockovčiaková, A., Jakabskýa, Š., Briančin, J. Modification of magnetic properties of siderite ore by microwave energy, Separation and Purification Technology, Košice, v.43, p169-p174, 2005.

Zou, Z., Xuan, A.G., Yan, Z.G., Wu, Y.X., Li, N. Preparation of Fe3O4 particles from copper/iron ore cinder and their microwave absorption properties, Chemical Engineering Science, Wuhan, v.65, p160-p164, 2010.

Capítulo 3. Artigo B - A Case Study of Pellet Size Fractions Influence on Pelletizing Operation

Maycon Athayde, Sergio Fernandes Nunes & Maurício Covcevich Bagatini

Artigo publicado em 15 de janeiro de 2018 na *revista Mineral Processing and Extractive Metallurgy Review, 39(4), 276-283.* DOI: 10.1080/08827508.2017.1423296

Abstract

Pellet production is constantly optimized considering different aspects of the production chain from run of mining (ROM) to metallic iron. Industrially, the trade-off between an optimum pellet-size-ratio and the maximum performance in the steel production chain is a relevant subject. The present case study of a Brazilian operation shows the impact of different pellet size fractions on performance of operation, improvements on the fired pellets, less fine generation during handling, and superior metallurgical behavior during the reduction process, resulting in the production of direct reduction iron (DRI) that add more value to the economic performance of the electric arc furnaces (EAF).

Key Words: Pellet Size Ratio, Process Optimization, Tumble Index.

3.1. Introduction

The steel production, from the iron ore green pellets until the direct reduction reactors, and finally the poured liquid steel on the EAF, has a large list of constraints, and some of them correlate the pellet size distribution to a maximum efficiency of the whole steel production

chain. Over the recent years, with the gradual increase in plant productivity, the need to understand and review the holistic effect of pellet size distribution in the processes has emerged, also ensuring a lower degradation during transport and a higher rate of reduction at the DRI production. This case study analyzes the different aspects of the problem, leading an understanding of this complex scenario. A common industrial way to express the size distribution of the pellets can be by the size ratio index, which refers to the relationship between the percentage of pellets on the large size range over the smaller size range, according to equation 1.

$$Size\ Ratio = \frac{\%\ (-16+12.5)}{\%\ (-12.5+9)} \qquad \text{Equation (1)}$$

The control of size ratio is challenging for whole production chain to obtain maximum output of each equipment; the correct adjustment of the different size fractions is key. In the present case study, all stages of the pelletizing process were evaluated in order to seek the global effectiveness reached in a proper selection of pellet size ratio, based on different size fractions.

3.2. The Case Study

The present study is about Samarco Mineração operation of Ponta Ubu in Brazil. The company has installed pipelines (about 400 km) which can supply slurry from the beneficiation plants. At the concentration site, the ore is screened, crushed, and classified to feed the primary balling mills. This circuit assures sufficient comminution of the iron ore ROM. Then, the ultrafine material is removed in a cyclones cluster before conventional flotation where gangue material such as silica is separated from the iron particles. The ore is reground and fed to a column flotation circuit. The slurry is then pumped to the pelletizing

plants. On the arrival, the slurry is stored in tanks and distributed to thickener (42 m), where its function is to densify the slurry (up to 69 % solid) and route this material downstream the process (clarification and water treatment ensure the water reuse in the process). From Figure 1, vacuum filters are installed in the plant (vacuum pressure of 25 inches of mercury). After filtration, the pellet feed (moisture at 10–11 %) is transported to the high pressure grinding rollers. This is a single crushing step to prepare the pellet feed (−325# of 87 %–89 % and Blaine surface area of 1800–2000 cm^2/g) to a desired particle size distribution (in general, increasing 2%–5% < 45 μm and Blaine surface area 200–400 cm^2/g) for the formation of the green pellets, allowing filters to operate with coarser pellet feed, improving its performance. The pellet feed pressed is then transported to a silo in the mixing line building. In the mixing building are also the additive silos, where raw materials are added and mixed to the pellet feed to form the green pellets: two types of binders are possible (organic binder or bentonite), limestone, and solid fuel (anthracite). For the dosing and mixing, silos are placed in the following order: limestone ground (in the plant), bentonite, ground coal, and organic binder. The mixture (pellet feed with additives) follows the lines of horizontal intensified drum mixers to acquire homogeneity for the balling process. The homogenous mixture follows to the agglomeration process, where discs (diameter of 7.5 m and 400 mm free height) are fed at 150 ton/h rate to produce green pellets controlling the range 16–8 mm% (70 %– 75 %), and pellets out-of-spec are in a close loop to a de-agglomeration system in the belt conveyor which receives the material from the mixers and returns it to the feeding belt of the discs.

Classification of the green pellets is performed just after the discs on a single-deck roller screener which withdraws the fines −9 mm and pellets greater than +18 mm. A second stage of classification is performed before the furnace where a double deck roller screen (DDRS) improves the 16–8 mm% range (more than 92 %). Recirculating load (pellets out of 8–16 mm range) corresponds to about 16 %–20 % of the material that is fed to the balling disc

and is coarser compared to the pellet feed (agglomerated), interfering in the process of the green pellets growing and contributing to the reduction of physical quality of the green and fired pellets (caused by the double-layer formation over the seed). The induration furnace is fed continuously by the DDRS which distributes the pellets through the entire section of the furnace over a hearth layer of 70 mm of fired pellets (bottom and side layers). The total height of the pellet bed, including the layer of fired pellets (bottom layer), may reach a maximum of 450 mm. The grate speed varies and it is automatically controlled to maintain a constant total bed height, with regard the production level setup. Furthermore, to remove fines from fired pellets (2–4%), after the furnace discharge, the pellets are screened. The screening installation has vibrating screeners installed in parallel, which separate the pellets by size (above 12 mm to hearth layer, −6,3 mm are fines, and 16–8 mm is the product). After this separation, the pellets are transported to the yard or directly load the ships.

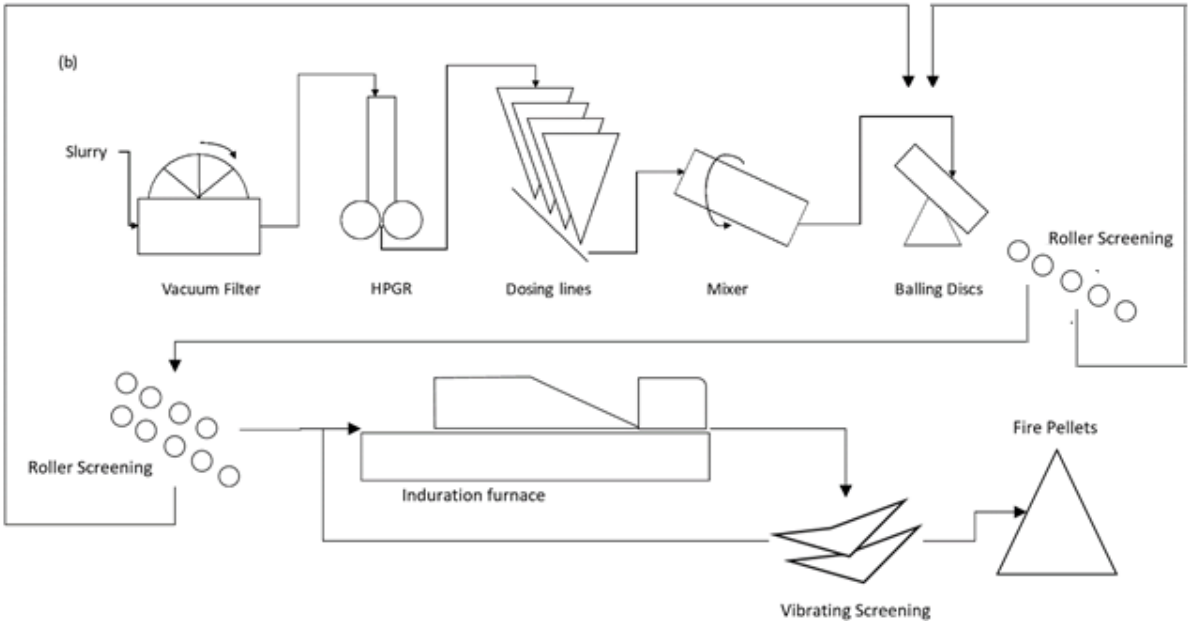

Figure 1 – Flowchart of the pelletizing operation

3.3. Pellet Size Fraction Impact on the Process

3.3.1. Influence of Pellet Size Fraction on the Balling Process

The optimization of agglomeration processes aims to have the best fired pellets physical quality which shall minimizes degradation and fine generation. Basically, the balling process is the agglomeration of solids bonded by a proper amount of water. Water is an important input to the formation and growth of the pellets, creating the surface tension which promotes the grain cohesion, allowing its handling previously to a later ceramic bonding. The outcome of balling is the green pellet which must have essential characteristics to resist the transport and process inside the pelletizing furnace. Among these properties, it can be highlighted the resilience (ability to resist without cracking after consecutive drops), wet compression and average diameter. These combined properties influence directly the performance of the firing step, reflecting in the quality of the fired pellets and overall plant output. If these parameters are not suitable, a partial sealing of the green pellets bed can be observed inside the furnace, as illustrated in Figure 2.

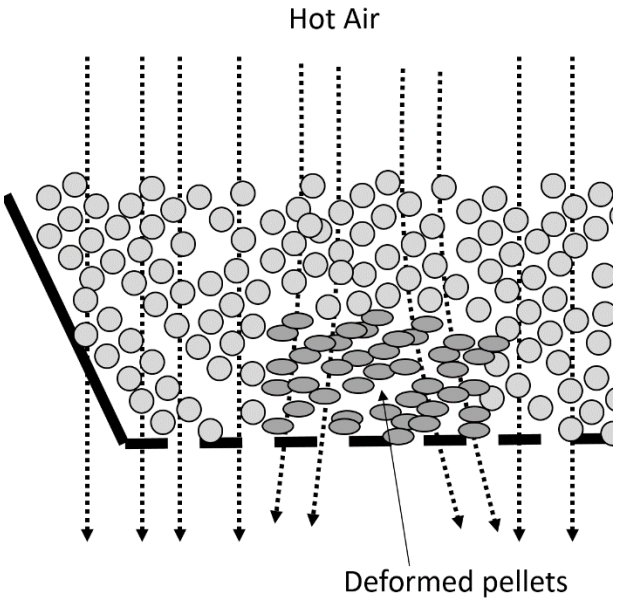

Figure 2 – Mechanism of pellet bed low permeability due pellet deformation.

The balling setup and operation are responsible for setting an average size of green pellet with lower variability. In general, it can be assumed that the average pellet diameter control will determine the size distribution of the pellets (with a fixed setting of the roller screen gap). In this process control one of the main parameters to be taken over is the recirculation load in the balling circuit. Nunes (2007) observed that moisture content of the recirculating load is directly influenced by the moisture content of the mixture (pellet feed plus additives). Nevertheless, a statistical analysis, with a confidence level of 95 %, shows an average shift of 0.38 % between those flow streams (Figure 3).

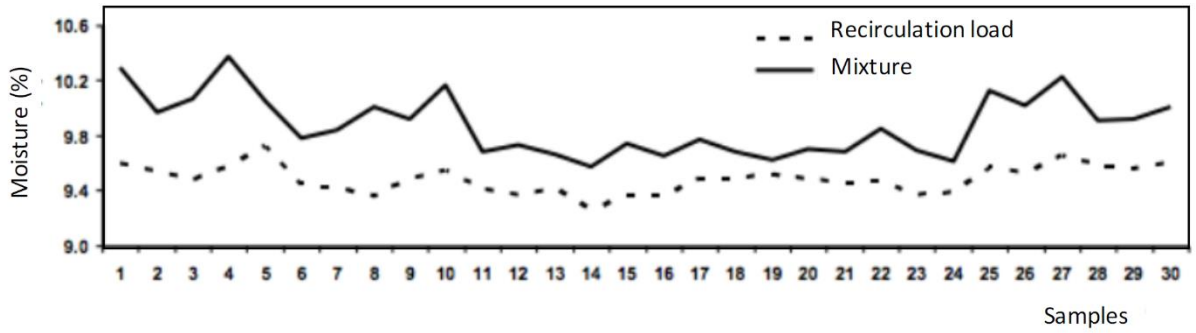

Figure 3 – Evolution of moisture in the green pellets mixture and circulation load (adapted from Nunes. 2007).

A lower moisture content of the recirculation load is explained by the moisture content of the small agglomerates discharged from the discs (-9 mm). Figure 4 presents industrial data with good correlation between pellets size discharged from a disc and moisture content. It is observed that a higher percentage of recirculation load is related to a greater amount of small dry agglomerates, and therefore a lower moisture content. The observation represents a major problem for the operation since the agglomeration depends on the moisture around the particles for the formation of capillary forces. There is a trade-off inside a disc, seeds drier than the rest of the particles grow by adhesion or the rest of the particles generate new seeds

by layering. Moreover, drier material actively influences the growth rate of agglomerates, where less capillary forces will act bonding the particles and consequently the agglomerate formed going to be weaker and size control more complex. A side effect that leads to the formation of double-layered pellet minimizes the quality of fired pellet, as the pellet shell easily separates from the core.

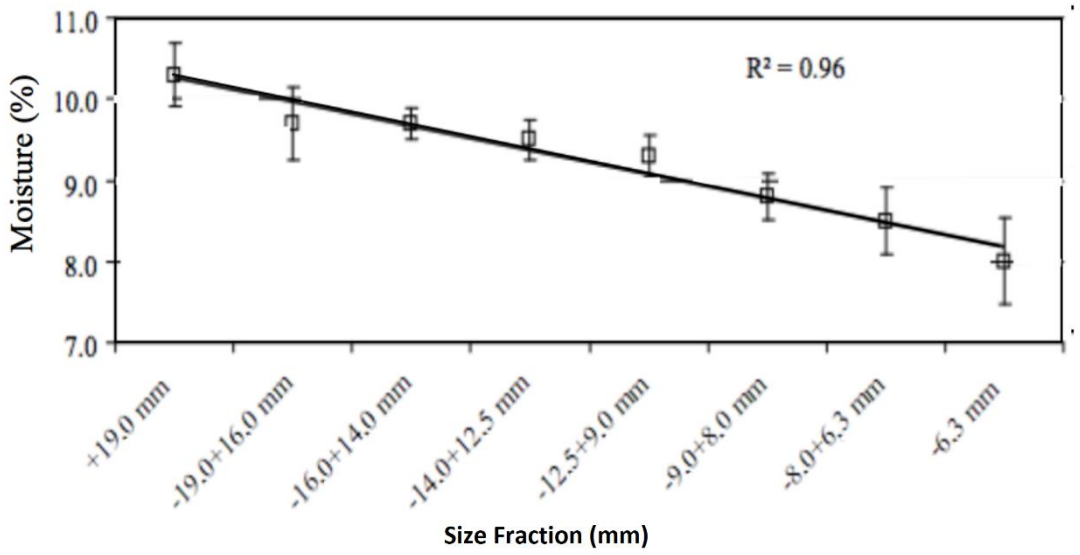

Figure 4 – Statistical analysis of moisture distribution by pellet size (adapted from Nunes 2007).

Operationally, the possibility of adjusting the balling discs to produce pellets with greater diameter (set up inclination, rotation, feed rate and binder dosage) usually depleting the overall efficiency (increasing the recirculation load and pellet out-of-spec). Industrial performance evaluations have shown that efficiency decrease can be observed in the reduction of the percentage of pellets concentrated in the range between -16.0 + 8.0 mm (Figure 5a) and an increasing in the recirculation load of the balling circuit. Additionally, greater average diameter is strongly related to the increase of the pellets size ratio. As seen in Figure 5, a production set to reach diameters greater than 11.8 mm lead to a reduction in the concentration of pellets in the range between -16 +8 mm and decreased homogeneity of

the size distribution (with a paramount importance for the following induration counter-flow processes).

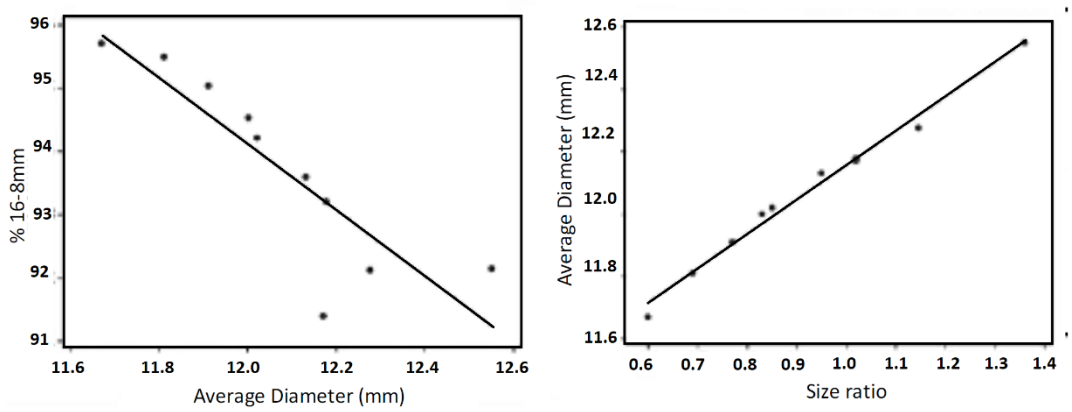

Figure 5 - Evaluation industrial average data (a) percentage of pellets from 16.0 to 8.0 mm diameter and (b) Correlation between the diameter ratio and size ratio (Werneck, 2010).

The pellet production of smaller average diameter leads an increase in the process stability through greater yield. Moreover, process optimization of balling disc (scrappers, feed point and disc hearth layer set up) has a clear effect on tumble index (pellet resistance to tumbling, which remain above 6.3 mm after 200 revolutions at 25 rpm according to ISO 3271). As shown in Figure 6 in terms of pellet size ranges year-average, the process is then optimized when the pellets are concentrated in the range between -12.5 + 9 mm, more likely comprising the pellet size ratio about 0.6 to 0.7. This is observed by reducing the formation of seeds within the pellet which reduces the quality of the fired agglomerate as the pellet shell and the core are not well consolidated. Additionally, similar results were obtained by Dwarapudi et al (2008) with Indian iron ore.

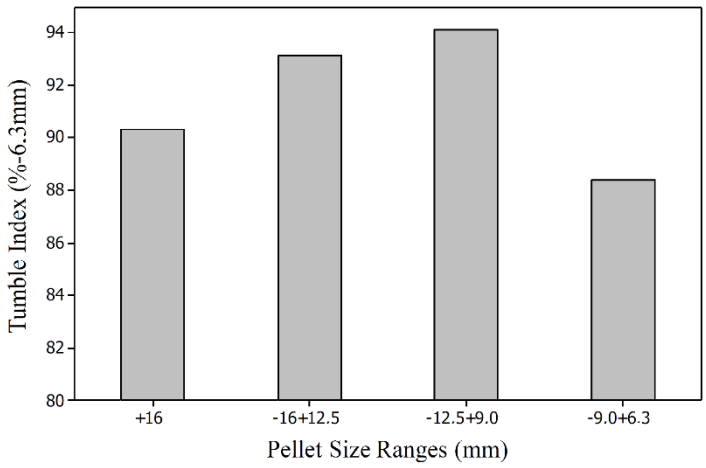

Figure 6 - Influence of Size Ratio in the industrial fired pellet tumbling index.

As far as pelletizing process control is concerned, among the 18 most important parameters monitored in the pelletizing plant (Figure 7) (e.g. average diameter, size ratio and %16-8mm range), the average pellet size is one of the most relevant variable which explains the tumbling index for the fired pellets produced. Additionally, the recirculation load has significant relevance (steeper trend line), but as discussed, this variable has a strict relationship with the control of size ratio (Passos et al 2014).

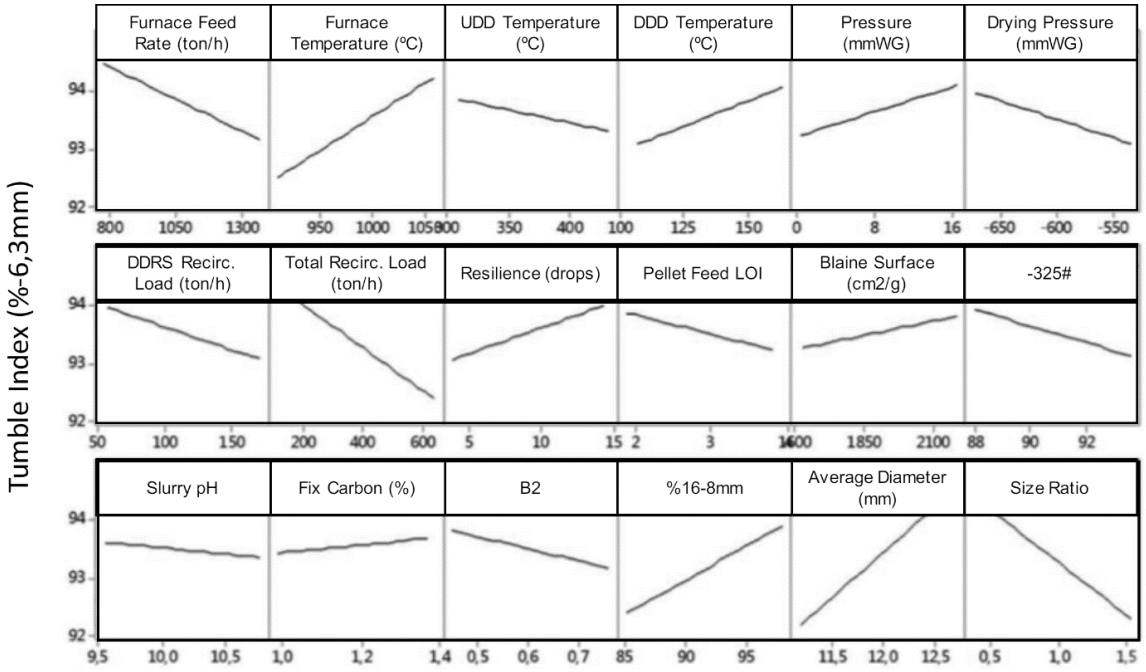

Figure 7 – Effects of process control parameters on the tumbling index. (Passos et al 2014).

The transportation from balling discs to the furnace requires from green pellets a minimum strength, the resilience, also has statistically significant difference among different size ranges (p-value> 0.05). Thus, increasing the tendency to break during transport until the furnace (after 6 consecutive falls) specially with the greater diameter, generating more fines that will lead to sealing of the pellet bed. These results are shown in Figure 8.

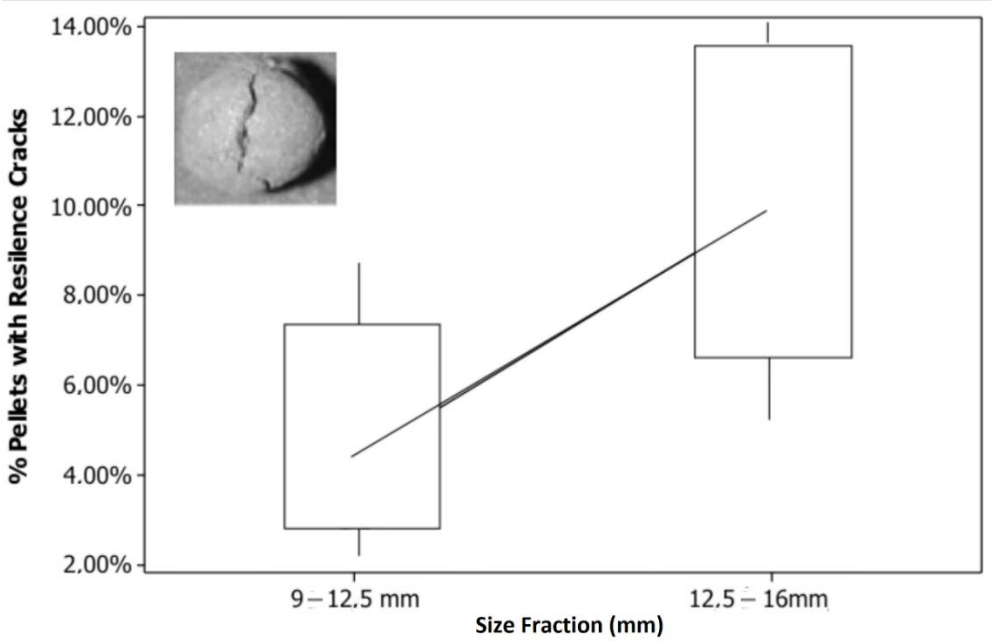

Figure 8: Influence of greater size ratio on the resilient crack generation.

The pellets that do not fully break apart in the transport to the furnace may present cracks. These pellets are fired with the presence of those cracks in the structure, which increases the probability to generate fines and/or fired pellets out of quality standards, which will collapse during handling to client, switching size ratio of the produced pellet and generating fines on the product (due the reduced tumbling index as shown above).

The balling process control has been optimized in Samarco, not just on the equipment level but also through advanced process control system which enables to reduce the process variability applying image analysis as online tool to pelletizing process control based on operational experience (Fonseca 2004).

3.3.2. Influence of Pellet Size Fraction on the Firing Process

The firing step is responsible to give physical strength to the green pellets so that it can withstand handling processes and be charged in the ironmaking reactors. This process is entirely carried out by pushing air through the bed of pellets. Basically, this process comprises three stages: drying, firing and cooling of pellets. In general, the most critical to maintaining the integrity of the pellet is drying stage. Larger pellets size diameter leads to slower drying rates. The temperature difference between the core of the pellet and its surface is larger as the pellet size is increased and, in this way, it is more difficult to evaporate the moisture from the central part of the larger pellets (Figure 9).

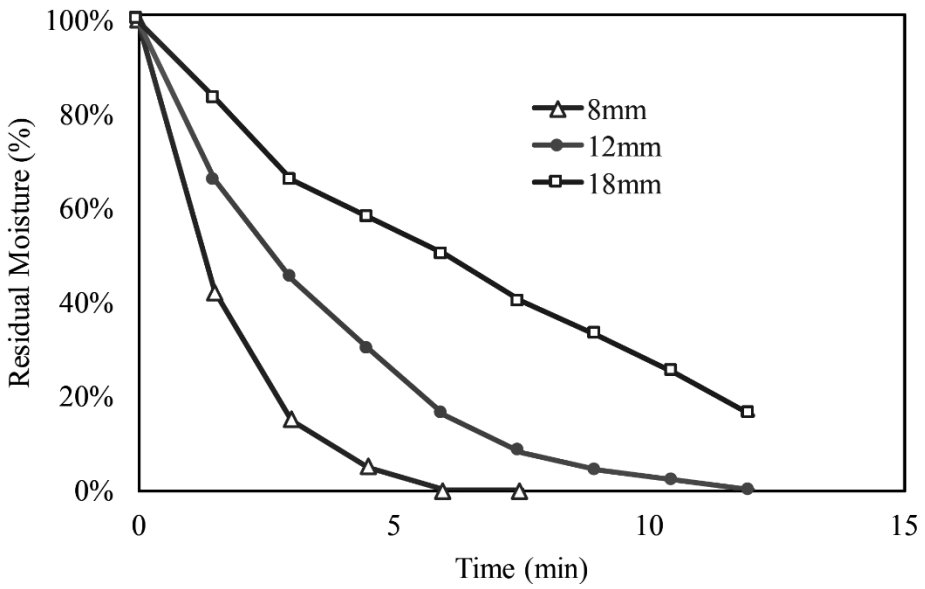

Figure 9 - Influence of the diameter of the pellets on drying.

The drying stage of the furnace in Samarco was optimized with an updraft stage followed by a larger downdraft stage, to maximize the drying of all layers of the bed, prior to the firing step. The next step is called firing and it aims to remove combined water minerals (e.g., goethite), calcination, and ignition of the coal mixed to the ore. Furthermore, it is the stage that sinters the grains of hematite and melts the slag that are key to add physical strength to pellets. The residual moisture inside the pellet is a physical parameter to the integrity of the

pellets (Pereira and Seshadri, 1985). However, the residual moisture will be removed from the pellet during the roasting on the firing zone, nonetheless in a much harsher condition in terms of heat exchange at a higher temperature, which may lead to a rupture due to high steam pressure inside the pellet. The tendency of generating thermal cracks is higher, one more time, because of the increase in the average diameter of the green pellets, most likely due to the residual moisture concentrated more on bigger size pellet, where the path to release the internal gases are indeed longer and more complex. Statistically, production data present a difference (p-value > 0.05) in the size range regarding the thermal crack occurrence (Figure 10). Cracked pellets will be fired in the furnace and will invariably generate fines during screening or handling.

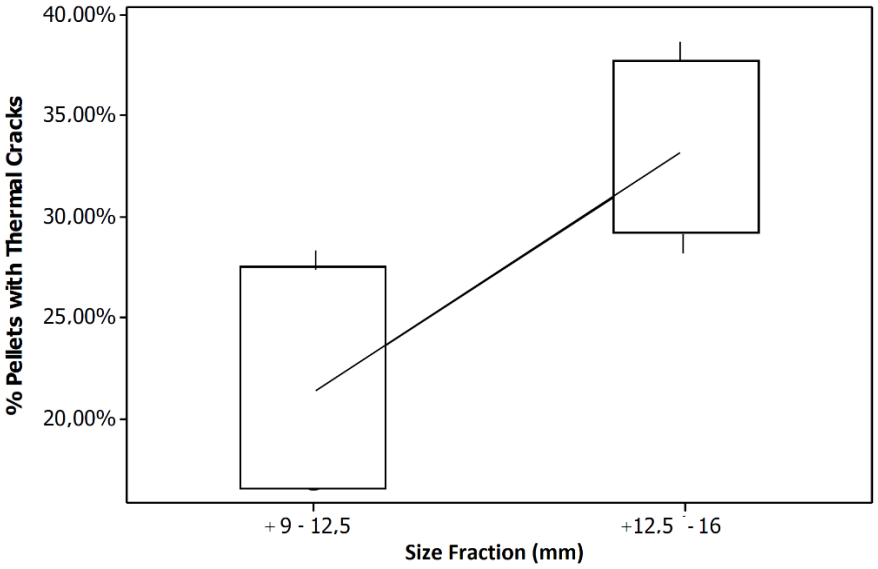

Figure 10 - Influence of the increase of the pellet size ratio in the generation of thermal cracks.

Additionally, temperature homogeneity along pellet bed height and natural gas saving develops on the addition of solid fuel (anthracite or pet coke) to pellet feed as an alternative energy source to the process. However, this may generate a secondary effect of generating thermal cracks during firing and consequent disintegration of the particles due to the volume increase of the hematite structure (rhombohedral structure) as thermally transformed into

magnetite (cubic structure). Dwarapudi *et al.* showed that the presence of non-re-oxidized magnetite (detected by increasing on %FeO levels) in the fired pellet becomes more significant with increase in the average diameter of the pellet (Figure 11).

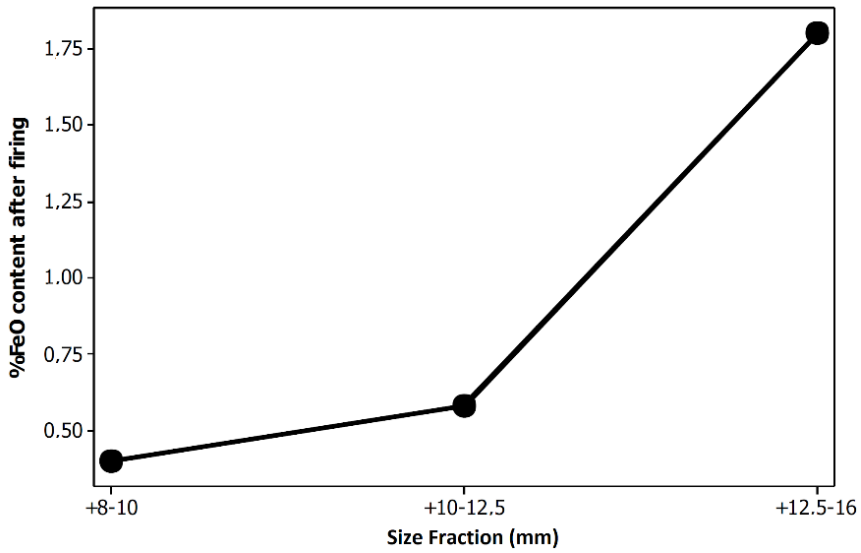

Figure 11: Influence of the pellet size ratio in the formation of magnetite (Dwarapudi *et al.*, 2014).

As can be seen in Figure 12, the mechanism of crack formation due to the reduction of the hematite happens because the gradient of the oxygen partial pressure inside the pellet (intensified by the diameter) where it leads to no re-oxidation of magnetite during cooling and a consequent the volume increase of the pellet core. This generates a strain state that very often forms branched cracks in the surface of the pellet during the cooling process in the end of the furnace.

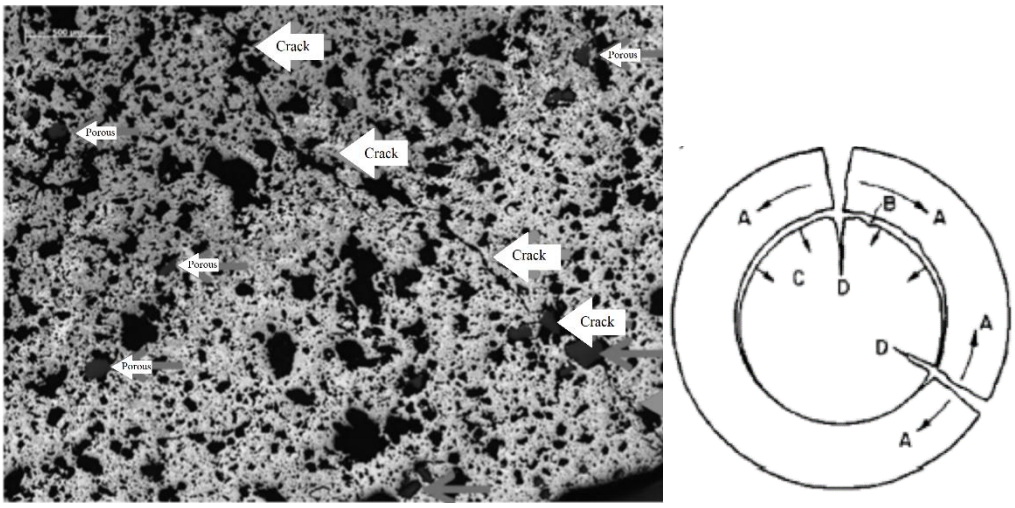

Figure 12: (A) Cracks formation due to thermal expansion of the pellet core and (B) proposed mechanism by Dwarapudi *et al.* (2014).

Therefore, to maintain the quality of the fired pellet, the operation of the pelletizing furnace is possible with a maximum size ratio of 0.9 with an average productivity estimated by 24.5 DMT/day/m². Nonetheless, it may represent a decrease of more than 10% in typical productivity of the Samarco pelletizing plants compared with the production of size ratio in the level of 0.6. The Figure 13 shows an analysis of historical data, from the later years, regarding furnace output productivity and size ratio, where it is shown a downward trend in productivity as a countermeasure to increases size ratio. As predicted, this occurs in order to avoid the deleterious effect to the pellet quality, as described above in this case study.

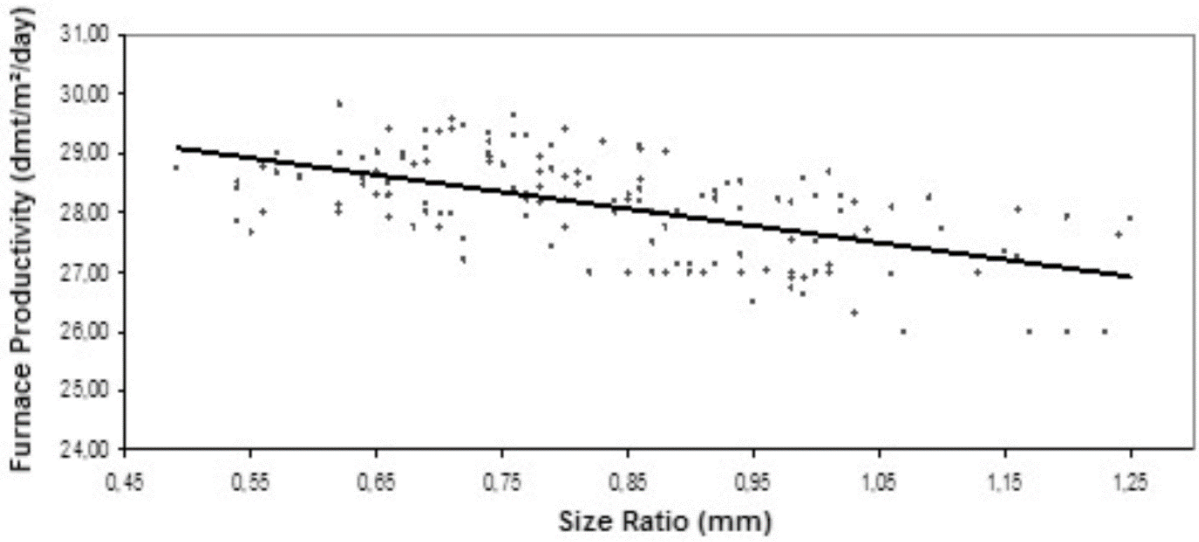

Figure 13 - Evaluation of the productivity decrease due to the increase of the particle size.

Even so, many factors also have influence on the productivity. However, the relationship between the pellet size ratio and the productivity is remarkable, which is critical to ensure that the handling of the pellets shall not be an issue. The next chapter presents the impact of pellet size ratio in the whole production chain, pellets with greater size presents complexities to downstream process.

3.3.3. Influence of Pellet Size Fraction on Handling and Pellet Degradation

The handling of pellets starts immediately with the screening of the pellets after induration furnace. The result shows that the pellets in the fraction of -12.5 +9 mm have a greater tendency of fines generation (-9 mm) as represented in the Figure 14a (green line). However, a probabilistic assessment demonstrates that the tendency to break of this range is much smaller than all the greater size ranges; 5 times less than the larger fractions of pellets. The study consider pellet with good and similar quality, although as presented in the present case, in general bigger pellets have lower quality. Average values of the fracture energies per pellet impact decreases significantly with increasing particle size. It shows that the

production of larger diameter pellets results in a greater risk of degradation due the impact, because of to its intrinsic fragility of the pellet.

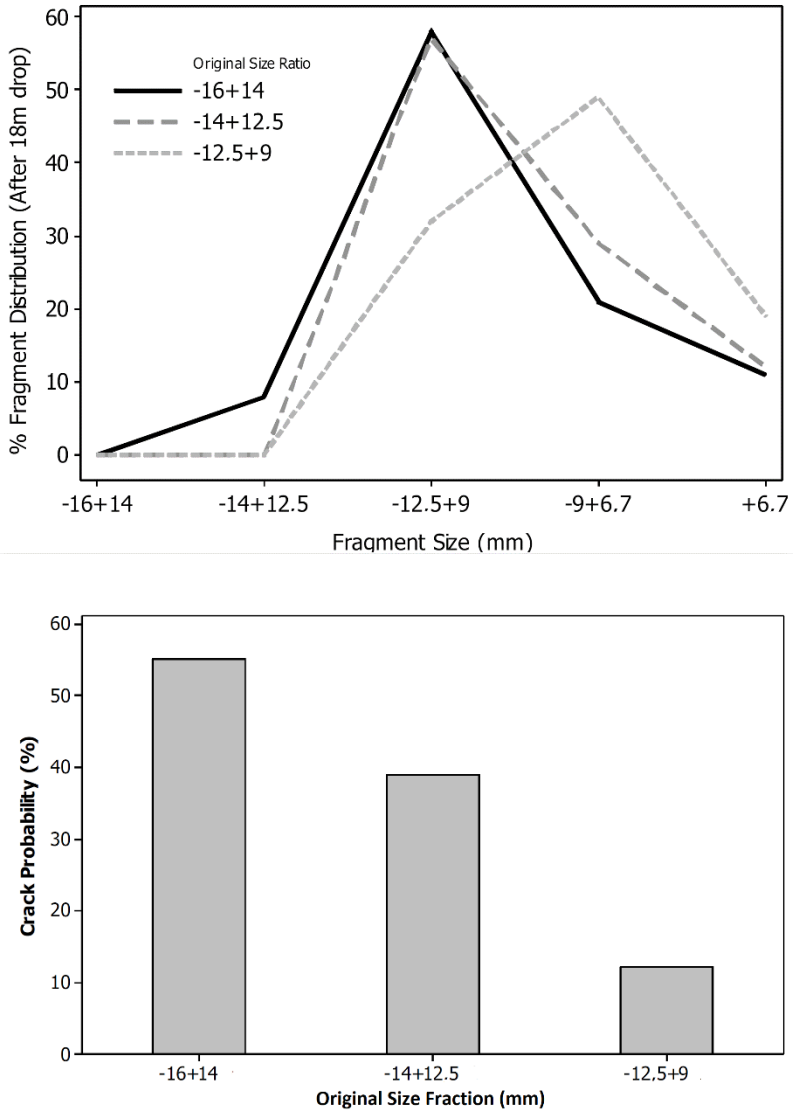

Figure 14 – Pellet degradation as a function of particle size ratio (a) Distribution of pellets degradation (b) Probability of degradation.

A lower tendency of pellets degradation in the smaller range (-12.5 + 9.0 mm) is a positive aspect to production and transport. Additionally, for the operations of stocking and reclaiming of pellets, Daniel (2013) shows for different pellet size the effect of aging phenomena after long periods of storage at environmental conditions. The pellet with smaller size ratios presents a better tumble index in average. Despite of that, over the stocking time,

this difference remains. Even after long periods of time representing a positive effect for degradation issues (Figure 15).

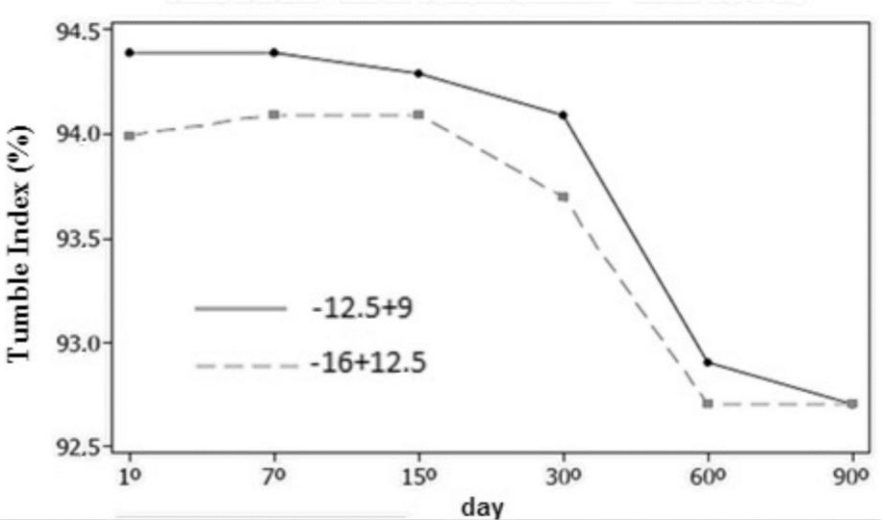

Figure 15 - Effect of size ratio with the aging of iron ore pellets after long periods stocked. DANIEL (2013).

Quality assurance in production operations and storage of iron ore pellets is a challenge key to maximize productivity and lower cost of direct reduction reactors, which also have requirements regarding optimal pellet size ratio.

3.3.4. Influence of Pellet Size Fraction on Direct Reduction Furnaces Performance

The mechanism that describes the reduction reactions of iron ore is called topochemical and it shows a strong dependence of the reaction rates with the radius of the particles (Szekely *et al.*, 1976). Either to lump or pellets, a better gas-solid contact happens using a bed of particles of smaller average diameter. This occurs because of the increasing of the specific surface area of gas-solid reaction. It also contributes to a higher rate of reduction; the fact arose from the average shorter distance between its surface and its central region. Metallurgical results show a strong tendency to increase the metallization of the pellet with reduction of its diameter (Figure 16).

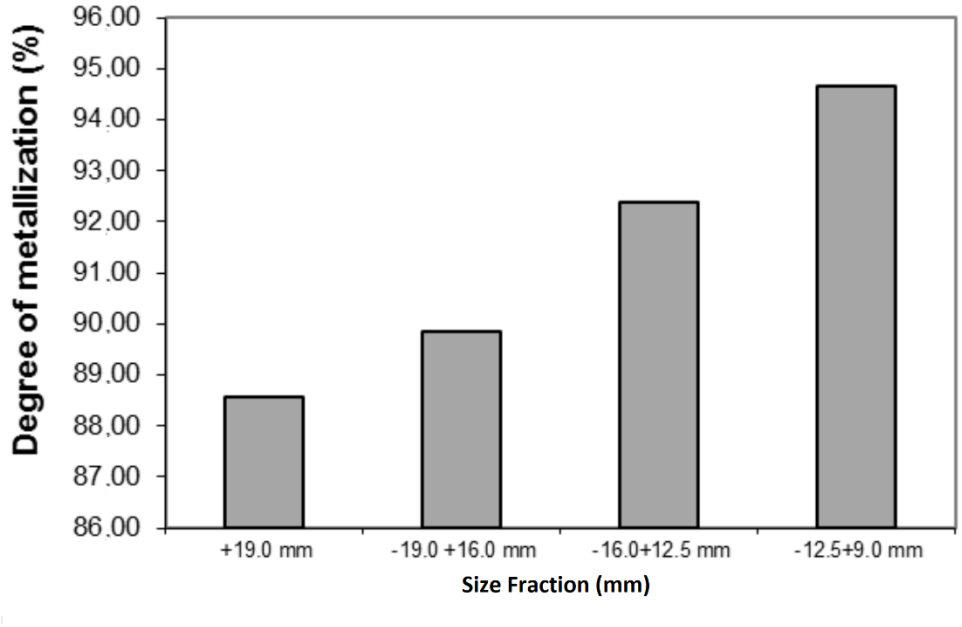

Figure 16 - Effect of size fraction on the degree of metallization pellet

Additionally, the direct reduction reactors are furnaces that operate in counter current flow with a pellet bed to be reduced to DRI. This generates the need to ensure a lower drop pressure in the system in order to minimize equipment power and further increase the kinetics of the reactions. Equation 2 has been proposed by Ergun to estimate pressure variation in the particle bed and is widely accepted in the literature. It shows dependence with characteristics of the bed of pellets, as well as inlet velocity and fluid viscosity.

$$\frac{\Delta p}{L} = 150\ \frac{(1-\varepsilon)^2}{\varepsilon^3}.\frac{\mu U}{\varphi d^2} + 1.75\,\frac{(1-\varepsilon)}{\varepsilon^3}.\frac{\rho U^2}{\varphi d} \qquad \text{Equation 2}$$

The size fraction also has influence on the fluid dynamic aspect of reduction reactors since they imprint a pressure variation on the reduced fluid flow. However, pellets of iron ore produced at Samarco are in a narrow range of size of about 95% between -16 and 9mm in order to lead the smaller pressure variation in the furnace. The Figure 17 shows pilot scale evaluation of different pellet size ranges and the impact to lower the pressure drop in the

furnace. Regarding the increase in absolute pressure drop in the reactor, the presence of fines in the ferrous burden charge is clearly the most critical problem, as the operational practice shows, also leading to a reduction of the void volume of the bed of material, far more relevant than the pellet size. Additionally, this also means that both reducing gases CO and H_2 as main products of the reduction gas, in particular CO_2 and H_2O, take a long time to release from the pellet core to the free pellet surface (Araujo, 2004).

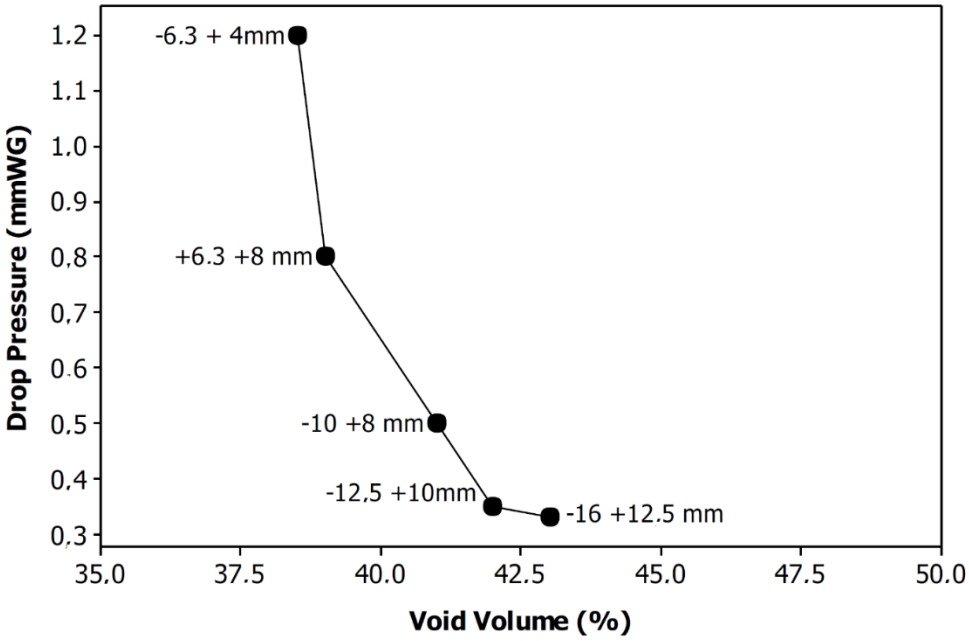

Figure 17 – Pressure variation along a column of pellets in pilot scale.

Therefore, the main objective to ensure and improve permeability of the bed is to reduce the fine fraction in the bed particle. As noted at this point, this can be achieved by the pelletizing with the balling disc set to concentrate the pellets in the range -12.5 + 9 mm around 60-70 %, thus focused on the aim to reduce degradation and with lower incidence of crack.

3.4. Conclusions

The correct definition of a size distribution has a great impact on the process efficiency, the average diameter of the particle size and the size ratio of iron ore pellets have a prominent

influence in the whole chain of the pellet production until the client, being a key parameter to optimization for the whole process.

Size ratio between 0.6 and 0.7, where there is most of the size fraction -12.5 + 9 mm, leads to a cost-effective optimization of the physical pellet quality by improving tumbling index, lowering the risk of pellets degradation.

In a holistic process view, optimizing the metallurgical characteristics of the reduction reactors to accelerate the reduction rates and without compromising the yield metallic of the steelmaking.

3.5. References

Araujo, D. R., 2004, Desenvolvimento de um modelo computacional de otimização e predição do valor de uso de pelotas de minério de ferro na rota redução direta – aciaria elétrica. Rio de Janeiro: PUC, p. 204.

Daniel, D. R., 2013, Estudo Da Influência da Relação Granulométrica No Envelhecimento Da Pelota De Minério De Ferro, Vila Velha: UVV, p. 50p. ((TRABALHO DE FINAL DE CURSO DE ENGENHARIA METALÚRGICA E DE MATERIAIS)).

Dwarapudi, S., Devi, T. U., Rao, M. S., and Ranjan, M., 2008, "Influence of pellet size on quality and microstructure of iron ore pellets." ISIJ International, 48(6). pp. 768–776.

Fonseca, C.M, 2004, INFLUÊNCIA DA DISTRIBUIÇÃO GRANULOMÉTRICA DO PELLET FEED NO PROCESSO DE AGLOMERAÇÃO E NA QUALIDADE DA PELOTA DE MINÉRIO DE FERRO PARA REDUÇÃO DIRETA, Ouro Preto: REDEMATUFOP, p. 133. (Dissertação, Mestrado em Engenharia Metalúrgica).

Nunes, S. F., 2007, Influência da Carga Circulante do Pelotamento na Qualidade Física das Pelotas Crua e Queimadas da Samarco Mineração, Ouro Preto: REDEMAT-UFOP. Vol. 133. (Dissertação, Mestrado em Engenharia Metalúrgica).

Passos, L. A. S., Peres, A. E. C., and Moreira, J. L., MODELAMENTO DO ÍNDICE DE TAMBORAMENTO DE PELOTAS DE MINÉRIO DE FERRO PARA REDUÇÃO DIRETA*44o Seminário de Redução de Minério de Ferro e Matérias-primas, 15o Simpósio Brasileiro de Minério de Ferro e 2o Simpósio Brasileiro de Aglomeração de minério de Ferro, 15 a 18 setembro 2014, Belo Horizonte, MG, Brasil.

Pereira, R. O. S., and Seshadri, V., novembro 1985, "Secagem de pelotas de minério de ferro." Metalurgia – ABM, 41(328). pp. 141–144.

Szekely, J., Evans, J. W., and Sohn, H. Y., 1976, Gas-Solid Reactions. Londres: Academic Press, p. 400.

Werneck, H. M., 2010, Avaliação da influência do tamanho da pelota no tamboramento, Vila Velha: UVV. Vol. 57. (TRABALHO DE FINAL DE CURSO DE ENGENHARIA METALÚRGICA E DE MATERIAIS).

Capítulo 4. Artigo C - Iron Ore Pellet Drying Assisted by Microwave: A Kinetic Evaluation

Maycon Athayde, Mauricio Cota Fonseca, & Maurício Covcevich Bagatini

Artigo publicado em 17 de janeiro de 2018 na *Mineral Processing and Extractive Metallurgy* Review, *39(4), 266-275* https://doi.org/10.1080/08827508.2017.1423295

Abstract

Drying is a critical process step to achieve excellent pellet quality in pelletizing process. The complexity and energy consumption towards moisture removing, especially for highly hydrated iron ore, increased the need for breakthrough enhancements to this process. The present study has evaluated kinetics parameters of the moisture release from iron ore green pellet using energy transmitted through microwave (frequency of 2.45 GHz). The influence of pellet size and output power on the moisture effective diffusivity (Deff) and the drying activation energy (Ea) were evaluated. The results make possible to compare the cutting-edge approach with traditional convective drying. Pellet physical quality was investigated through the green crushing strength (GCS) which shows smooth reduction in earlier stages, however not affecting the final dry GCS results. Bonded hematite reduction and calcination of goethite was identified at the microstructure through reflected light microscopy, SEM showed micro cracks formation in several grains.

Key Words: Pelletization, Drying, Iron Ore, Microwave

4.1. Introduction

In recent years, increase the availability of fine iron ore concentrated with high iron content, moreover it has been developed a growing interest to produce pellets as burden charge towards production of primary iron. Despite of that, pellets needs to attend suitable mechanical properties to withstand transportation and avoid degradation during reduction in high shaft reactors, which became one of the major challenges for the mining industry. However, the pelletizing furnace operators has seen their productivity decreasing along the years, one of the reasons are the iron ore quality deterioration due to reserves depleting, concentrate is becoming finer and moist leading to restriction in the furnace drying zone, in operations where wet concentration is applied. Actually, the moisture removal must happen with diligent temperature control to prevent thermal spalling and in order to minimize condensation phenomena within the pellet bed, due the dew point at low temperature intermediate layer (Fan *et al.*, 2014; Thurbly *et al.*, 1980). Additionally, from the cost-efficiency point of view, drying can represents about 25% of the total amount of energy required for pellet induration (Patisson *et al.*, 1991). Even though, proper moisture content is a key parameter to guarantee cold cohesion of particles during the formation of the green pellet, this trade-off between right moisture content and restriction of moisture removal into the furnace is a challenge for the actual pelletizing technology.

The drying process for pellets is traditionally carried out by convective heat transfer, based on up- and downdraft hot air. This process has kinetic limitations which are intensified in ore with high level of mineral hydration (goethite/martite usually with higher level of microporosity, higher slimes content and moisture generated during concentration process to be released in the furnace) and even larger pellet size (Thurbly *et al.*, 1980; Patisson *et al.*, 1991; Ljung *et al.*, 2011). An alternative, in order to overcome this limitation in iron ore pellet drying is the use of microwave irradiation, which has been extensively studied in

mining and extractive metallurgy (Haque 1999). The dielectric heating is the interaction between the electro-magnetic field of microwaves with matter, where dipoles align and flip around, since an alternate field is applied and the internal energy convert in heat due to friction. Industrial electromagnetic frequencies are typically 915 and 2450 MHz (Haque, 1999; Menendez *et al.*, 2010).

The ability to absorb and convert the energy into heat is in fact an electrical material property (Menendez *et al.*, 2010). Sahoo *et al.* (2015) demonstrated that iron ore can warm up at 1.2 °C/s. The degree to which the iron ore will absorb microwaves depends on the real component of the complex permittivity (ε') and the imaginary component of the complex permittivity (ε"). The first measure the mineral ability to store electrical energy. The second represents the generation of heat. Besides ε' and ε", another parameter that is used to express how the microwave energy is dissipated is known as loss factor and defined by equation 1.

$$\tan\delta = \varepsilon''/\varepsilon' \quad (1)$$

Considering the constitution of a typical pellets, one can observe (Table 1) that moisture plays an important role as an absorber of microwave and convert into heat ($\tan\delta>0.1$). Despite of other carbon-based materials, coal is a poor absorber. Menedez et al (2010) attribute to an insufficient large graphene lattices not enough to allow delocalized π-electrons to move in order to couple with the electromagnetic field of the microwaves. Limestone is a transparent material for microwave. The hematite is the main constituent of the pellet and have good dielectric properties (He *et al.* 2016).

Table 1 – Loss Factor for pellet main constituents (2.45 GHz and 298 K)

Material	Tanδ	References
Water	0,118	Haque, 1999
Coal	0.02-0.08	Menendez *et al.*, 2010
Bentonite	0.01-0.05	Luan *et al.*, 2015
Magnetite	0.02 - 0.03	He et al, 2015
Hematite	0.01-0.02	Pickles et al, 2015
Limestone	0.0012-0.0021	He et al, 2015

Pellet drying can be optimized by dielectric heating as it is not limited by heating conduction throughout the material like the convective process, which should affect the release of moisture. This effect can be represented by, the effective diffusivity of moisture, Deff, which comprehend several mechanisms such as molecular diffusion, capillary flow, Knudsen flow, hydrodynamic flow and surface diffusion, (Ljung *et al.*, 2011). For conventional drying, Ljung *et al.*, measured to iron ore pellets Deff to 3.3×10^{-8} m^2/s (150 ºC and 1.7 m/s) and pellet drying simulation was carried out adopting the equation 2 (Menezes *et al.*, (2010)) showing the dependence with hot gas properties and the void fraction within the pellet.

$$D_{eff} = \frac{1.18.10^{-9} T_g^{1.75}}{P} . \varepsilon^{1.41} \quad (2)$$

Where P is the pressure (atm), Tg is the gas temperature (K) and ε is the pellet porosity. This paper presents an experimental investigation of iron ore pellets drying assisted by microwave power for different pellet sizes. The drying out capacity of green pellets was investigated and operational parameters were assessed. A comparison with convective drying was established and the productivity of both process compared.

4.2. Experimental

Pilot plant iron ore pellets were tested at microwave oven to evaluate drying out time, drying rates and mechanical strength. The techniques and theoretical approach for drying will be explained.

4.2.1. Green Pellet Preparation

Iron ore concentrate (Mariana mining complex - Brazil) was prepared from run of mine (ROM) in pilot scale concentrator by mechanical flotation and ball milling (Table 2). Other raw material for the pelletizing mixture was Brazilians bentonite and limestone and South African anthracite coal. Limestone was added to achieve a binary basicity of 0.8 and anthracite added to achieve 1 %C. The final moisture content was 10 % added at a pilot Erich mixer.

Table 2 - Chemical Characterization of the Iron ore for the test work.

FeT (%)	FeO (%)	SiO_2 (%)	Al_2O_3 (%)	CaO (%)	MgO (%)	P (%)	Mn (%)	LOI	EW
65.95	1.62	1.59	0.32	0.02	0.02	0.046	0.083	3.65	4.798

Green pellets were produced in a pilot scale pelletizing disc Dravo - Lurgi model W-3511-1. (Inner diameter 100 cm and total depth 20 cm), rotation of 15 rpm and 45° with horizontal. The mixture feed rate was kept constant at 630 kg/h. The pellets produced at the size ranges, namely: + 9.0-12.5 mm, + 12.5 -14.0 mm and + 14.0- 16.0 mm.

The pellet generated in the disc was hand sieved to generated green pellet for the test. Three average pellet diameters were obtained after careful sieving not to break the pellets: 10.75

mm (+9.0-12.5 mm), 13.50 mm (+12.5 mm -14.0 mm), 15.25 mm (14.0-16.0 mm). The pellets have presented a highly homogeneous size distribution within the fraction (Fig. 1).

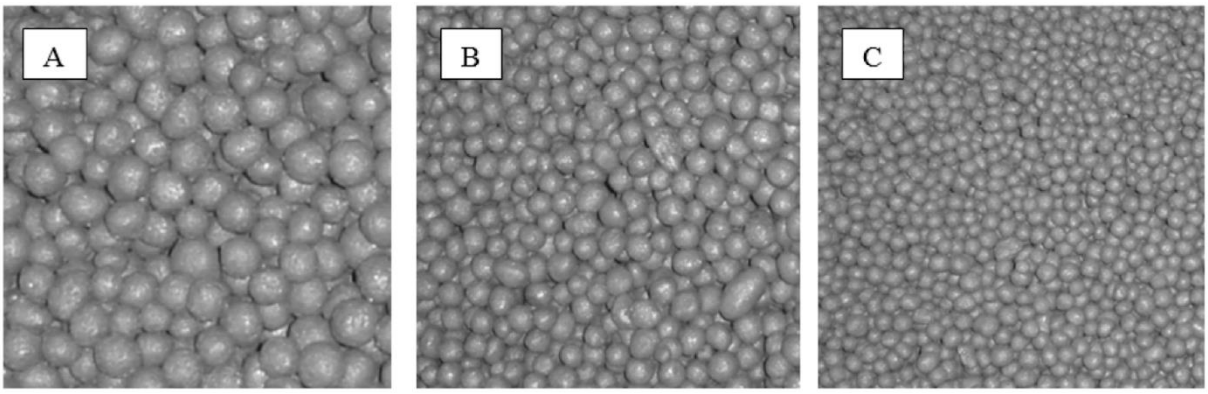

Fig. 1 - Green Pellets from the standard concentrate sized: (a) +14.0-16.0 mm, (b)+12.5mm-14.0mm and (c) +9.0-12.5 mm.

4.2.2. Microwave Drying Technique

The green pellets (100 g) were irradiated for 180 seconds at intervals of 30 seconds, in a turntable-tray microwave oven model LG MH7048G (2.45 GHz, maximum power of 1000 W) adapted with additional exhaust system (1 L/min) to standardize the steam withdrawal with a Teflon high-temperature resistant plate (Fig. 2). At the end of each time step, average surface temperature was measure by pyrometer. To determine the initial moisture content, sample of 100 g were dried in an oven at 105 °C for 8 hrs. The power setting was selected from 300, 600 and 1000 W, adjusting the controlling of the microwave oven.

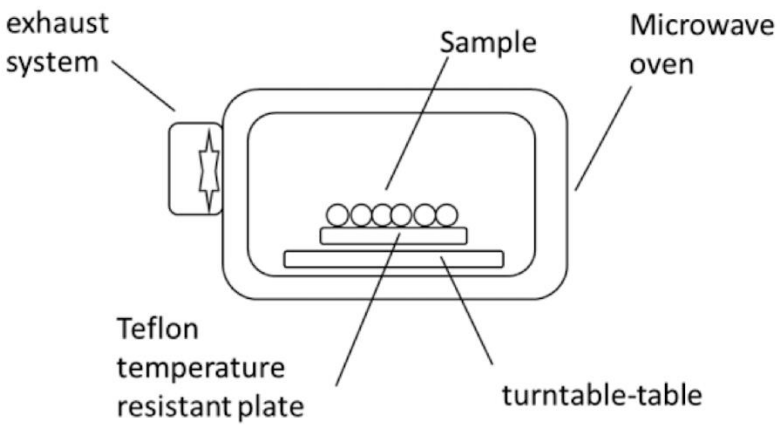

Fig. 2 – Scheme of the drying furnace.

For each step, three tests repetitions were carried out with 100 g of green pellets, in a single layer spread over a Teflon plate. Then residual moisture was recorded every 30 s (with 100 g of fresh green pellets) after switching off the microwave. The data reported from each time interval is an average of these three repetitions. The reproducibility of the experiments was within the range of ±5%. Moisture determination procedure was completed in less than 10s during the drying process.

Due to the Teflon restriction, the microwave irradiation was applied until the sample temperature was less than 500 ºC (measured by pyrometer).

4.2.3. Pellet Microstructure and Mechanical Strength Evaluation

Evaluation of possible microstructural modifications was conducted using the reflected optical microscope Zeiss model 65 Imager.M2m coupled with a digital camera. A Scanning electron microscope (SEM) JEOL –JSM 35C Model was also used.

The pellet quality was accessed to evaluate the effect of the drying, after pellet irradiation with microwave, through the green crushing strength (GCS). This was performed in a group of 10 pellets, placing a single pellet at the center of the plate of the testing machine. Load at

a speed of 10 mm/minute was applied on the pellet for compression to record the maximum load (kgf/pellet) at the pellet undergoes, then the arithmetic average value was noted.

4.3. Theoretical Approach for the Drying Kinetics

In order to standardize the effect of microwave power on drying as a function of drying time, the weight loss was converted to the moisture ratio (MR) (Eq. 2).

$$MR = \frac{M_t - M_e}{M_o - M_e} \quad (2)$$

Where, Mt is the moisture content at a specific time, Mo is the initial moisture content, Me is the equilibrium moisture content (in the case of unsaturated air is zero). Several authors (Barati *et al.*, 2008; Patisson, 1991; Umadevi *et al.*, 2010) use an assumption that diffusivity based on Fick's diffusion equation can be a single physical mechanism to transfer the moisture to surface of several materials. To iron ore pellets heated by microwave power the effective moisture diffusivity (D_{eff}), which is affected by composition, moisture content, temperature and porosity of the raw materials, could be assumed by the same mechanism, because the heat conduction within the pellet is not a limiting step due to the characteristic volumetric heating attributed to the microwave (Miranda and Silva, 2006). In the case of a sphere, equation 3 is the analytical solution for the Fick's law and the effective moisture diffusivity can be obtained (Dadali *et al.*, 2007; Crank, 1975). The D_{eff} is defined by the sum of infinite terms of the equation, although 100 terms show sufficient accuracy (deviation less than 10^{-5}).

$$MR = \frac{6}{\pi^2}\sum_{n=1}^{\infty}\frac{1}{n^2}exp\left[\frac{-n^2\pi^2 D_{eff}}{r^2}t\right] \quad (3)$$

Where MR is the moisture ratio, n is the term, D_{eff} is the effective moisture diffusivity (m^2/s), r is the average pellet radius and t is the drying time (s). As a thermal-activated process, the drying activation energy (E_a) can be also assessed based on the Arrhenius equation (Equation 4).

$$D_{eff} = D_0 \exp(\frac{-E_a}{RT}) \quad (4)$$

Microwave drying studies (Menendez *et al.*, 2010; Kingman *et al.*, 2004; Rayaguru *et al.*, 2011) have considered a modified approach proposed by Dadali *et al.*, using microwave output power density instead of the temperature, in order to show the dependency of the microwave power with the moisture ratio (MR).

$$D_{eff} = D_0 \exp(\frac{-E_a m}{P}) \quad (5)$$

Where D_{eff} is effective diffusivity (m^2/s), D_0 is the pre-exponential factor (m^2/s), E_a is the activation energy (W/g and kJ/mol), P is microwave output power (W) and m is the mass of raw sample (g).

4.4. Results and Discussion

4.4.1. Effect of the Microwave Power on the Pellets Drying

The pellet sample submitted to the irradiation shows sensible behavior to the microwave power level (Fig. 3). Higher power density (10 W/g) reached to fully release the moisture in

less than 150 s for all pellet size, faster than any reported drying study investigated. Against convective drying, the smaller pellet size shows substantial slower dry out time. This presents an important practical effect of the dielectric drying, most likely because of high relation area/volume (which is proportional to one third of radius, in sphere cases). Microwaves requires matter to be absorbed and then convert it into heat subsequently, heating may be slower than the losses of heat per pellet unit in earlier moments of drying, conventionally highly dependent of the pellet size (Pereira and Seshadri 1985; Tsukerman *et al.* 2007).

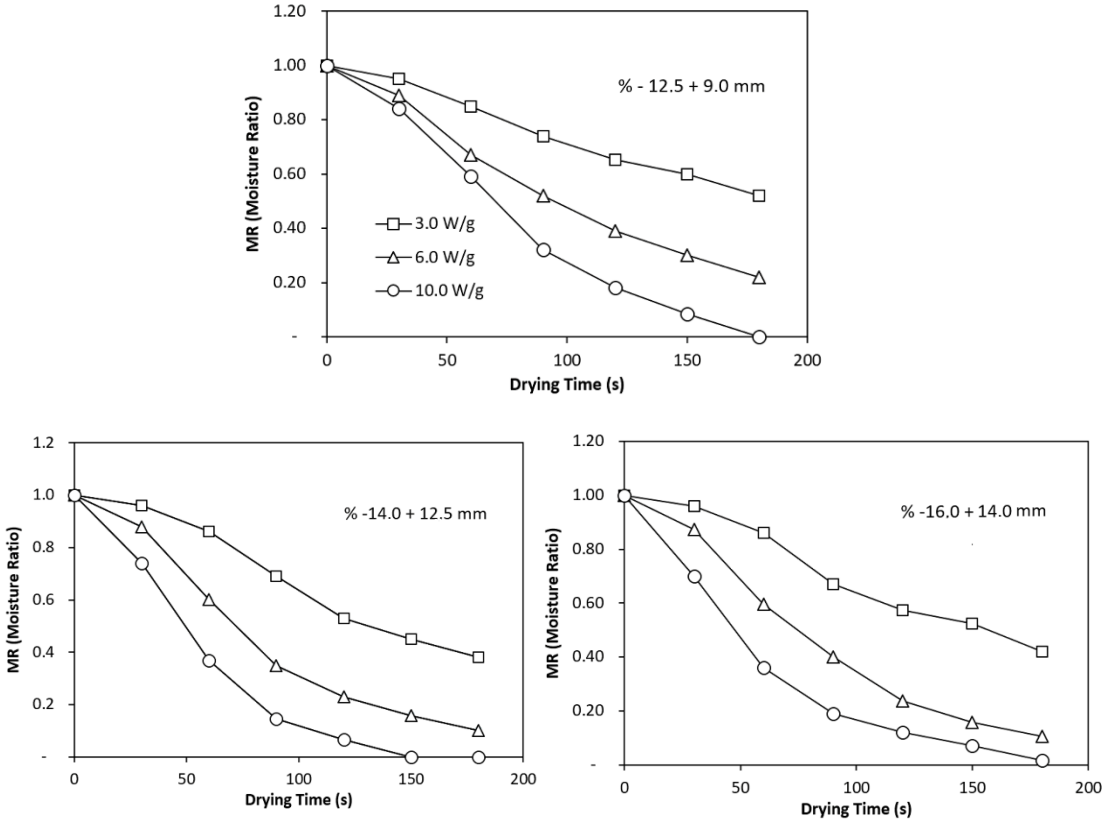

Fig. 3 – Effect of microwave power on moisture ratio versus time, at different conditions of pellet size and power density.

Initially, the green pellet is saturated, moisture is distributed throughout the pores (funicular state), higher absorption of microwave power is expected. As the drying progress, moisture reduction in the bulk decreases the absorption of microwave and lead to falling in the drying rate.

4.4.2. Drying Mechanism

Convective pellet drying of iron ore green pellets has been intensively investigated and it is represented by multi-stages model. Nevertheless, the present study focus on the impact on drying out and dry pellet quality resultant from a use of microwave for further industrial application. Drying rate curves, presented at Fig.4, shows that an initial stage is responsible for 20-40 % of the drying time. This induction period is normally attributed to the increase of the surface temperature, increasing the saturation of the gas in vapor. The stage ends at a critical moisture level of MR=0,39, initiating a falling rate period, related to small amount of moisture diffusing to the outer shell. Apparently a second falling rate period is also formed. It may be assumed that the surface dried and a plane of separation has moved into the pellet, due to the high initial heating rate at the surface specially at high power density. In this case, the final rate of drying is controlled by the vapor diffusion, and related most to internal tortuosity and porosity than outside conditions (as suggested by eq. 1), initiate at MR=0.19, independently of the pellet size.

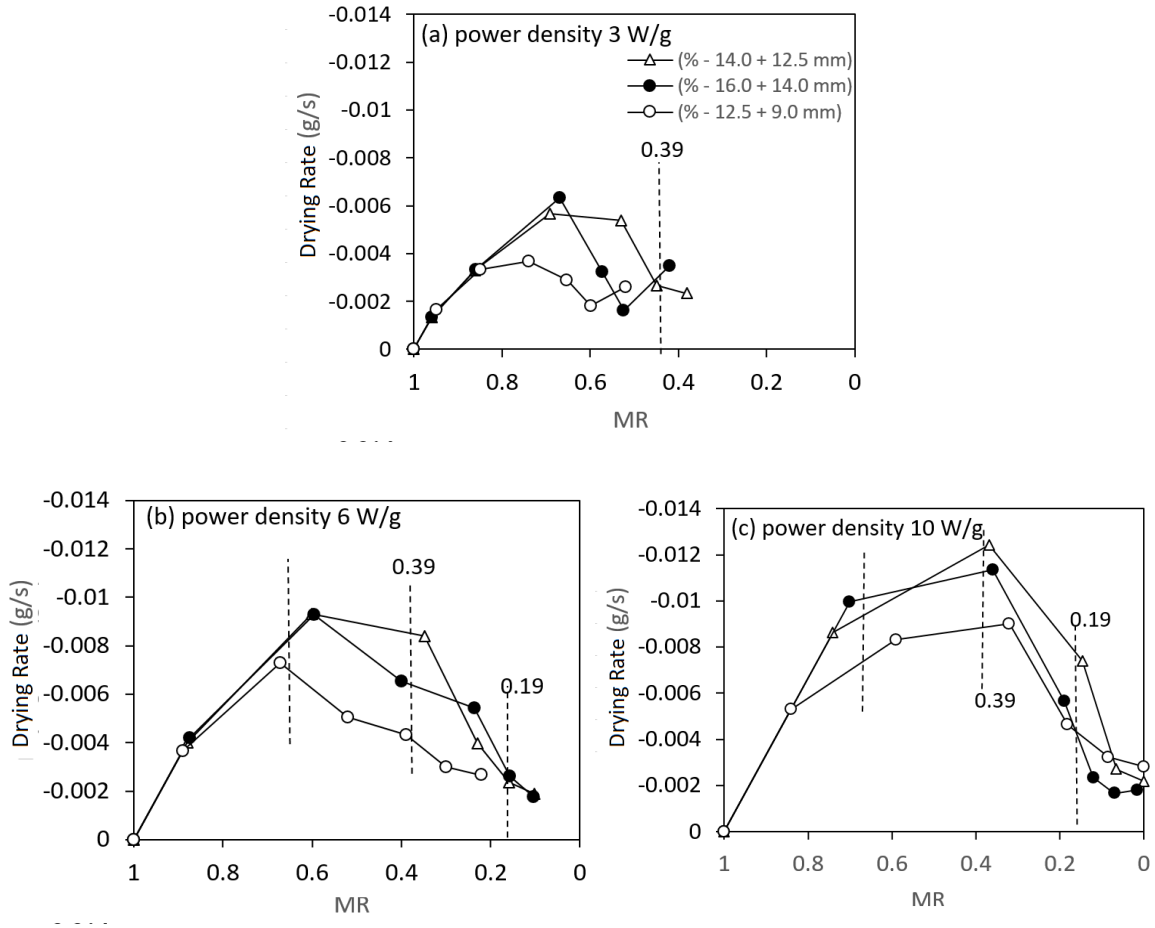

Fig 4 – Drying Rates Curves versus MR, at different conditions of pellet size and power density.

Lower initial drying rates were observed (closer than convective drying), consuming energy as the wave moves into the solid heating the whole particle. Pellet surface temperature increases together with the pellet core, in a different mechanism than convective drying. A constant drying rate period was not observed, as observed in convective drying studies at low heating rate (Pereira and Seshadri 1985). The heated core ease vapor diffusion to the outer shell, increasing the drying rates. Falling rate period happens along with minimum moisture content, also likely because of lowered dielectric properties, which is directly proportional to the moisture content. This mechanism observed is summarized at Fig 5.

Despite of the constant temperature of convective drying, the dry pellet keeps warming up at least 1 °C/s (Sahoo *et al.*, (2015)).

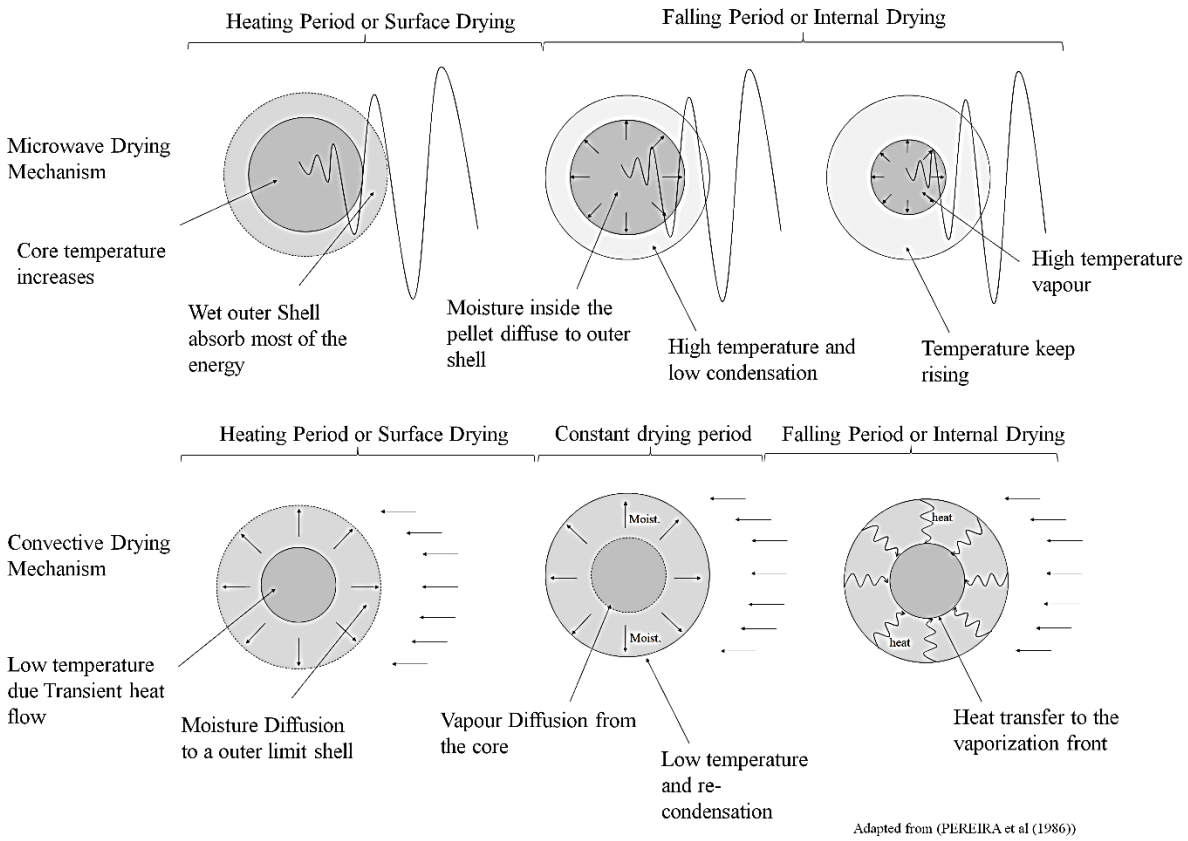

Fig 5 – Comparison between the mechanisms of drying via Microwave heating and Convective.

The interaction microwave power density and pellet diameter on drying rate was investigated with a model built based on the variables with 5 % confidence level. The ANOVA results and coefficient values were reported in appendix 1 and Fig 6. Higher value of R^2 and Adjusted R^2 indicates a high dependency and correlation between the observed and the predicted values. However, no significant difference (p-value > 0.05) of drying rates (assumed at 50 s) for different pellet size levels, expected because of the ease access of the wave through the mass. Conversely, the power density shows major influence on the kinetic rates as demonstrated in Fig 6.

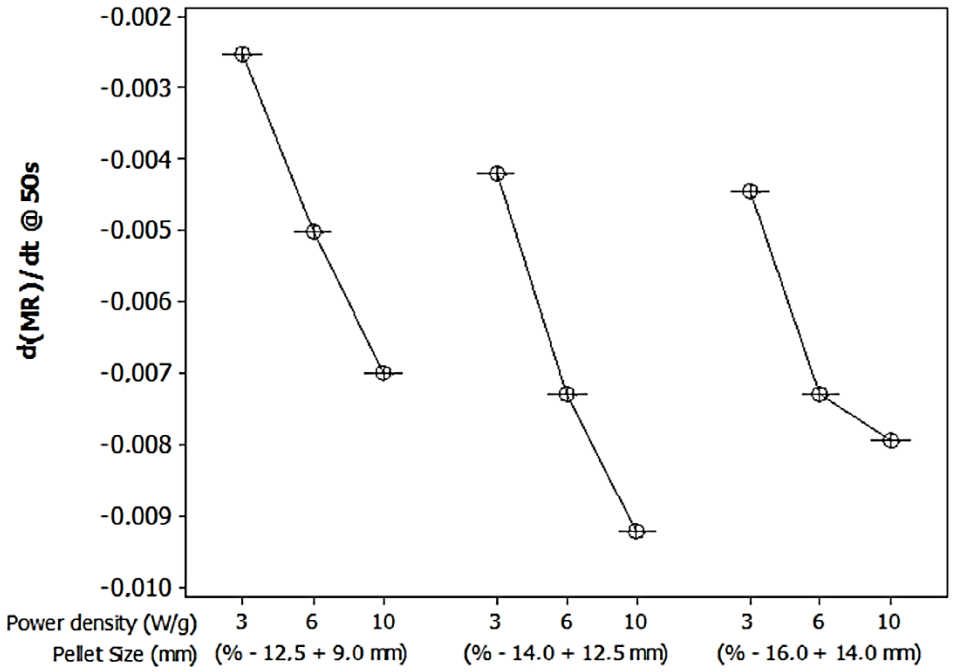

Fig 6– Influence of the power density and pellet size on the drying rate at 50s.

4.4.3. Maximum Drying Rates

Fig. 7 shows maximum drying rate as a function of power density and pellet average diameter. It can be seen that drying rate linear increases with power density, but intermediate pellet diameter achieved higher drying rates (most likely no relationship). This power density behavior is expected since the vapor pressure exerted by liquid water rises with increasing temperature. Also, capillarity is improved due to the decreasing surface tension of water as the temperature increases with the power density.

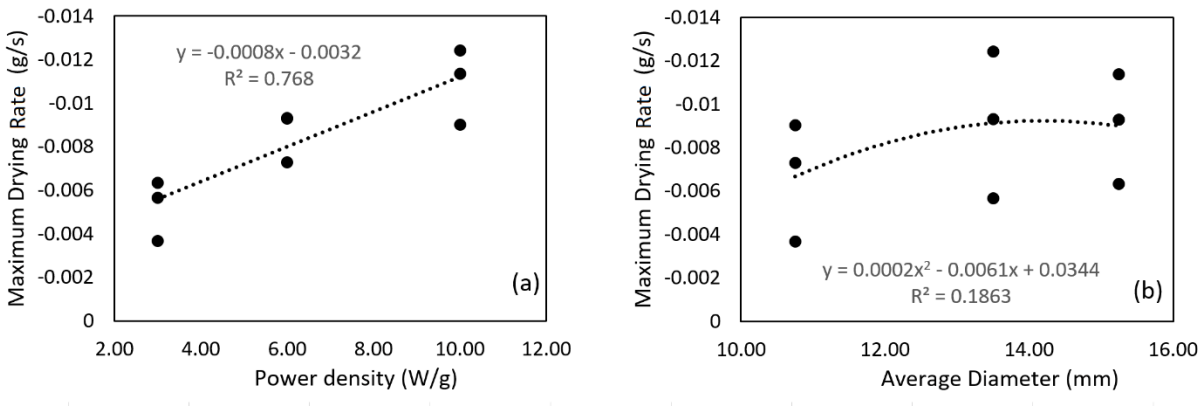

Fig 7 - Maximum drying rate as a function of (a) power density (b) average diameter.

Moisture Diffusivity and Activation Energy

The variation in D_{eff} with moisture ratio is a complex and system specific function. Although, the literature is scarce in values for effective moisture diffusivity for pellet drying, various research workers (Dak *et al.*, 2012; Dadali *et al.*, 2007; Rayaguru *et al.*, 2011) have carried out evaluation with organic materials. In Fig. 8, Deff is calculated based on Eq 3. To the green pellet, shows an exponential decrease with temperature achieved to all conditions experimented. Differently of organic material, porous structure became tighter and worse as the steam flow goes outside of the pellet. At higher temperature, D_{eff} is reported to pellet convective drying by Ljung *et al.*, but with an inverse relation to the temperature and a hundred times greater than the observed in several organic materials experimented in the literature (Montevali *et al.*, 2011). Miranda *et al.* describe the curve shape of Fig. 8 as small presence of moisture in microspores as in alumina, compared with material such as kaolin and silica.

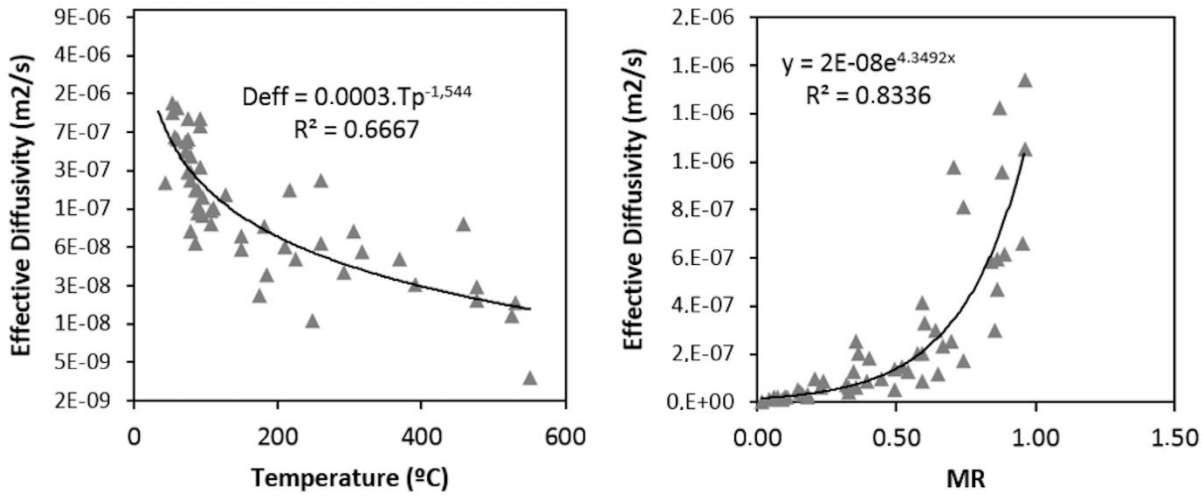

Fig.8 – Evolution of Effective Diffusivity with (a) the temperature and (b) MR.

Activation energy for the drying process at the three size ranges was calculated based on the Arrhenius equation (power density). The three pellet diameter presented similar curve inclination which shows a low dependence of the activation energy with the size (Fig.9), also this is highlight the effectiveness of the microwave to dry compared to the convective process.

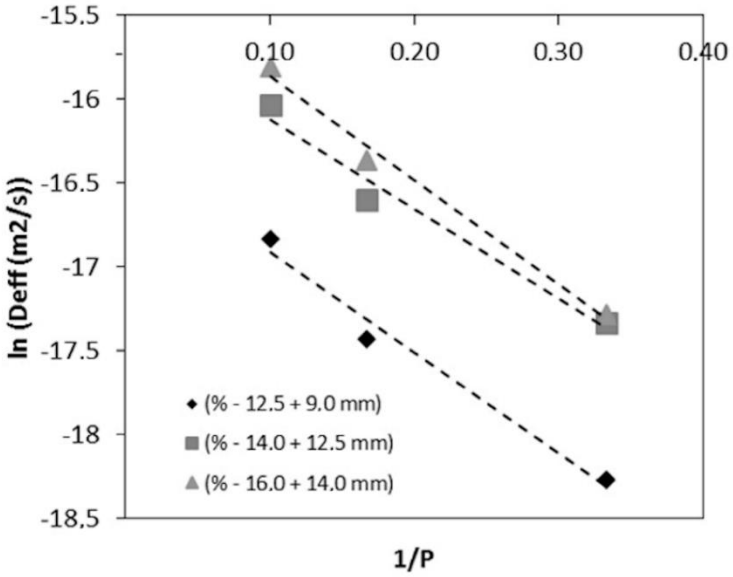

Fig. 9 – Variation of Activation Energy with the pellet diameter.

Literature testwork with single green pellet (Thurbly *et al.*, 1980; Pereira and Seshadri 1985) using convective drying can be applied to compare the drying efficiency, with the process presented in this paper (Fig. 10). The drying tests reported by Thurbly *et al.* (1980) are similar compared with Seshadri *et al.* (1985). The microwave shows an accelerated process, where moisture content is reduced by half more than three times faster the literature results.

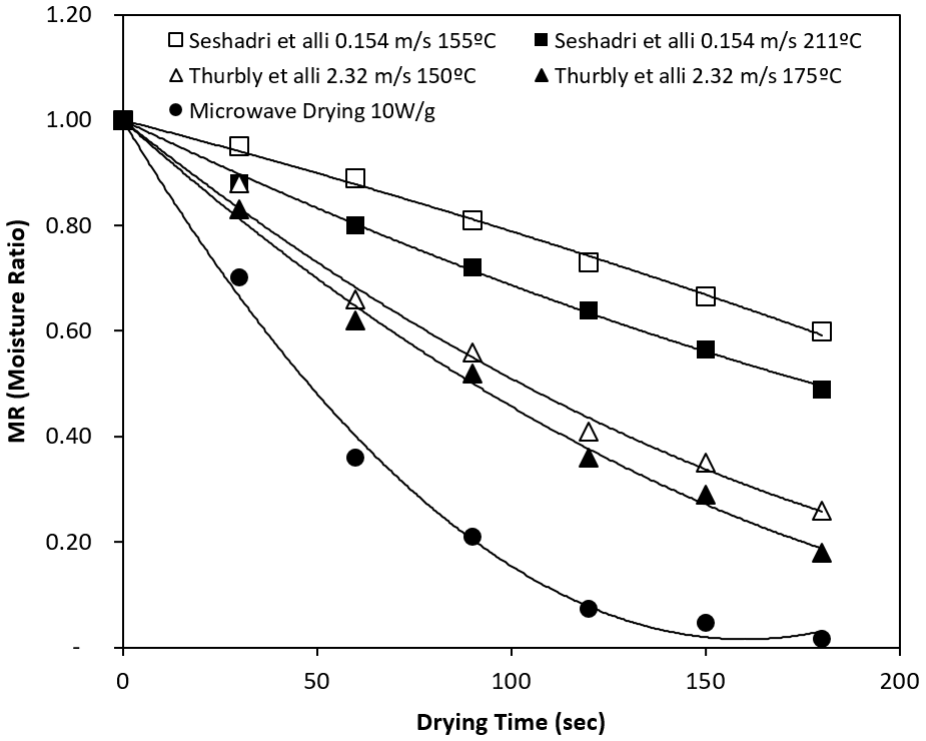

Fig. 10 – Several convective drying conditions compared with the dielectric drying curve at 10 W/g.

Kinetics parameters were calculated from the drying rate curves. The results demonstrated that green pellet dried assisted by microwave shows an intermediate Deff value compared with calculated from literature (Table 3). The drying via dielectric heating presented a lower level of energy to initiate the process, which was estimated at almost twice lower than the convective drying. It can be explained by the homogeneous, volumetric and faster heating of the pellet immerse into the electro-magnetic field, reducing steam condensation inside the

pellet, due to dew point. Another contribution is the heated core of the pellet, which may reduce drag force against the steam flow.

Table 3 – Comparison of convective and dielectric heating on drying kinetics parameters

Author	Pereira et al	Pereira et al	Thurlby et al	Thurlby et al	Dielectric Heating
Air speed (m/s)	0.154	0.154	2.32	2.32	0.0
Power density (W/g)	16	19	232	256	10
Temperature (ºC)	155	211	150	175	*
D_{eff} (m2/s) x 10^{-8}	2.95	3.92	15.1	18.4	9.8
E_a (kJ/mol)	8,8		12,8		5.8

4.4.4. Effect of Drying on the Pellet Quality

Conventional drying process, in general, influences the quality of the pellets, based on that the pellet quality were assessed via GCS. In Fig.11, green crushing strength (GCS) behaves differently with the intensity of irradiation. The larger pellet size ranges +14-16 mm and +12.5-14.0 mm have had a strength reduction in early stages of the drying. On the other hand, the smaller pellet size range +9-12.5 mm kept almost the same GCS until 100 s, where a steeply increase on the GCS was observed specially for density power of 6 W/g and 10 W/g, at this last one achieving 2.5 Kgf/pellet.

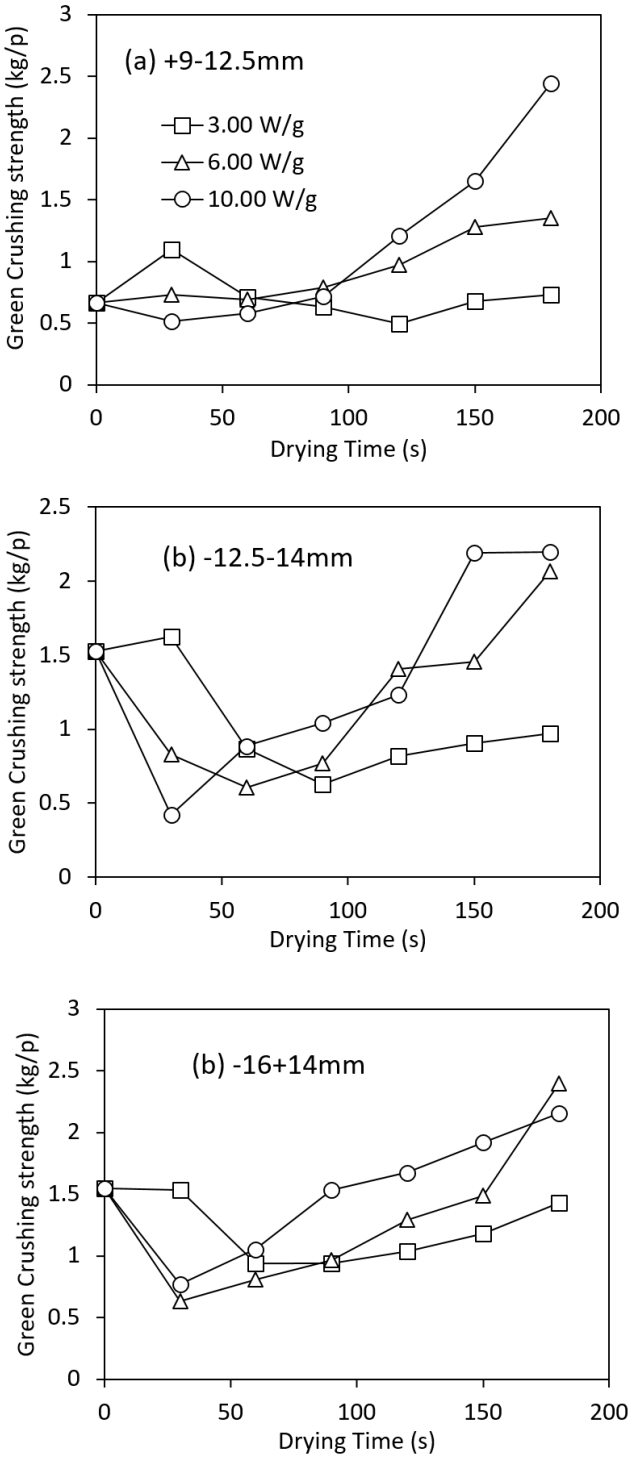

Fig. 11 – Evolution of green crushing strength (GCS) during the drying assisted by microwave.

Although the GCS presented are likely sufficient for most industrial operations and in good agreement with reported by other authors (Umadevi *et al.*, 2010), it is below the average results obtained after standard experiment for GCS of dried pellets where they were gently dried in an oven at 105 ºC/2h (5.2±0.5 Kgf/pellet). The lower values seem to be due to the generation of micro-cracks on the hematite and goethite mineral even before the calcination of the mineral, such cracks appear either in the center or in the mantle of the pellet, as SEM analyses demonstrated (Fig 12). Some authors have already investigated the mineral cracking due to the microwave power in several different minerals and they attribute that to differences in heating rate and linear expansion among different minerals (Kumar *et al.*, 2010; Kingman *et al.*, 2004). This phenomenon has been appointed as positive on the reduction of energy in mineral milling (Kumar *et al.*, 2010; Haque 1999), but it results in a worsening in the properties of dried pellet that likely will need to be enhanced during the firing process. Optical microscopy of the pellets shows that the gangue minerals (silica and carbonates) responsible for the slag bonding mechanism have not reacted yet (Fig. 10A). The test was conducted at temperatures lower than 500 °C but goethite has initiated the de-hydroxylation and hematite reduction to magnetite showing locally heat generation (Fig. 10). The goethite to hematite transformation takes place at a temperature above 250-300 °C (Maqueda et al, 1999, Pickles et al 2005), however, hematite to magnetite originate higher temperature spots within the pellet, one called the phenomenon of thermal runaway (Pickles, 2004), hard to detect with the optical pyrometer used in the study. Pickles et al (2005) explain the increase in the real permittivity due to the movement of ions during the de-hydroxylation process.

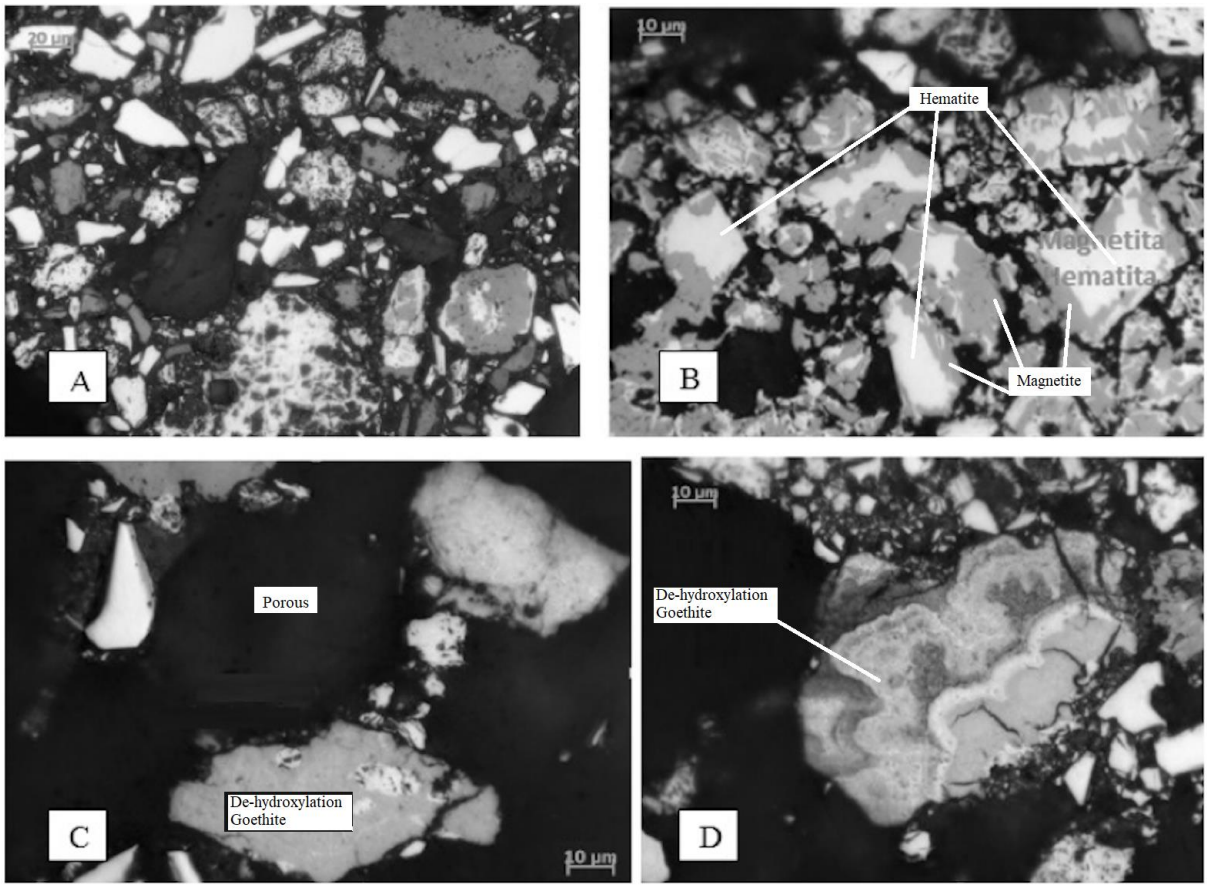

Fig 12. (a) Green pellet microstructure at 100s drying time (10 W/g), no slag has been formed. (b) Topo chemical transformation of hematite in Magnetite (c) De-hydroxylation of the earthy goethite mineral (d) De-hydroxylation of the earthy goethite mineral.

Additionally, the partially reduced particles indicate that coal particle coating hematite grains have burned, although larger coal particles unchanged was identified on the SEM images (darkest particles in Fig. 13D), which may lead to a thermos-decomposition of the hematite. These events normally are not seen in convective drying because the temperature of the process does not exceed 250 ºC.

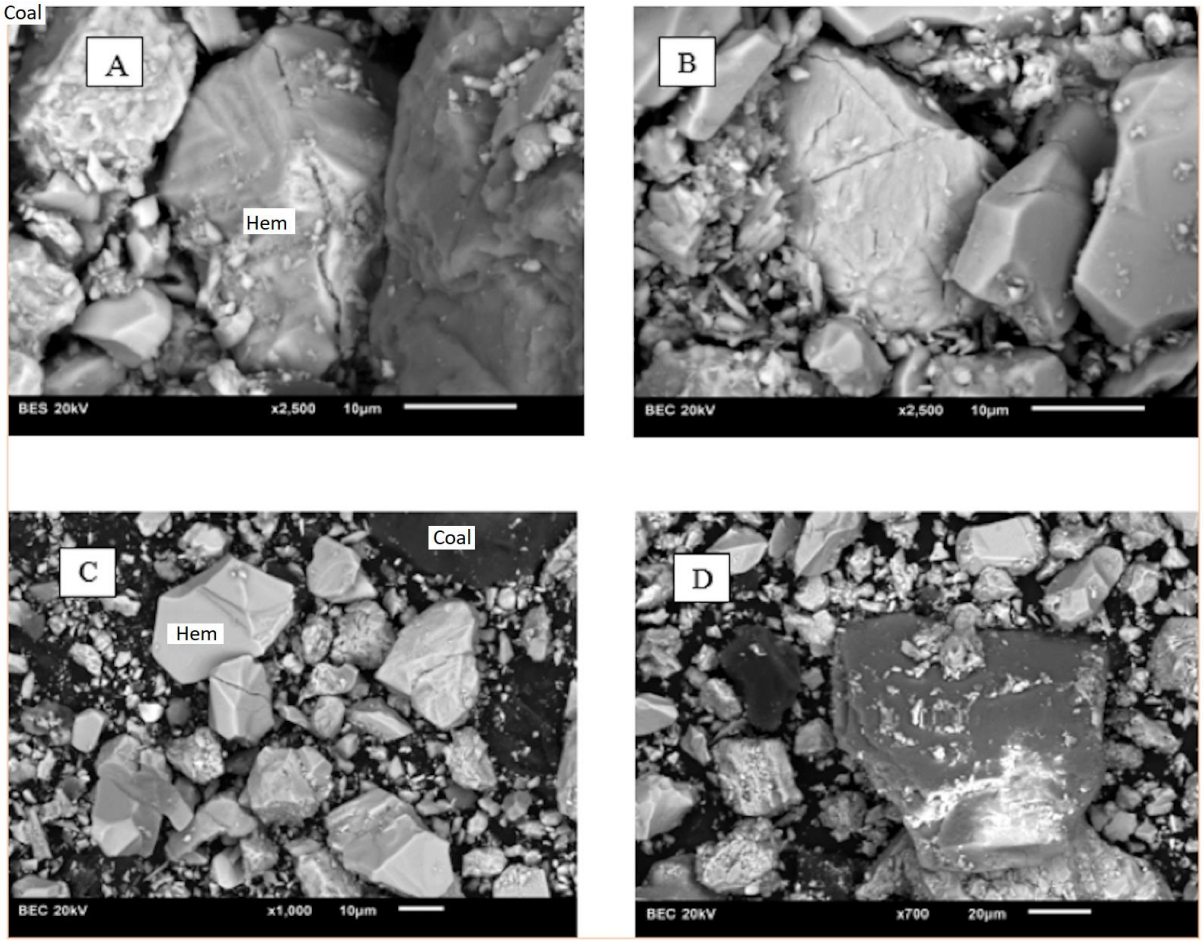

Fig. 13 - Green pellet microstructure at 100 s drying time (10 W/g), SEM image showing hematite and Martite with longitudinal cracks.

4.5. Industrial Relevance of the Microwave Drying

In pelletizing operation, moisture removal need to happen prior to the pre-heating zone, to avoid spalling and guarantee energy saving. Earlier release of moisture has linear relation on productivity, as the time save could be converted in machine speed. Based on the data presented at Fig 8, moisture reached safe residual at 100 s (10 W/g). It represents a process debottlenecking, which going to depend of the furnace operation.

4.6. Conclusions

The iron ore pellet drying assisted by microwave was evaluated to be a potential technique to increase the productivity of drying. The main conclusions obtained are as follow:

- The effect of microwave power output and pellet size on the drying rates were compared and show only the first has significant impact on the drying rates.
- Drying rates by microwaves shows an intense heating stage previously to a falling period, expected due to the reduction of moisture at the pellet core.
- Micro cracks generation was observed mainly in hematite grains, which can contribute to reduce cold crushing strength in early drying process.
- Effective moisture diffusivity was assessed and values ranged from $1.7x10^{-7}$ (at 100 ºC) up to $3.6x10^{-9}$ (550 ºC) showing an exponential decrease with temperature. The drying activation energy shows values of 5.8 KJ/mol are almost twice lower than the energy involved in convective process.
- Further study might be carried out to understand the hardening behavior after drying and the individual influence of the mineral phases on the crack generation, along with other mineral such as magnetite for which the oxidation is also relevant. Additionally, further studies shall be done to evaluate the energy efficiency of the process and influence of raw materials quality such as binders or flux.

4.7. References

M. Barati, Dynamic simulation of pellet induration in straight-grate system, Int J Miner Process, 89 (2008), pp. 30-39

Crank, J., The mathematics of diffusion. Oxford University Press, U.K., 1975.

Dadalı, G.C.B.C.A., Apar, D.K., and Özbek, B., 2007. Microwave Drying Kinetics of Okra. Drying Technology, 25 (5), 917–924.

Dak, M. and Pareek, N., 2014. Effective moisture diffusivity of pomegranate arils under going microwave-vacuum drying. Journal of Food Engineering, 122, 117–121.

Fan, X., Yang, G., Chen, X., He, X., Huang, X., & Gao, L. (2014). Effect of carboxymethyl cellulose on the drying dynamics and thermal cracking performance of iron ore green pellets. Powder Technology, 267, 11-17. doi:10.1016/j.powtec.2014.07.011

K.E. Haque; "Microwave energy for mineral treatment processes – a brief review"; Int. J.Miner. Process, 57 1-24 (1999).

He, C. L., Ma, S. J., Su, X. J., Mo, Q. H., & Yang, J. L. (2016). Comparison of the Microwave Absorption Characteristics of Hematite, Magnetite and Pyrite. Journal of Microwave Power and Electromagnetic Energy, 49(3), 131-146. doi:10.1080/08327823.2015.11689903

Kingman, S., Jackson, K., Bradshaw, S., Rowson, N., & Greenwood, R. (2004). An investigation into the influence of microwave treatment on mineral ore comminution. Powder Technology, 146(3), 176-184. doi:10.1016/j.powtec.2004.08.006

Kumar, P., Sahoo, B., De, S., Kar, D., Chakraborty, S., & Meikap, B. (2010). Iron ore grindability improvement by microwave pre-treatment. Journal of Industrial and Engineering Chemistry, 16(5), 805-812. doi:10.1016/j.jiec.2010.05.

Ljung, A., Lundström, T. S., Marjavaara, B. D., & Tano, K. (2011). Convective drying of an individual iron ore pellet – Analysis with CFD. International Journal of Heat and Mass Transfer, 54(17-18), 3882-3890. doi:10.1016/j.ijheatmasstransfer.2011.04.040

Menéndez, J., Arenillas, A., Fidalgo, B., Fernández, Y., Zubizarreta, L., Calvo, E., & Bermúdez, J. (2010). Microwave heating processes involving carbon materials. Fuel Processing Technology, 91(1), 1-8. doi:10.1016/j.fuproc.2009.08.021

M.n.n., M., & Silva, M. (2006). Moisture Effective Diffusivity in Porous Media with Different Physical Properties. Defect and Diffusion Forum Diffusion in Solids and Liquids, 207-212. doi:10.4028/3-908451-36-1.207

Motevali, A., Minaei, S., & Khoshtagaza, M. H. (2011). Evaluation of energy consumption in different drying methods. Energy Conversion and Management, 52(2), 1192-1199. doi:10.1016/j.enconman.2010.09.014

Patisson, F., Bellot, J. P., Ablitzer, D., Marlière, E., Dulcy, C., and Steiler,. J. M., (1991), Mathematical-modeling of iron-ore sintering process. Ironmaking and Steelmaking, 18, pp. 89–95.

Pérez-Maqueda, L. A., Criado, J. M., Real, C., Šubrt, J., & Boháček, J. (1999). The use of constant rate thermal analysis (CRTA) for controlling the texture of hematite obtained from the thermal decomposition of goethite. Journal of Materials Chemistry, 9(8), 1839-1846. doi:10.1039/a901098j Pereira, R. O. S, Seshadri, (1985) V., Secagem de Pelotas de Minerio de Ferro, Metalurgia – ABM, V.41, n.328, p.141-144.

Pickles, C., Mouris, J., & Hutcheon, R. (2005). High-Temperature Dielectric Properties of Goethite From 400 to 3000 MHz. Journal of Materials Research, 20(01), 18-29. doi:10.1557/jmr.2005.0012

Pickles, C. (2004). Microwave heating behaviour of nickeliferous limonitic laterite ores. Minerals Engineering, 17(6), 775-784. doi:10.1016/s0892-6875(04)00021-4

Rayaguru, K., & Routray, W. (2010). Effect of drying conditions on drying kinetics and quality of aromatic Pandanus amaryllifolius leaves. Journal of Food Science and Technology, 47(6), 668-673. doi:10.1007/s13197-010-0114-1

Sahoo, B., De, S., & Meikap, B. (2015). An investigation into the influence of microwave energy on iron ore–water slurry rheology. Journal of Industrial and Engineering Chemistry, 25, 122-130. doi:10.1016/j.jiec.2014.10.022

Tsukerman, T., Duchesne, C., & Hodouin, D. (2007). On the drying rates of individual iron oxide pellets. International Journal of Mineral Processing, 83(3-4), 99-115. doi:10.1016/j.minpro.2007.06.004

Thurlby, J.A., and Batterham, R.J. (1980) Measurement and prediction of drying rates and spelling behaviour of hematite pellets. lnst. Min. Metall., Trans, Sect. C, 89 , C125-C131.

Umadevi, T., Kumar, P., Lobo, N. F., Prabhu, M., Mahapatra, P., & Ranjan, M. (2011). Influence of Pellet Basicity (CaO/SiO_2) on Iron Ore Pellet Properties and Microstructure. ISIJ International, 51(1), 14-20. doi:10.2355/isijinternational.51.14

Appendix

Table 5 – Summary ANOVA for average effective moisture diffusivity.

Source	DF	SS	MS	F	P	Significance
Pellet size (mm)	2	7E-06	0.0000037	16.76	0.011	Non Significant
Power density (W/g)	2	3E-05	0.0000144	65.96	0.001	Significant
Error	4	9E-07	0.0000002			
Total	8	4E-05				
S = 0.0004680			R-Sq = 97.64%	R-Sq(adj) = 95.28%		

Capítulo 5. Artigo D - Novel Drying Process Assisted by Microwave to Iron Ore Pelletizing

Maycon Athayde and Maurício Covcevich Bagatini

Artigo aceito para publicação em 17 de julho de 2018 na revista Material Research 2018; 21(5) DOI: http://dx.doi.org/10.1590/1980-5373-MR-2018-0170

Abstract

Drying has become critical to iron ore pellet production, due to increasing inability to withdrawal moisture from the green pellets, especially faced by Goethitic iron ore producers. Existing pelletizing furnaces do not support increase more heating rates nor changes in furnaces length, without compromise pellet quality. The present study evaluates an innovative alternative for the actual fully convective drying process composed by an up-draught drying (UDD) and down-draught drying stage (DDD), through the application of microwave energy to assist the existing process. In the present work, the process was simulated in a pot grate where industrial parameters can be simulated. The microwave generator (power input of 10 MW and 915 MHz) was connected in a traditional static pot grate at the hood by a microwave conductor. The experiments show elimination of the over-wet zone at the upper layer of pellet observed at the traditional process. A reduction greater than 7 % of the moisture in UDD was achieved, while the convective process adds extra moist to the green pellets modifying the pellet shape.

Keywords: Drying, Microwave, Travelling Grate, Pellet

5.1. Introduction

Pelletizing has great importance in iron ore mining, ensuring optimal use of mineral reserves and increases the overall blast furnace efficiency. In general, the process involves two main steps, firstly the balling, where green pellets are formed with the addition of a binder to enhance agglomeration, induced by water and capillary forces formed within the iron ore grains (Forsmo *et al.*, 2008). Secondly, the pellets are treated in induration furnace to attain mechanical resistance and appropriate metallurgical characteristics required by the ironmaking facilities (Meyer, 1980).

The travelling grate furnace, where the induration process is carried out, is typically divided into 4 zones: drying, pre-heating, firing and cooling. A large amount of energy are consumed during the induration process, normally in the form of natural gas, oil, tar, anthracite or coke. Due to fossil fuel scarcity and global warming issues, at least partial substitution for renewable energy is desirable (today, the main energy sources in Brazil are generated by hydropower).

Moisture guarantees the consistency of the green pellet during the balling process and cannot be fully avoided in the processing. On the other hand, high presence in the furnace feed is one of the main bottlenecks for the drying process, where the complete release needs to take place prior to the preheating stage. In modern induration furnace operations, drying initiates up-draught (UDD), where hot air pushed upwards in temperatures around 150-200 ºC through the pellet layers heating the pellets evaporates free water, which moves out from the lower layer, giving these pellets enough dry strength to resist upper layers load during the process. Nevertheless, during drying, whether the heat carrier is not hot enough (where an industrial trade-off between grate speed/feed rate, moisture content and gas temperature is normally take in consideration), an over-wet zone may occurs at upper layers where the pellet are colder, losing its green resistance properties due moisture saturation over a certain

limit (Meyer, 1980), and become too plastic (generating clusters) and even break, due to excessive moisture (even over initial values fed to the furnace). Regarding the following zones, bed permeability will be affected thereby compromising the quality of fired pellets and performance of the operation. In addition to that, for the subsequent DDD (down-draught drying) the heat requirements to evaporate the condensed moisture increase considerably (latent heat is consumed to vaporize the condensate moisture again over the pellets) compromising energy efficiency and productivity of the furnace (Pereira and Seshadri, 1985).

The downward flow has temperature limitations due to top layer pellet spalling and heat recovery restriction (Thurbly *et al.* 1980). Feng *et al.* (2012) have gathered temperatures in the grate zone of a grate-kiln process, half of bed height of a travelling grate process, the hot air when firstly contacts the upper layers makes a rapid pellet bed temperature rising, while the temperature in lower layers increases no more than 10 %, which can be even lower if gas sensible heat is consumed to vaporize moisture at upper layers. Pereira and Seshadri (1986) described that a single pellet drying is led by three main steps: at the earlier stage, the driving force for withdrawal moisture from the surface of wet pellet is the equilibrium moisture of the hot gas. The removed moisture is replaced by vapor that migrates from the pellet core to the surface in a continuous process. Furthermore, evaporation from the surface reduces the moisture content throughout the system at a virtually constant volumetric rate. At an end of the constant rate period, the moisture content of the pellet surface reaches a minimum, initiate a falling in the drying rates. From this point on, the access of heat in the pellet core limits the diffusion of moisture through the pellet, thus achieving its critical moisture value. Recently, microwave has been introduced to assist the complex heating process of several materials. Huang *et al.* (2012) evaluated that the method of drying iron ore with microwaves in terms of efficiency and energy is superior to conventional methods. The major advantages

of using microwaves in the industrial process are the heat transfer rate, the directional heating, the size of the equipment, the agility in the switching, the absence of combustion products that contributes to the reduction of process residues and, in addition to these advantages, the equipment allows a good heating control, not requiring direct contact with the materials (Haque, 1999; Guo *et al.*, 2009).

According to Haque (1999), materials behave in three ways in front of microwave radiation, they may not have any influence (transparent to the microwaves, such as silica), reflect (as with metals) or absorb these waves (water or iron-bearing materials). The same author state that when such waves are absorbed, an energy transfer occurs from the microwaves to the material and as a result, the temperature increases. The increase in temperature, or dielectric heating, is caused by the friction of the spinning dipoles or because of the migration of ionic components. By different mechanisms, iron ore and moisture are the materials that control the heating by the microwave (Shaohua *et al.*, 2017). In the case of iron ore pellets Athayde et al (2018) explained that moisture plays an important role as a good absorber of microwave and convert the energy into heat. Despite of other carbon-based materials, coal is a poor absorber. Limestone is a transparent material for microwave and finally hematite, main constituent of the pellet, have good dielectric properties.

In the present study, the application of microwave in order to support the drying process for a travelling grate furnace was studied in a pot grate. For this purpose, it was implemented a microwave generator, associating the microwave heating together with convective heating. It was assessed the benefit of over-wetting minimization at the UDD and the moisture withdrawal, pellet bed aspect was also investigated.

5.2. Materials and Methods

5.2.1. Materials

Industrial itabirite concentrate obtained from an industrial pelletizing plant located at Anchieta, Brazil was used in the laboratory pelletizing experiments. Representative samples were generated by quartering and riffling sampling methods. (ASTM E 877-03, 2003). Iron ore concentrate had a particle size of 90% passing (325# mesh), and Blaine specific surface area was found 2030 cm^2/g measure according to ASTM standard (ASTM C 204-07, 2007). Additional raw material was Brazilian bentonite (0,5 %), limestone (1,3 %) and anthracite (1 %). Chemical analysis of representative pellet generated is shown in Table 1.

Table I – Chemical Analysis of the Pellet

Fe (%)	FeO (%)	SiO_2 (%)	Al_2O_3 (%)	CaO (%)	MgO (%)	P (%)	Mn (%)	LOI
66.9	0.12	1.96	0.32	0.65	0.02	0.04	0.083	2.6

5.2.2. Laboratory Pellet-Making Procedure

The green pellets were prepared according to the following balling procedure: The moist concentrate sample was weighted with defined portions of the raw. Mixing was conducted in an Erich mixer for 120 s. Then, the mixture was agglomerated into pellets by continuously feed into a pelletizing disc (150 cm dia.) rotating at 40 rpm and pellet growth rate controlled by feed rate. During the mixture, the green pellet moisture was adjusted to batches of 10.26 % and 9.98 %. Two batches of green-balls were made for each condition of final moisture, adjusted with pre-weighted moisture.

The green pellet was sieved and classified in size range from 16.0 to 8.0 mm and initially separated into 4 samples of 45 kg for tests. The growth speed of pellets was controlled to

increase the fraction between -16+8.0 mm. The size distribution of pellets produced is shown in Table II and the quality parameters of wet pellets are shown in Table II.

Table II – Pellet size distribution of the pellets

%moisture	9.98	10.26
(mm)	(%)	(%)
+19.0	0.00	0.0
-19.0+16.0	4.25	5.80
-16.0+12.5	32.55	34.80
-12.5+9.0	58.02	55.10
-9.0+8.0	1.89	1.70
-8.0+6.3	1.42	1.34
-6.3	1.89	1.50

Table III – Quality parameter of the pellet batch produced

Parameter	Batch 1	Batch 2
Moisture (%)	10.26	9.98
Wet-CS daN/pellet	2.2	1.95
Drop number (from 450mm height)	6	6.5
Dry-CS (150 ºC) daN/pellet	5.5	6

After producing green pellets and after the pot grate experiment, 100 g of wet pellets were randomly selected immediately. The weight of the remaining pellets was recorded and then put in a laboratory oven to dry them at 378 K until constant weight. A laboratory scale was used, the moisture content was calculated by wet and dry weight difference. The calculation of the percentage of humidity was performed, according to the ISO3087 standard.

5.3. Drying Experimental Procedure

The pot grate furnace has the objective of simulate conditions of an induration process. The main constituents of the furnace are: (1) the combustion chamber where a burner containing

LPG (liquefied petrol gas), oxygen and atmospheric air are ignited and the hot off-gases generated flows through the (2) pot, where the pellets are placed during the test and fully convective heated (radiant heat from flame are retained inside of the chamber). The input energy (LPG) is a control loop with the temperature set up at the lower layer of the pot. The pot is assembled with 37 cm of green pellets to be burned over a 7 cm layer of fired pellet, placed over stainless-steel grate bars. Furthermore, the pot is located between the (3) hood (connected with the combustion chamber) and the (4) windbox, which conduct the gas flow (down- or upwards). For the present study, a microwave applicator was implemented at the hood (Figure 1), directing microwave generated to the pellet bed using (5) waveguides made out stainless steel (non-magnetic) for safety purposed of no leakage. The (6) microwave generator inserted was a SAIREM FRANCE microwave generator with maximum capacity of 18 KW, which operates at frequency of 915 MHz.

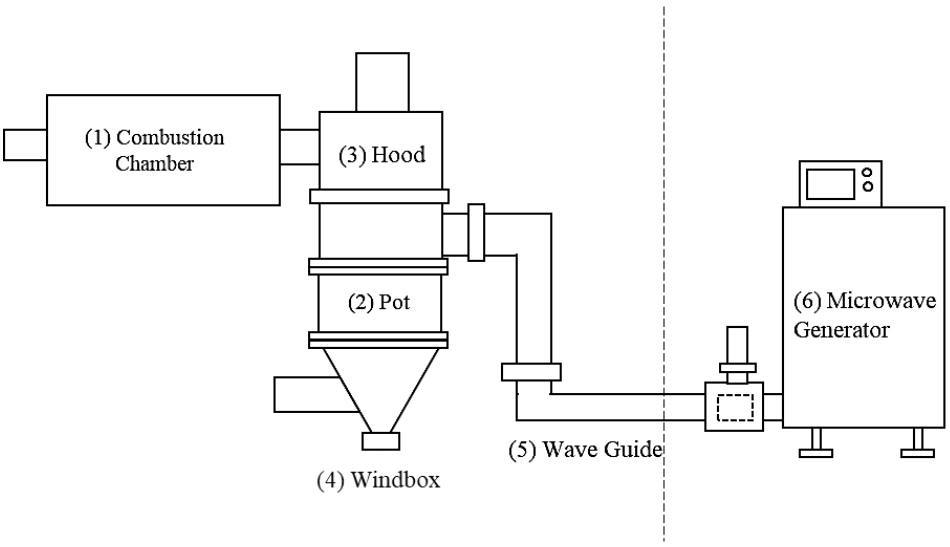

Figure 1 – Scheme of pot grate adapted for microwave drying.

For this experiment the conditions for drying as well as other parameters of the experiments are given in table IV, which were defined based on operation induration data available for industrial operations. The conditions applied in the test were: (1) Fully convective, following

standard conditions and (2) mixed heating profile where the microwave was set continuously at 10 kW during the first UDD stage.

Table IV– Heat pattern applied in the present study operation

Zone	Reaction Zone Length (m)	Time (s)	Pressure Drop (mmWg)	Temperature inlet (ºC)
UDD	16	175	-290	290
DDD	31	340	250	280

After the test, moisture was measured at four-bed height (30, 60, 240, 360 mm). The pot grate was opened after the tests and thermal images acquired using FLIR i7 Thermal Imager.

5.4. Results and Discussions

5.4.1. Pot Grate temperature evaluation

The constant pressure drop control-loop leads to increase of inlet air flow if the resistance through the pellet bed is lower (improving the heat transfer across the bed), in order to make the trials comparable and correlated with the industrial operation. In the fully convective mode, the pellet temperature at 60 mm depth from the surface does not rise to a great extent from the initial temperature in the first 200 s, as the gas flow is cooled down across the bed. Figure 2 indicate that firstly gas heat was consumed turning moisture into steam on the lower layers and secondly consumed in latent heat when moisture is re-condensate on the intermediate layer. On another hand, the microwave assisted experiment warm up pellets downwards into the pellet bed, sharply increasing the temperature of the first pellets of the upper layer showing heating rates as high as 1.5 ºC/s and an average of 0.79 ºC/s against only 0.14 ºC/s, when only convective heating is applied at the UDD. In Figure 2, it was observed a significant increase in the temperature at 60 mm depth, reaching the temperature

of 115 ºC against 71 ºC at the end of the UDD. Afterwards, the DDD chilled the top layer, transferring the heat downwards. The pellet surface temperature above the gas dew point (100-110 ºC) avoid the condensation of moisture.

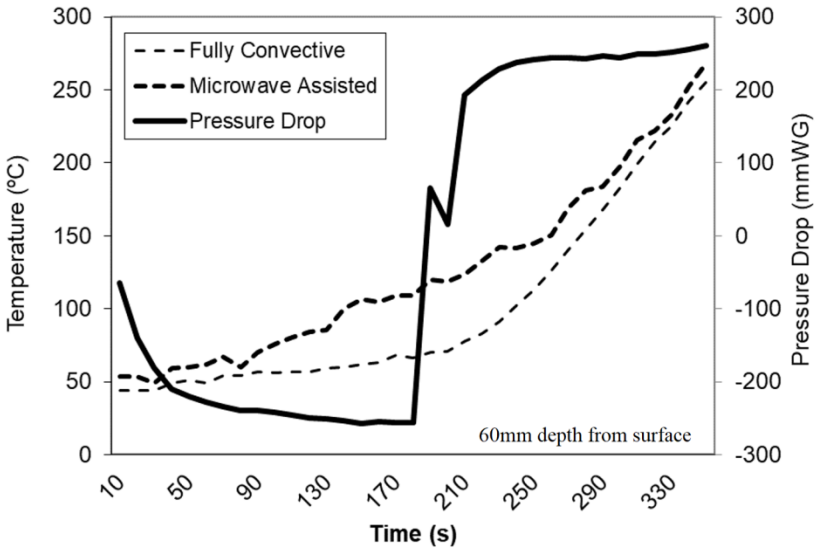

Figure 2 – Temperatures profile at 60mm depth from surface.

Nevertheless, the dielectric heating is restricted to the first layers of pellets, once the wave is attenuated through the pellet bed. Saito *et al.* (2011) have observed low penetration depth of microwave materials with good dielectric properties such as iron ore. Figure 3 demonstrate that the lower layer closer to the hearth layer (340mm depth from surface) has no significant difference in the temperature profile between the two treatments, most likely the wave did not reach these pellets, but moisture was properly released during the UDD, which normally occurs in the region.

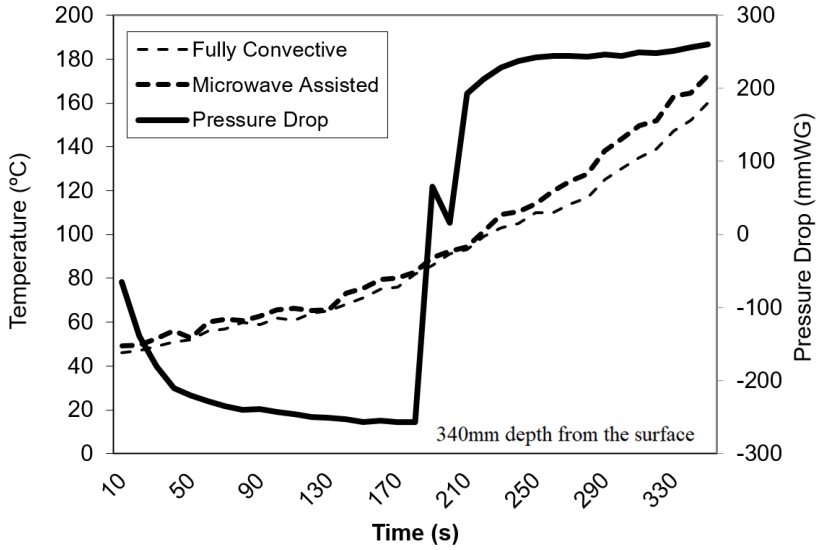

Figure 3 – Temperatures profile at 340mm depth from surface.

The mitigation of the overwetted region had an impact on the windbox temperature, based on the similar inlet temperature at the DDD zone (280 ºC) and pressure drop in the experiment. Figure 4 indicate an improvement in the overall heat transfer rate across the pellet bed, with lower moisture at upper level it allowed increase the windbox temperature by 37 ºC. A critical point at the DDD is guarantee that heat transfer gas-pellet is sufficiently low to avoid a high steam release from the pellet core and consequently spalling, which could lead to spalling as observed by Tsukerman (2007). Additionally, Matos (2007) presented from industrial correlation that temperature increased are responsible for +0,01 MTY/ºC in pelletizing throughput, because of the possibility to shorten the residence time of pellets inside of the furnace.

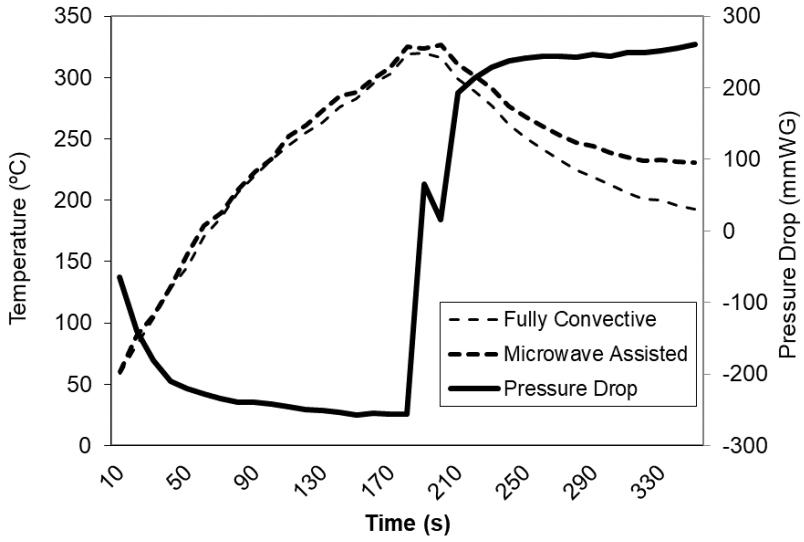

Figure 4 – Windbox temperatures

The effect of the temperature changes in the pellet bed on the moisture was measure and it is described in the following chapter

5.5. Moisture Released at Pot Grate Experiments

Figure 5 shows the impact of the heating distribution across the pellet bed moisture released after the experiment. The upward hot air absorbed the moisture until the saturation limit, decreasing its temperature. The moisture measured at the lowest layer, shows no difference between the heating methods (360 and 240 mm depth), because of the similar level of temperature achieved, as observed previously at Figure 3. On another hand, at upper layers (60 and 30 mm), for the fully convective experiment, moisture presented higher than initial values (10.2 % and 10.5 % above the initial 10.12 %), indicating that the air flow cooled down until the dew point, where moisture condenses over the surface of the cooler pellets, especially at 60 mm depth. The use of microwave at UDD had a considerable impact on those layers of pellets where moisture reduced considerably (9.3 % and 10.0 % from initial 10.12 %) compared with the fully convective drying, do not allow condensation. The mitigation of condensation has a direct impact on the bed permeability, as far as the physical

aspect of pellets is concerned no visual cracks or deformation were observed, inferring that the drying rates were sufficient smooth for microwave power applied. According to Ljung, (2011) drying is a function of an initial surface evaporation period succeeded by a period of increase in internal evaporation. Based on that, the mechanisms co-exist during a certain period of time. However, Figure 4 demonstrates that the microwave accelerates the pellet temperature towards the wet bulb temperature, making possible increase the pellet temperature sooner as the moisture content at the surface is lower.

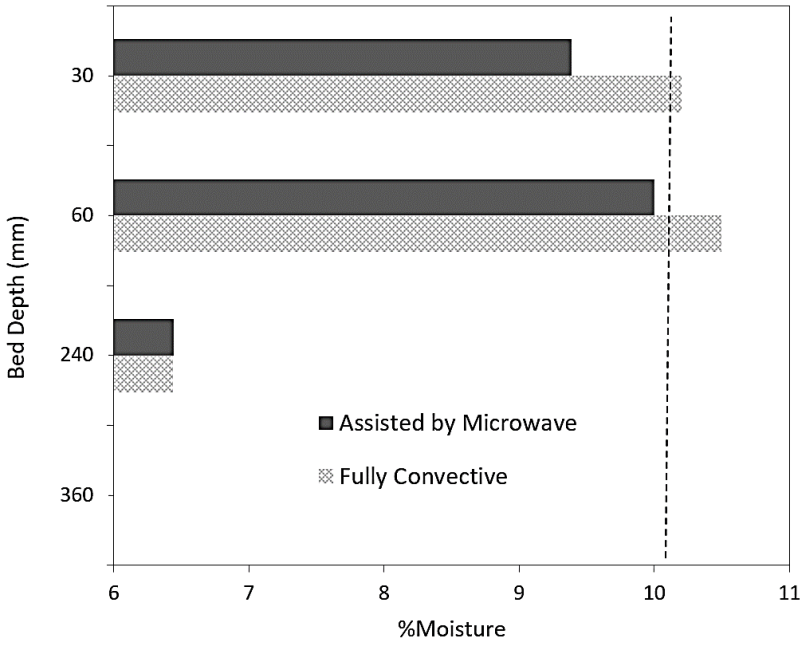

Figure 5 – Effect of the Microwave on the UDD efficiency

In Figure 6, the variation of moisture in two different level of moisture has demonstrated a better efficiency with microwave assisted heating compared to the fully convective heating. The heating assisted by microwave mitigate the over-wetting of in both levels of initial moisture at the end of the UDD. However, the fully convective drying generates an over-wetting condition, which increases moisture in the upper layer by +3.7 % per +1 % of increase in initial moisture, this behavior can be explained by Thurlby et al (1980), since, in their view, it is well established that the moisture stuck in the medium-upper layer jeopardize

the pelletizing operation due the collapse of the pellets when the porous saturation is achieved (Forsmo, 2006), also referred by Meyer (1980) due an increase in the resistance of the air flow.

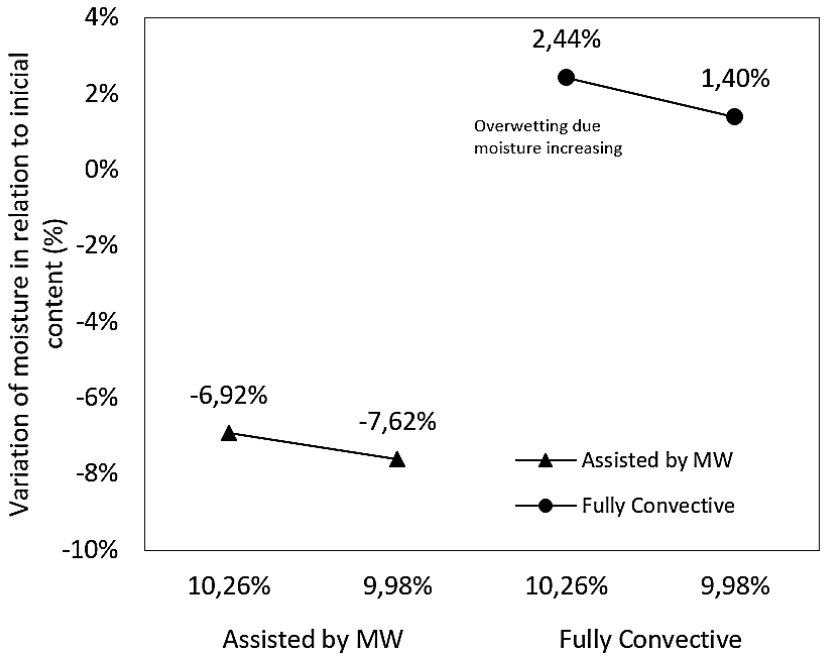

Figure 6 – Effect of the total moisture content on the drying efficiency, at the top layer at the end of UDD

5.6. Pellet aspect after Pot Grate Experiments

In figure 7, the over-wetting zone formed can be clearly observed. Although the pot was carefully dug through the layers, some pellet cracked.

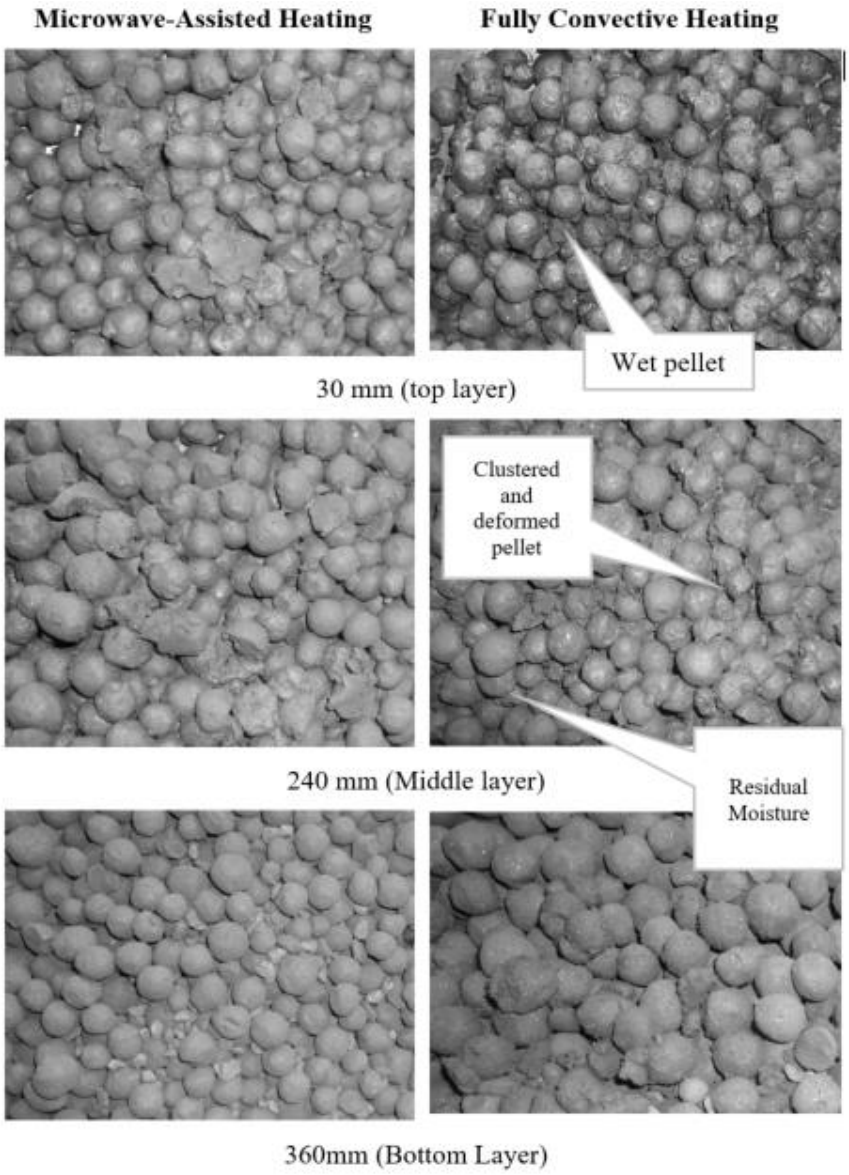

Figure 7 – Visual appearance of the pellet after UDD experiment

At the end of the UDD stage of each experiment, a thermal image was obtained in order to verify the heat distribution effect on the temperature of the pellet bed surface. The top layer, in Figure 8, demonstrated cross-section specific patterns for both experiments. In the microwave assisted experiment, the central part of the pot grate shows an energy concentration (Figure 8b), temperature reached 130 ºC against 55 ºC in the fully convective heating (Figure 8a). The reason I the oscillating behavior of the microwave in multimodal ovens which generates a homogeneous electromagnetic field, distributing radiations towards

different directions through pot grate hood. However, these stationary waves heat more some spots of the area exposed, where the power density is considerably higher. The complex oscillating pattern of the waves could lead to thermal runaway effect (Ogunniran *et al.* (2017), Lovas et all (2011)) and degradation of the pellets, which was not observed due to the moisture release at the surface. Additionally, spalling was not observed, indicating the heat rates applied were not sufficiently high despite the high temperature achieved.

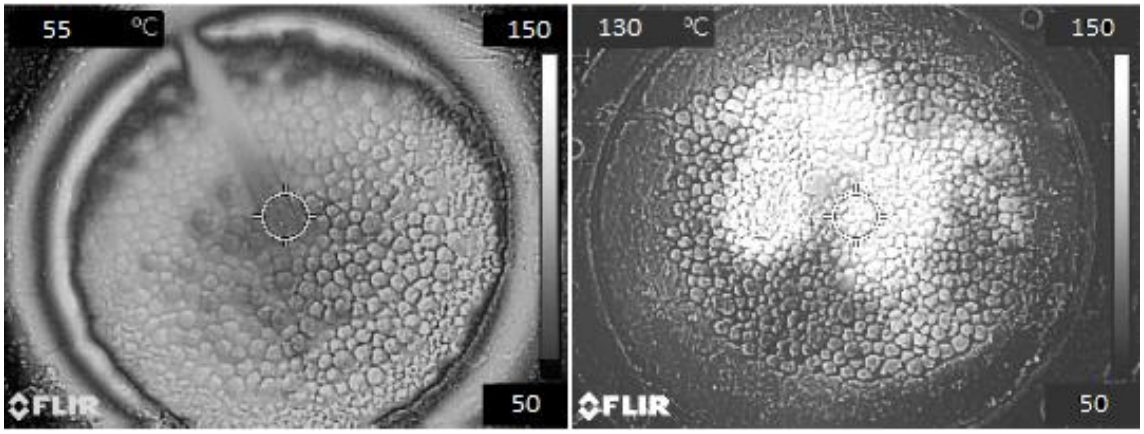

(a) (b)

Figure 8 – Heating pattern over the pan of the pot grate (a) fully conventional heating (b) assisted by Microwave.

5.7. Comparison of the heating mechanisms

The fully convective heating, in general, over-wet pellets in the intermediate and upper layers, the increase in moisture reduced the green pellet strength resulting in clusters, deformed and clogged the pellet bed voids where the gases should percolate at further downdraught steps. However, the application of microwave during the UDD stage to assisted heating minimized the clustering and deformation, in Figure 9 the mechanism is compared. The wave penetration is a function not just of wavelength, but also energy converted in heat in the first layer of the bed, which in this case is high due the high amount of moisture. Nevertheless, pellets at 240 mm depth were almost dried (showing how deep microwave

reached) whereas moist pellet (darker) at top layer is far less compared to the fully convective heating.

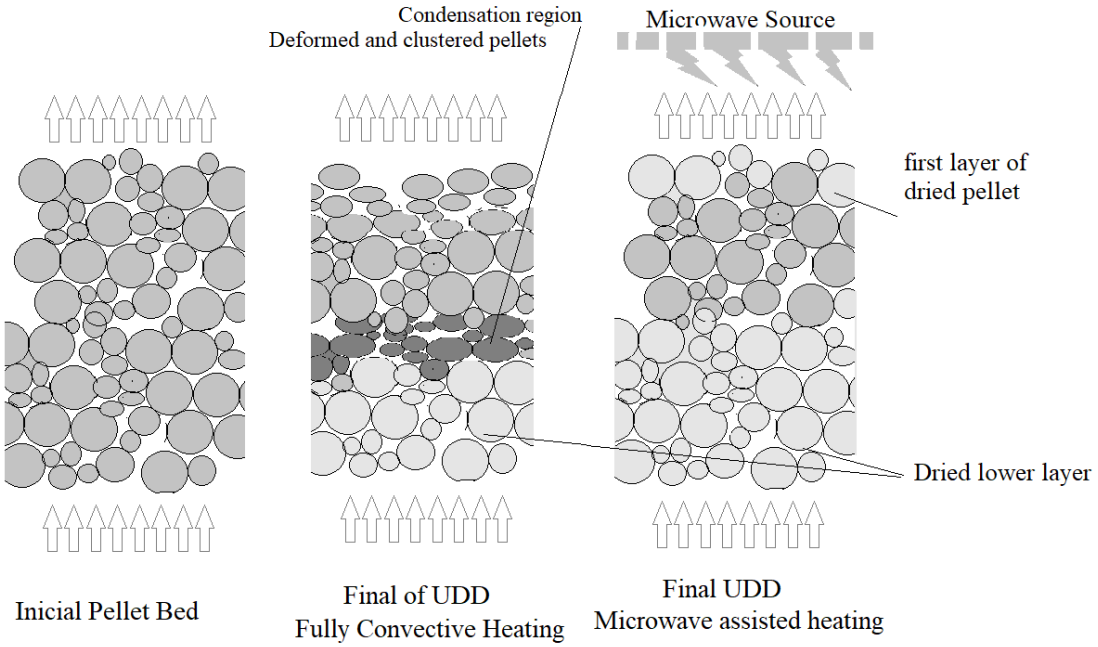

Fig 9 – Mechanism of the heating and drying with fully convective and microwave assisted in the pellet bed.

The results represent may a significant increase in productivity of travelling grate furnaces, as DDD can operates without constraints and higher temperature. The main constraint is to eliminate water before the preheating zone, then maximizing the operation.

5.8. Conclusion

The present paper demonstrated through a pot grate study a breakthrough technique to improve drying efficiency through the application of microwave. The process permit:

- Dielectric heating is much complex than fully convective heating, and a new operation mode are expected due the nature of heat transfer and absorption from a different material;

- Although high heating rates may lead to spalling of the green pellets, in the present experiments it was not observed, concluding that energy transfer was sufficient low to release the moisture from the pellet core.
- The heterogeneous behavior of the application should be improved to increase energy efficiency of the process. The work must continue improving the applicator in order to minimize the heat distribution.
- The microwave application minimized the dew point of the heat carrier and retention time of the green ball with excess humidity, allowing a more efficient process, for the same green pellet strength at upper layers (minimizing the influence of static load on the pellet with excess wetting).
- The microwave assisted heating shows low influence of the initial moisture, which impact the fully convective system leading to increase in residence time of the pellet in the furnace.

5.9. Reference

Athayde, M., Cota, M., & Covcevich, M. (2018). Iron ore pellet drying assisted by microwave: A kinetic evaluation. Mineral Processing and Extractive Metallurgy Review, 1-10. doi:10.1080/08827508.2017.1423295

Saito, Y., Kawahira, K., Yoshikawa, N., Todoroki, H., and Taniguchi, S., 2011. Dehydration Behavior of Goethite Blended with Graphite by Microwave Heating. ISIJ International, 51 (6), 878–883.

PEREIRA, R. O. S, SESHADRI, V., Secagem de pelotas de minério de ferro, Metalurgia – ABM, V.41, n.328, p.141-144, novembro 1985.

Haque, K.E., 1999. Microwave energy for mineral treatment processes—a brief review. International Journal of Mineral Processing, 57 (1), 1–24.

Huang, Z., Yi, L., Jiang, T., & Zhang, Y. (2012). Hot Airflow Ignition with Microwave Heating for Iron Ore Sintering. ISIJ International, 52(10), 1750-1756. doi:10.2355/isijinternational.52.1750

Guo, S., Li, W., Peng, J., Niu, H., Huang, M., Zhang, L., Zhang, S., and Huang, M., 2009. Microwave-absorbing characteristics of mixtures of different carbonaceous reducing agents and oxidized ilmenite. International Journal of Mineral Processing, 93 (3-4), 289–293.

Feng, J., Xie, Z., & Chen, Y. (2012). Temperature Distribution of Iron Ore Pellet Bed in Grate. Journal of Iron and Steel Research, International, 19(2), 7-11. doi:10.1016/s1006-706x(12)60052-1

Forsmo, S., Samskog, P.-O., and Björkman, B., 2008. A study on plasticity and compression strength in wet iron ore green pellets related to real process variations in raw material fineness. Powder Technology, 181 (3), 321–330.

Ogunniran, O., Binner, E., Sklavounos, A., & Robinson, J. (2017). Enhancing evaporative mass transfer and steam stripping using microwave heating. Chemical Engineering Science, 165, 147-153. doi:10.1016/j.ces.2017.03.003

Thurlby, J.A.; Batterham, R.J. (1980) Measurement and prediction of drying rates and spalling behaviour of hematite pellets. Transactions of the Institution of Mining and Metallurgy. Section C.; 89C:125-131p.

MATOS, A.P., Influência da temperatura, pressão, produção e granulometria no processo de secagem das pelotas cruas, Ouro Preto: REDEMAT-UFOP, (2007), 115p

Meyer, K., Pelletizing of Iron Ores, Wurzburg: Druckerei K.Triltsch. (1980)

Ljung, A.-L., Lundström, T.S., Marjavaara, B.D., and Tano, K., 2011. Convective drying of an individual iron ore pellet – Analysis with CFD. International Journal of Heat and Mass Transfer, 54 (17-18), 3882–3890

Tsukerman, T., Duchesne, C., and Hodouin, D., 2007. On the drying rates of individual iron oxide pellets. International Journal of Mineral Processing, 83 (3-4), 99–115.

Forsmo, S., Apelqvist, A., Björkman, B., and Samskog, P.-O., 2006. Binding mechanisms in wet iron ore green pellets with a bentonite binder. Powder Technology, 169 (3), 147–158

Shaohua, J., Singh, P., Jinhui, P., Nikoloski, A.N., Chao, L., Shenghui, G., Das, R., and Libo, Z., (2017). Recent developments in the application of microwave energy in process metallurgy at KUST. Mineral Processing and Extractive Metallurgy Review, 1–10.

Capítulo 6. Artigo E - Iron Ore Concentrate Particle Size Controlling Through Application of Microwave at the HPGR Feed

Maycon Athayde and Maurício Covcevich Bagatini

Artigo aceito para publicação em 12 de abril de 2018 *na revista Minerals & Metallurgical Processing journal*.

Abstract

Nowadays, the HPGR (high pressure grinding rolls) is an intermediate step between filtering and balling in most modern iron ore pelletizing operation. The operation debottlenecks filtering process and reduce pressure over the typical milling process to control particle size to the balling. The present study evaluated aspects of microwave application to the iron ore concentrate fed to HPGR in a bench scale unit. Iron ore concentrate was irradiate varying the exposure time to the microwave and the grinding efficiency was evaluated. The influence of moisture in the HPGR efficiency was also assessed. The pellet feed blaine surface area (BSA) improved by 300 cm2/g and % < 325# fraction by 3 %. Scanning electron microscope (SEM) images show the formation of micro-cracks onto the particles surface induced by microwave, the effect observed helped improve the milling process performance, in addition to the moisture reduction observed due the temperature increase.

Keyword: HPGR, Microwave, Moisture, Pelletizing

6.1. Introduction

Pelletizing is one of the most efficient processes to prepare fine iron ore to reduction reactors. Its flexibility to adjust pellets composition for each operation (tailored-made) and the uniformity/stability of size distribution, chemical composition, physical and metallurgical properties are key factors to reactor's stable operation. A critical production trade-off is a relationship between the iron concentrate moisture and its particle size distribution (Sportel et al., 1997; Kawatra, 2001 and Nunes et al., 2014). Usually, wet grinding circuits reduces run-of-mine ore particle size to liberate the wanted mineral from the gangue, nevertheless in the case of pelletizing it is also necessary to adequate particle size and surface area, i.e. ore fineness, to obtain high cohesion among the particles, a proper green pellet growth rate and resistance at the balling process. Pellets strength occurs through capillary adhesion forces that bond mineral particles all together and reach its maximum when the porosity is properly filled with moisture. Forsno et al. (2005) measured the maximum compressive strength, observing an inverse correlation with particle size and efficient moisture level control. The porous network saturation inside the green pellet need to be achieved. However, the moisture control at the dewatering process is greatly influenced by the ultra-fine particles fraction (% < 325#) in pellet feed and generated during milling. This particle size clogs the filter cloths void reducing the and the permeability through the filter cake. Therefore, particle size distribution (PSD) has a strong impact on the downstream processes. Holistically, the balance between moisture and PSD greatly affects the induration furnace, not only because the agglomerates growth rate, but also due to the green pellet strength and surface finishing control (Kapur et al., 2003). The mentioned green pellet properties are key to prevent deformation and minimize fine generation within the furnace, leaded by cracked green pellets during the drying stage inside the furnace. A permeable pellet bed eases the drying

process and lowers energy consumption at higher throughput, as the heat transfers are more intense and temperature for induration reactions can be achieved (Forsmo et al. 2008).

The fine ground ore is a requirement to pelletizing process, although the filtering operation are jeopardized. Technological innovations have been proposed to solve the traditional mineral processing trade-off and to control moisture level at the high presence of ultra-fine-fraction, as a proper feedstock to pelletizing process (Leonel et al., 2013). In the last decades, the HPGR (High Pressure Grinding Rollers) was introduced as an additional comminution step to the beneficiation plants flowchart, as represented in Figure 1. The first motivation to support HPGR use as an alternative comminution process is its greater energy efficiency compared to conventional crushers and mills (Meer et al., 2015). By applying the load slowly on ore particles, the HPGR breaks the grains, minimizing energy loss as heat and noise. The possibility to regrind the mineral to adjust the surface area for pelletizing needs after dewatering, without any addition of water to the process, it is a second strong motivation.

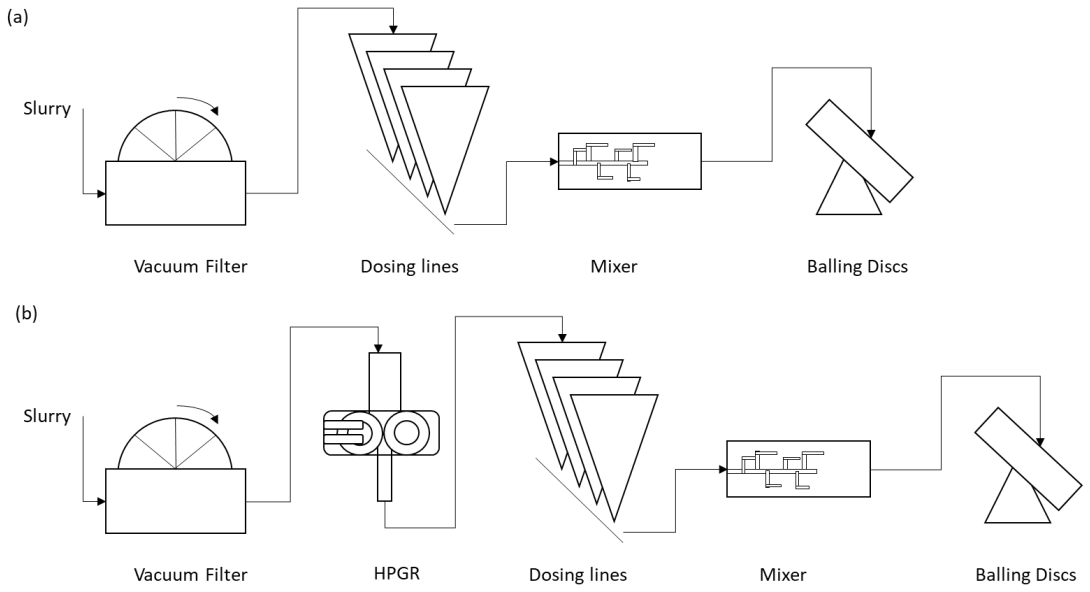

Figure 1 – (a) Traditional Pelletizing process (b) Pelletizing process with HPGR

The equipment consists of two opposing rotating rollers as shown in Figure 2, coupled to traction resistant bearings, coated with abrasion resistant structure and studs. The pressure is

applied by means of a hydro pneumatic system. The roller slides or floats on shock absorbers, reacting to the forces of the material on the roller and the spring system. The mineral is fed by means of a chute or column positioned in the upper part of the equipment, based on a level control that assures the uneven continuous feeding above the rollers. Usually the feed column is sufficient to exert a force of separation between the rollers (Abouzeid et al., 2009).

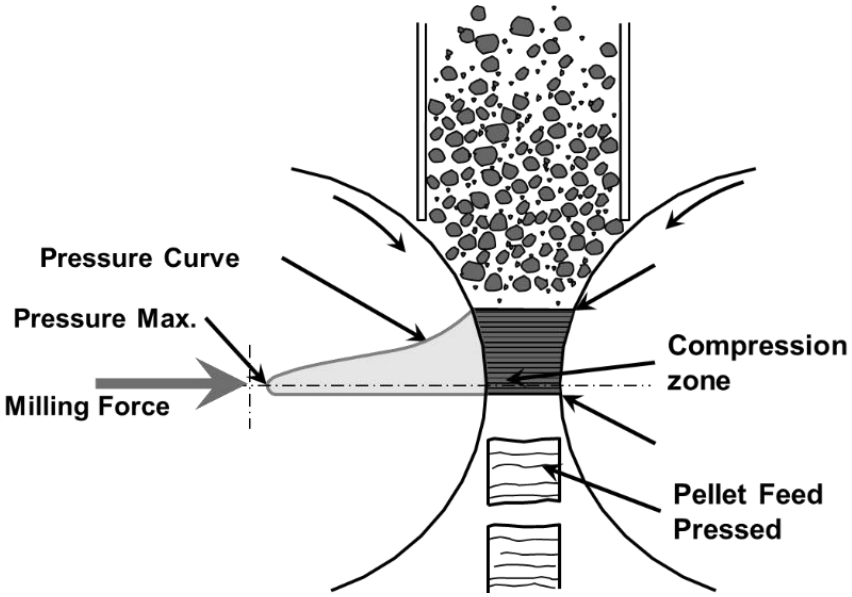

Figure 2 – Mechanism of comminution in an HPGR.

The HPGR advantages for the iron ore pelletizing are: pellet feed moisture reduction, lower energy consumption, and capability to adjust PSD after dewatering instead of at beneficiation unit (Ribeiro et al., 2010). Nunes et al. (2014) demonstrated that a better pellet feed PSD (where % < 325# fraction is higher than 90 %) improves considerably the physical green pellet quality. In the microstructural point of view, the particles processed at HPGR (Zu et al., 2004 and Meer et al., 2015) have a modified morphology (less angular edges) and enhanced surface activity (due to the cracks generated) which allows an easier growth rate control during the balling process. Moreover, Zu et al., (2004) demonstrated that concentrated processed through HPGR improves green pellets to support 3.3 to 4.9 additional drops number and dosage of bentonite reduces from 2 to 1 $\%_{w/w}$. Also, Meer et al.

(2015) observed a reduction in green pellet porosity in the range of 3-5 %, which may represent an increase in throughput of an induration furnace.

Differently than a tradition wet-milling flowchart, the comminution through HPGR generates higher ultra-fines portion. Consequently, the HPGR installed ahead of the dewatering process eases the moisture control and have benefits to the balling process. Additionally, the particle breaking mechanism is induced not by the impact but by attrition and shearing forces among particle (Meer et al., 2015; Barrios et al.,2016). These forces may generate 3 to 5 % more ultra-fine particles (% <10 μm) than a ball mill, for the same BSA and throughput (Abazarpoor et al., 2017). However, the moisture level is critical to achieve an increase of 300 to 400 cm2/g for the reason of the slippage (drifting) among particle covered by water, when pressed between the rollers. The moisture content increase reduces parabolic the HPGR throughput, especially on the level above 7 % (typical for pelletizing process). The studies reported flake generation in this moisture level (Saramak et al., 2013 and Meer et al., 2015). Recent models developed correlate particle reduction rate and moisture content, it has been shown that flake generation increases specific energy consumption and lower net throughput due to the high pressure used to avoid slipping when moisture increases. The throughput stability is critical by due the high capital investment for an HPGR compared with the traditional grinding circuit, and new technologies which can improve the HPGR performance are needed.

In the last two decades, several studies of hard ores pre-grinding have evaluated extensively the use of microwave radiation (Kingman et al.,1998; Kumar et al., 2010; Rizmanoski, 2011). Although Ali et al (2011) advise that a high-power density is required for treat fine-grained ores. In contrast, Kingman et al. (2004) shows that microwave generates inter-granular fractures in an extensive number of different minerals, easing the cracking of the particles during the ball milling process, in applications with less than 0.5 s (< 3kW).

Rizmanoski (2011) explained that reduction in strength of different mineral is related to applied microwave power level and mineral liberation, the degree at which mineral component of the ore will absorb microwaves depends on the complex permittivity ε, which is defined by Eq. (1).

$$\varepsilon = \varepsilon' - i\varepsilon'' \quad (1)$$

Where ε' is the real component of the complex permittivity, and ε'' is the imaginary component of the complex permittivity (He et al., 2011). The dielectric heating, as it is known, is the interaction of the electromagnetic field of microwaves with the mineral, where dipoles align and flip around since an alternated field is applied and the internal energy converts in heat due to the friction (Haque et al., 1999). The real component measures the mineral ability to store electrical energy. The complex permittivity represents the ability of heat generation. Besides ε' and ε'', another parameter that is used to express how the microwave energy is dissipated is known as loss factor and defined by Eq. (2).

$$\tan\delta = \varepsilon''/\varepsilon' \quad (2)$$

Iron minerals have higher dielectric property than gangue minerals, consequently Shaoxian et al. (2013) explained that different absorption rates among the minerals (especially in mixed particles) generates stress within the lattice with the increase of temperature, leading to intergranular and trans granular cracks. Each ore has different thermal expansion rate because of crystal size, electrical properties or ore composition. Besides, the present study will evaluate how HPGR can take advantage of this effect.

The main goal of the study was to investigate the effect of microwaves irradiation on the ability of the HPGR improve pellet feed BSA and generation of fine particle portion, important for iron ore pelletizing process. The abovementioned moisture influence on the

HPGR grindability needs to be considered during the experiments as the heated pellet feed release moisture, an effect of the microwave applied. An improvement in the pellet feed PSD will allow better operation of the induration and balling process.

6.2. Materials and Methods

6.2.1. Raw Materials

Industrial itabirite concentrate obtained from an industrial pelletizing plant located at Anchieta, (Brazil) was used in the experiments. Representative samples were generated by quartering and riffling sampling methods (ASTM E 877-03, 2003). Blaine specific surface area was measured according to ASTM standard (ASTM C 204-07, 2007). The chemical composition and physical properties are shown in Table I.

Table I – Chemical, physical and mineral characterization of the iron ore concentrate

FeT (%)	FeO (%)	SiO2 (%)	Al2O3 (%)	CaO (%)	MgO (%)	P (%)	Mn (%)
65.95	1.62	1.59	0.32	0.02	0.02	0.046	0.083

Blaine Surface Area (cm2/g)	+100# (%)	-200# (%)	-325# (%)	+325 # (%)	Loss of Ignition (%)	Specific Density (g/m3)
1838	0.2	7.3	89	3.6	3.65	4.8

%Specular Hematite	%Porous Hematite	%Magnetite	%Goethite	%Quartz
42.3	33.7	1.2	20.8	2

6.3. Experimental Procedure

6.3.1. Microwave Treatment Experiments

The concentrate was treated in a microwave oven, multimodal, provided with a turntable-tray model LG MH7048G (2.45 GHz, power of 1000 W). An additional exhaust system (1L/min) is placed on the lateral side to standardize the steam withdrawal. The sample holder is a Teflon high-temperature resistant plate (Figure 3) to keep the irradiation power density constant in the sample.

In every treatment, the iron ore was irradiated in 100 sub-samples of 150 g, in order to keep the power density and electromagnetic field homogeneous on the whole sample. The treatments were conducted in time step of 0, 10, 30 and 50 s, in duplicate. The sample temperature was gathered after every treatment and the average recorded for each time-step. The average temperature on bulk surface was measured using a model Raytec ranger 3I infrared thermometer after switch-off the microwave power. In order to access the heat efficiency, 100 ml of water (c_p = 4.18J/g/ºC) was placed in the same sample position to evaluate the amount of heat absorbed in regarding the power input setup. The result is a 68±1 % furnace efficiency (E) for absorption in relation to the nominal power input, the complement is dissipated as heat, mostly in the magnetron tube.

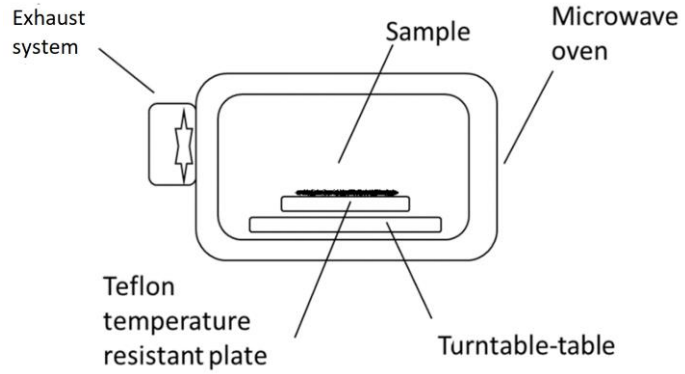

(a)

(b)

(c)

Figure 3 –Microwave furnace used during the application (a) scheme of microwave furnace (b) image of the microwave used in the test (c) sub-sample heated.

Figure 4 illustrates the position of an industrial application in the flowchart, the irradiation time can be translated into the distance over a conveyor belt, before feeding the HPGR.

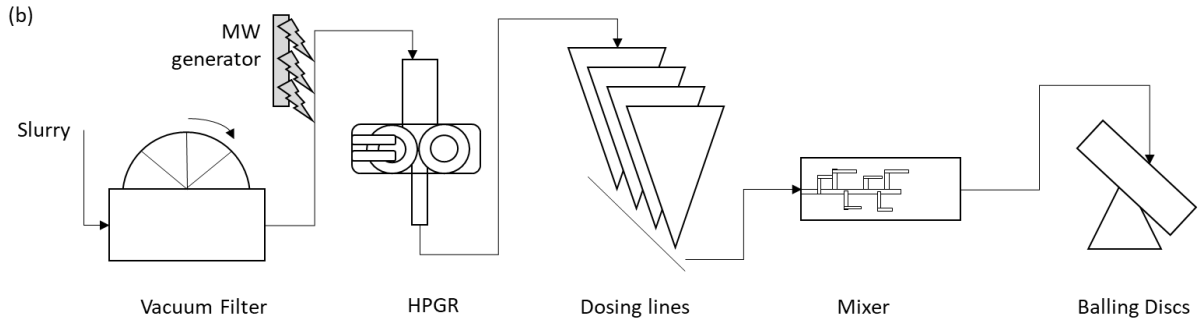

Figure 4 – Flowchart of a pelletizing process including MW generator to support HPGR process.

6.3.2. Milling experiments at the HPGR

A bench scale Polysius LABWAL HPGR (250 mm diameter and 100 mm length), shown in Figure 5, processed the concentrate irradiated. Every test used a 15 kg sample (feed rate of 30 kg/h). Alves et al (2015) determined that good quality results could be obtained from samples of only 5 kg, where a typical standard is in the range of 25-30 kg.

Comminution was achieved by compressing the particle bed using two-rotating rolls, where one is forced against the other by a hydropneumatics piston system. The setup oil pressure was 50 N/mm2, roller speed kept constant at 0.3 m/s (zero gap 2.91 mm).

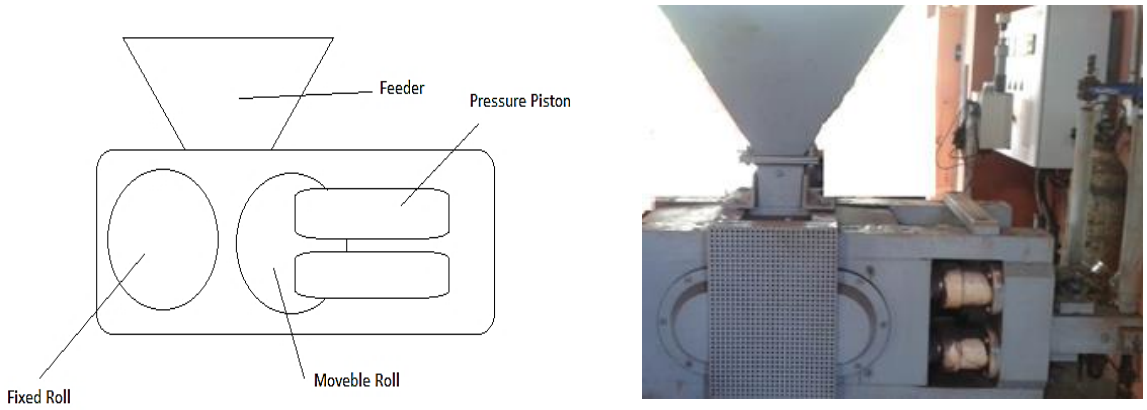

(a) (b)

Figure 5 – (a) Scheme and (b) picture of the bench scale HPGR

The milling experiment was conducted by two feeding methods:

(1) "Original": A part of the representative samples generated by quartering and riffling sampling methods, reposed at room temperature for 2 h.

(21) "Treated and pressed only": 100 concentrate sub-samples obtained from the microwave treatment were homogenized and reposed at room temperature for 2 h.

(3) "Treated and pressed remoisturized.": 100 concentrate sub-samples, after the previous procedure had the moisture adjusted to reach the initial 10 % w/w and then homogenized

again. The procedure intends to evaluate the influence of the microwave, without considering the moisture released during the heating.

6.3.3. Particle size analysis

The particle size distribution was performed with a Mastersizer 2000E, capable of analyzing particles between 0.02–1000 μm. Parameters were fixed at a pump speed of 3000 rpm, the measurement time of 6.5 min and pulp concentration of 0.01 $\%_{w/w}$. The sample was prepared in distilled water.

6.3.4. Specific surface area

The measurement of the air permeability of a bed of fine particles was measured in the instrument based on the ASTM C-204 (2011), to obtain the BSA.

6.3.5. Particle aspect ratio by SEM using image analysis

The samples were analyzed using a scanning electron microscope (SEM) JEOL –JSM 35C Model. The sample was coated with a thin layer of carbon in order to get the sample sufficiently conductive. The images were taken at 500x in different zones of the sample in order to map randomly the particles. ImageJ software was employed to provide the aspect ratio. The aspect ratio is always either equal or greater than 1.0 (ratio length/width). A symmetrical particle shape in all directions, such as a sphere has an aspect ratio of one, while an elongated particle has a higher than one aspect ratio. The images were analyzed after calibration for dimensions, contrast improvement, background noise minimization, a threshold to extract particle from the background through a binary image.

6.4. Results and Discussion

6.4.1. Microwave Heating Profile

Figure 6 shows the pellet feed temperature evolution during microwave application. In the earlier moments, it was found a high heating rate of 1.31 ºC/s, while after the 30 s the heating rate reduces to 0.72 ºC/s. Sahoo *et al.* (2010) and Athayde et al (2018) also observed iron ore warming up at 1.2 ºC/s. The heating efficiency was assessed based on Eq. (3) and the results are presented in Figure 6.

$$\%Heating\ Efficiency = \frac{mc_p\Delta T + \Delta H_{Vap}\ .\ \Delta_{moisture}}{PtE}\ x\ 100 \quad (3)$$

Wherein, "m" is the mass of pellet feed (g), "c_p" is the specific heat (J/g/ ºC), "P" is the power input supplied by the microwave oven (W), "t" is the irradiation time (s), "ΔT" is the temperature variation during the trial (ºC), "ΔH_{vap}" is the heat of vaporization of water (J/g), "Δmoisture" mass variation of the sample (g) and "E" is the furnace efficiency (%).

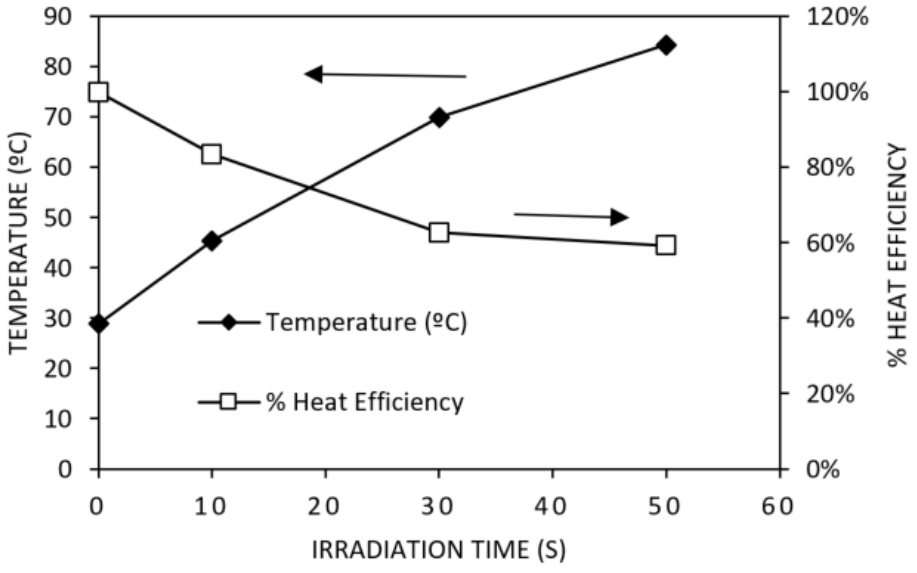

Figure 6 – Evaluation of temperature with the irradiation time

The maximum exposition time was defined due to the generation of incandescent spots which consumes more energy, defined as thermal runaway (He et al., 2015). The effect happened after the irradiation time of 50 s, defining a maximum residence time in the furnace. The complex occurrence of this spots depends on how the region is cooled by heat diffusion to the material surrounding, which it is also dependent of the thermal diffusivity and temperature gradient across the sample. The heat generation has a strong influence on the moisture loss. Moisture has stronger microwave absorption characteristics than hematite. The mineral has a lower loss factor (Tanδ 0.01-0.07) compared to water (0.12-0.16), which decrease even more because of an increase in temperature (Haque, 1999), reducing the heat efficiency with the increase in the irradiation time. Figure 7 shows a drying rate of 8.0 ± $0.2x10^{-4}$ g/(g.s) in consequence of the dielectric heating, which represents a positive aspect for the pellet drying process in a subsequent induration process.

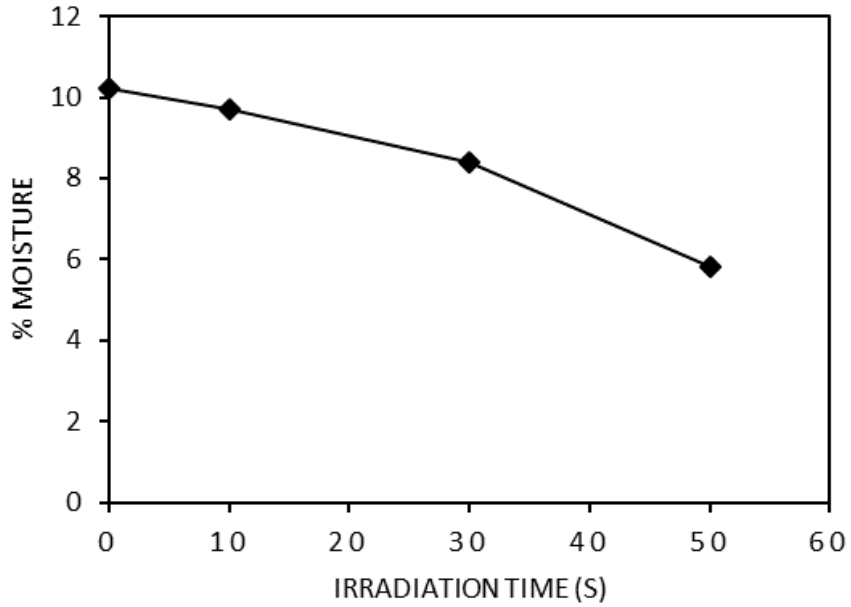

Figure 7 – Moisture reduction during the irradiation time

6.4.2. Microwave irradiation impact on the HPGR Efficiency

The grinding efficiency at bench scale HPGR was assessed based on the evolution of the iron ore concentrate BSA and % < 325# fraction. As shown in Figure 8, microwave irradiation induces a significant increase in BSA and % < 325# fraction. Similar applied load and feed rate at the HPGR reduced the particle size, due the application of compressive forces (increasing the portion of ultra-fine, represented by a higher BSA), but also the microwave irradiation time increase has influence in the result. The BSA increased at a rate of 3.5 ± 0.3 $cm^2/g/s$ of irradiation, the rapidly increase was followed by % < 325# fraction increase, also essential to better balling efficiency (Zhu et al., 2004). The causes for the improvement in the HPGR efficiency conditions are the particle fragility, during the time where the ore is exposed to the microwaves and as described earlier the second reason for this observation lies on the nature of the moisture reduction impact on the particle bed between the rolls.

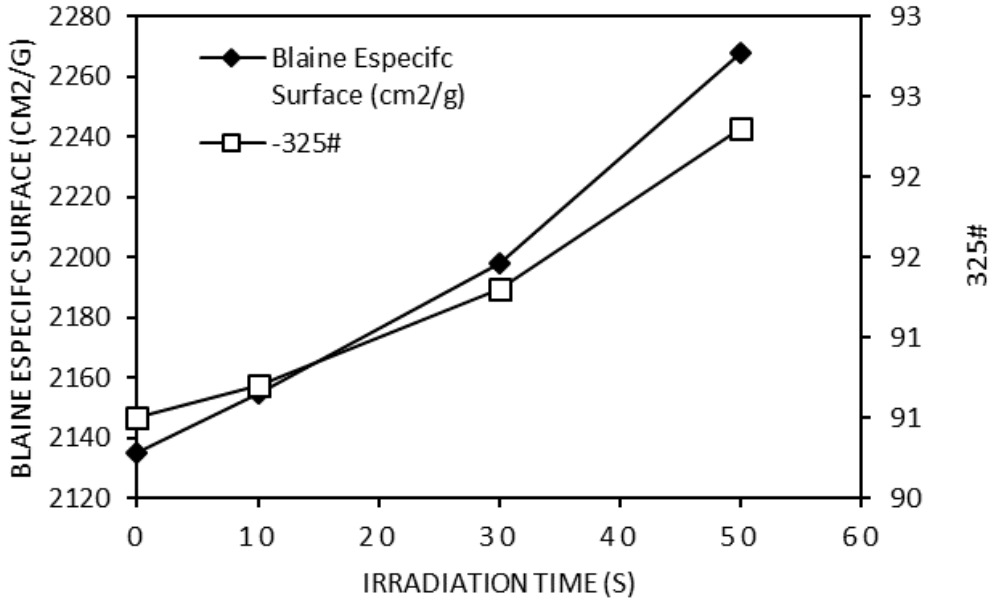

Figure 8 – Effect of the irradiation on the concentrate particle size (initial BSA = 1838 cm^2/g).

The microwave effect on the HPGR efficiency was evaluated, also excluding the HPGR improvement expected due the lower moisture after microwave heating. Figure 9 shows the particle size results of the “pressed and treated remoist.” sample and the "treated and pressed only". The samples "treated and pressed only" had an increase of BSA and % < 325# fraction after grinding of 534 cm^2/g and 4 % respectively, but the moisture content of the sample heated was 4 % less than the initial sample (Figure 7). Several authors report a reduction in HPGR grinding efficiency because of the moisture increase (Abazarpoor et al., 2017 and Meer et al., 2015), nevertheless these results show that dielectric heating of the microwave, may have an additional effect on the sample. The “pressed and treated remoist”, where the moisture are at the same level as the “original” sample, shows a value of BSA and % < 325# fraction of 104 cm^2/g and 0.7 % respectively lower than the “treated and pressed only" sample, which can be attributed to the moisture reduction effect alone.

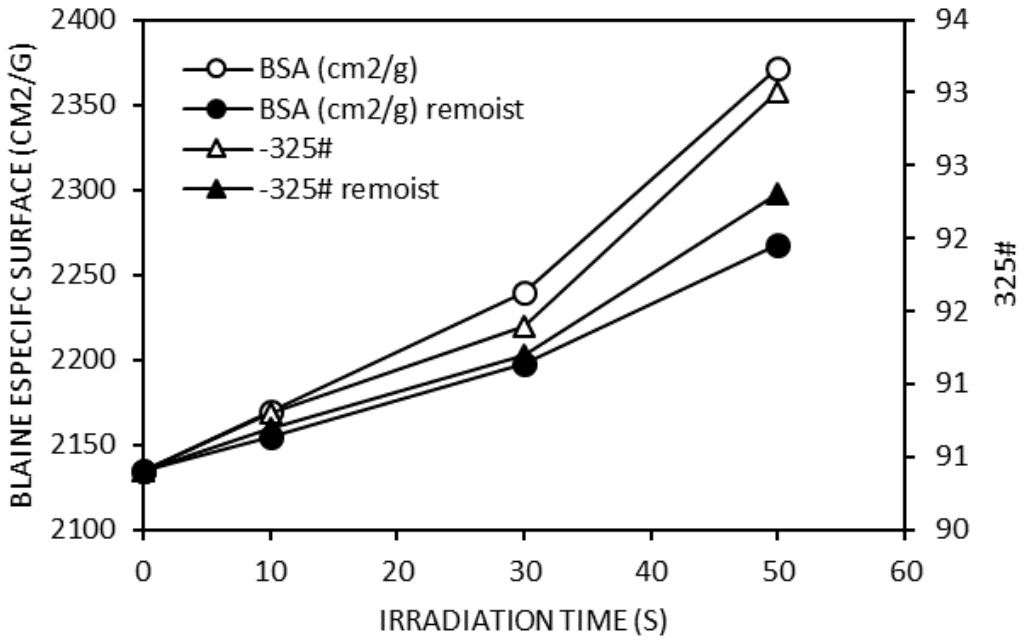

Figure 9 – Effect of the irradiation time on the concentrate wet and partially dried BSA and %<325# fraction after being pressed.

The variation of BSA and % < 325# fraction shown in Figure 9 with microwave irradiation can be split between a microwave effect and moisture reduction. In Figure 10, the total variation was considered when moisture was not added to the concentrate (moisture reduction + microwave effect), but partial variation (%Delta) can be also calculated, as in Eq. (4) and (5). The microwave effect contributed with 42 ± 1 % of the BSA increase and 24 ± 2% of the % < 325# fraction increase, the complement to the total variation are due the moisture reduction effect. In summary, the microwave influence is more than twice more relevant for the BSA than to the % < 325# fraction. The microwave irradiation affects the generation of the very fine particle, which has greater surface area per unit of mass (bellow 10 µm). Consequently, the moisture reduction had a stronger influence on the increase of % < 325# fraction than BSA.

$$\%Delta\ (BSA) = \frac{BSA_{treated}^{remoist} - BSA_{original}}{BSA_{\ treated} - BSA_{\ original}} \quad (4)$$

$$\%Delta\ (\%325\#) = \frac{\%325\#_{treated}^{remoist} - \%325\#_{original}}{\%325\#_{treated} - \%325\#_{original}} \quad (5)$$

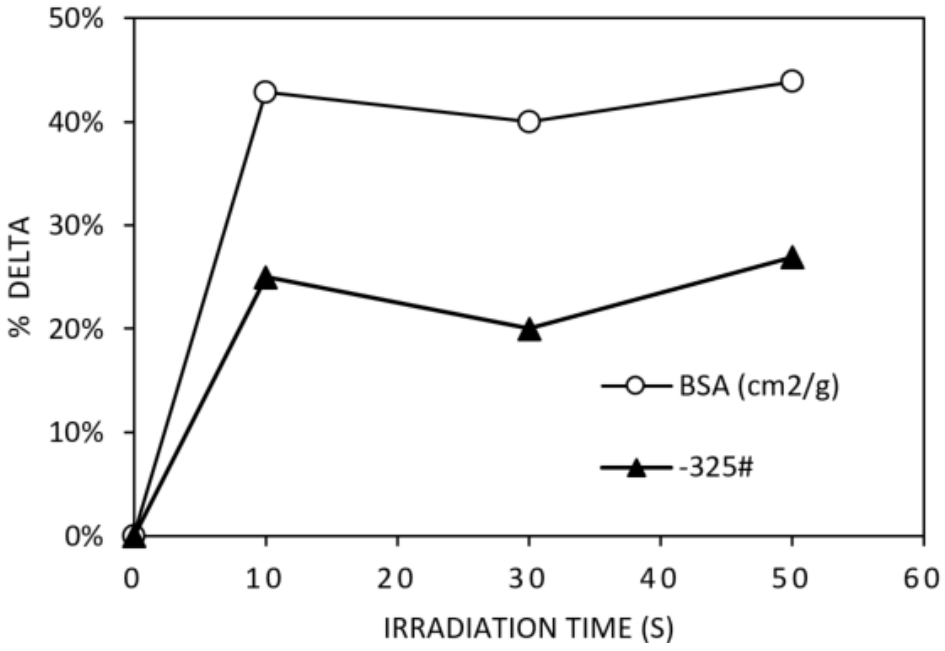

Figure 10 – Influence of only microwave on the BSA and % < 325# fraction after HPGR.

.

Meer et al., (2015) explained that high moisture content increase material slippage (drifting) on the roll surface and add abrasive wear, markedly shorten the wear life of the rolls. From the operational point of view, the purging of water to the edge of the rolls and the high moisture material handling affect the stability of the operation.

6.4.3. Microscopic characterization

Figure 11 shows SEM images conducted on the original sample and after the 30 s of irradiation. Particles before grinding but just irradiated shows already some degradation, with fine micro-cracks all over the surface of the particles. There are mainly two mechanisms supporting the localized cracks and fractures throughout the treated sample (Ali et al., 2011 and Shaoxian et. al., 2013), firstly the uneven distribution of thermal expansion by cause of the different minerals present in the sample and secondly, different energy absorption rates of the microwave energy by each mineral. Several micro-cracks observed in the minerals in Figure 11b occurred because different mineral responds to the electric field in different ways, which leads to different heating rates (Kingman et. al., 2004). No internal pressure release can be attributed to the fact as the crystallized moisture are the same from the initial value after irradiation, which is expected seeing that low temperature was achieved.

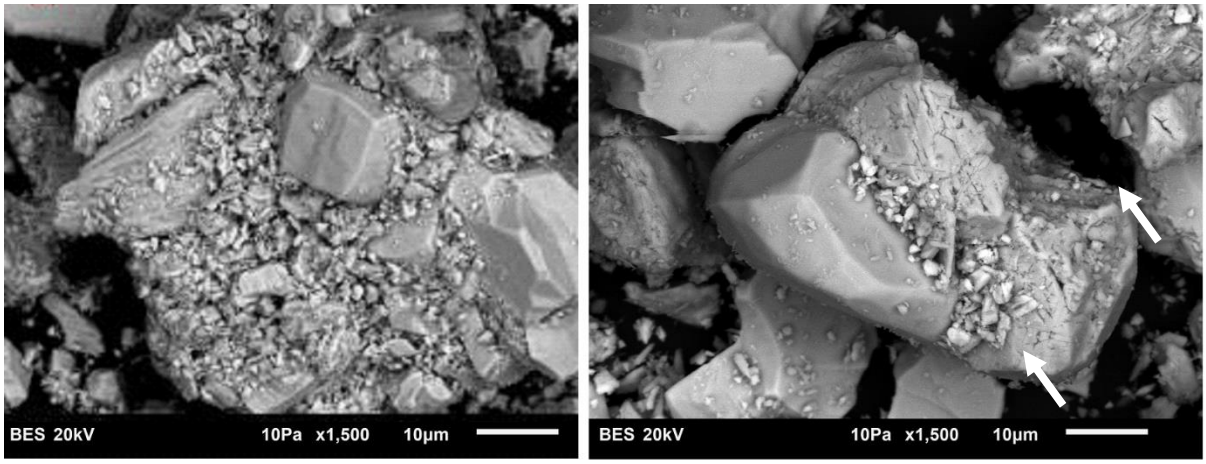

Figure 11 – Mixed particles (a) without microwave treatment and (b) treated with 30 s.

The absorption by the silica, goethite, and hematite presented in the concentrate creates different linear thermal expansion leading to an internal stress in the lattice between mixed particle, which generates ramified micro-cracks propagated through the mineral particle to release the tension generated, also observed by Kingman et al., (1998). Figure 12 shows an example of a martite particle with micro-cracked rooted in several directions, which lower the needed milling energy to break the particle.

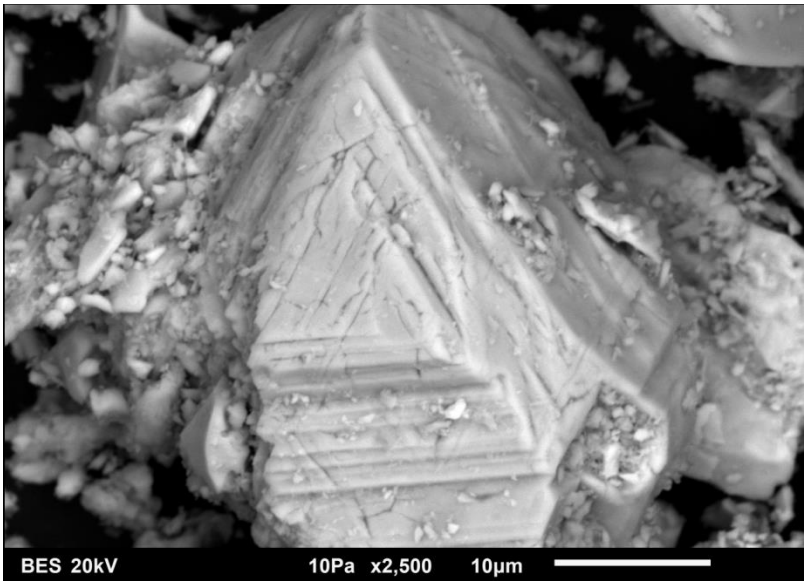

Figure 12 – Example of a martite particle micro-cracked observed in the sample treated for 30s.

.

The particle shape of the sample after the HPGR was also analyzed by SEM. The HPGR increases the proportion of ultra-fines in the sample, shown in Figure 13. Compaction and inter-particle abrasion were chiefly responsible for breakage, then resulting in a lower presence of elongated particles. Consequently, shorter and rounded particles without sharp edges in the "Only pressed" sample replaced those particles in the "Original" sample. Additionally, Figure 13 shows in "Treated and Pressed" sample that an additional increase of ultra-fines covers the main particles, which support the observed increase of BSA in this

sample. On the particles of "Only Treated" sample the microwave absorber minerals hematite, goethite and martite shows branched micro-cracks not following any specific direction, characteristic of the microwave effect into the minerals. Charikinya et al. (2015), Kingman et al. (2004) and He et al. (2015) had observed the same behavior in coarser ores.

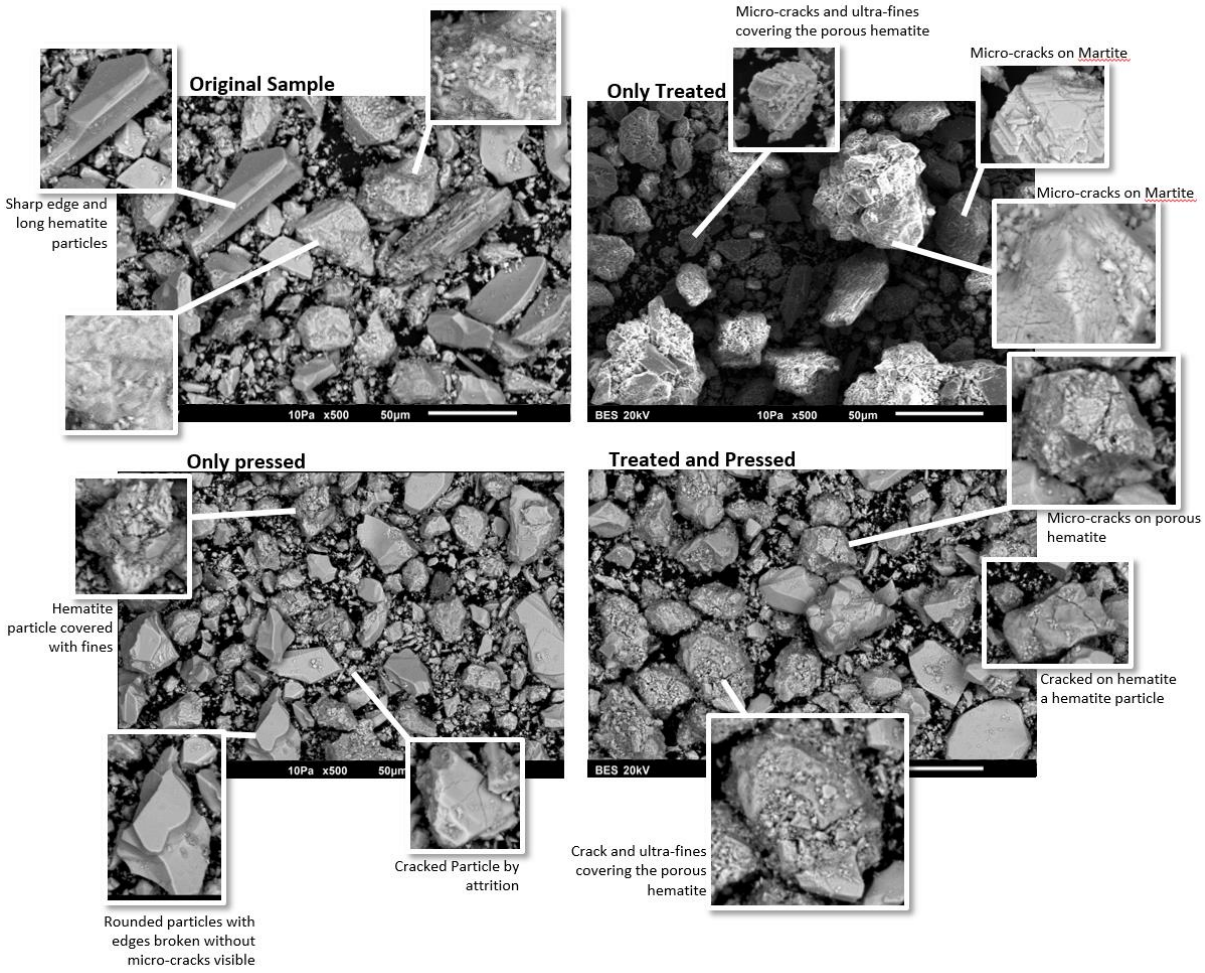

Figure 13 – Concentrate SEM treated at the microwave and pressed at HPGR (500x).

The particle aspect ratio shown in Table 2 corroborates with the observed distinct breakage behaviors of the particles. Some particles became more brittle by the introduction of the micro-cracks. In general, breakage is a strong function of the specific energy level in the HPGR, as observed by Abiyzeid et al. (2015), but the micro-cracked particle is not significantly affected, it is explained by the lower energy needed to break. This effect on the

size is dependent on differences in brittleness of feed components. The cracked particle (soften) tends to generate ultra-fines, whereas the other stronger particles break down into large parts, only reducing aspect ratio.

Table 2 – Statistics of Particle Aspect Ratio (width/length)

Sample	Mean	Standard Deviation	Q1	Q2	Q3
Original Sample.	2.06	0.99	1.40	1.94	2.72
Only Pressed	1.26	0.50	0.90	1.248	1.55
Only Treated	2.03	1.05	1.32	2.006	2.30
Treated and Pressed	1.29	0.45	0.96	1.261	1.60

The PSD curves (Figure 14) show that samples treated with microwave and then ground by HPGR present more fine particles than the sample only ground in the HPGR, at the same size fraction. Therefore, pellet feed preparation for pelletizing may take advantage of a microwave pre-treatment prior to HPGR, because a higher BSA are desirable to improve the capillarity forces within the grains. The pre-treatment increased from 25 % to 34 % the fraction % < 10 μm (responsible for 11.1% increase in the BSA), while the fraction %<325# fraction slightly improved by 3%.

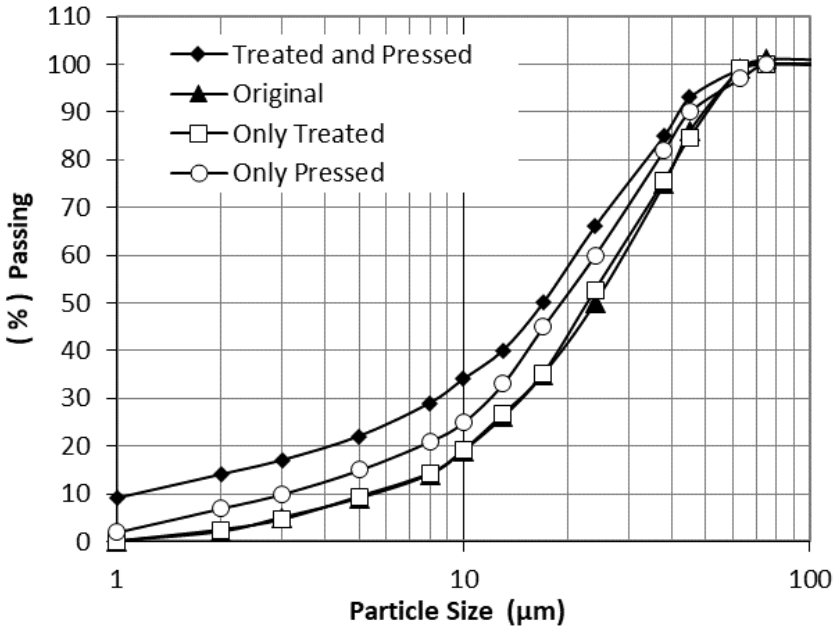

Figure 14 – Effect on concentrate particle size distribution treated in the microwave and pressed in the HPGR.

6.5. Conclusions

The study quantified the microwave effect on the milling by HPGR in order or minimized the requirements for the balling process and consequently furnace drying, the following conclusions can be drawn:

- The microwave irradiation shows a 3.5 cm2/g/s improvement on the BSA after grinding on the HPGR, which should be attributed to an increase in size fraction % < 10 µm from 25 % to 34 %.

- Although influenced by the higher moisture level, the pellet feed has an excellent heat up fast. The sample reached 80 ºC within the 50s, which may improve the balling and drying process and need to be study in future.

- The moisture released contribution during the heating was isolated. The microwave effect on the particle size reduction was quantified as 40 % for BSA increase and 22 % for % < 325# fraction increase.
- The BSA and % < 325# fraction increase was related to the generation of microcracks onto the particles, observed on the SEM images.

6.6. Reference

Abazarpoor, A., Halali, M., Hejazi, R., & Saghaeian, M., 2017, "HPGR effect on the particle size and shape of iron ore pellet feed using response surface methodology". Mineral Processing and Extractive Metallurgy, 127(1), 40-48. doi:10.1080/03719553.2017.1284414

Abouzeid, A. M., & Fuerstenau, D. W., 2009, "Grinding of mineral mixtures in high-pressure grinding rolls". International Journal of Mineral Processing, 93(1), 59-65. doi:10.1016/j.minpro.2009.05.008

Ali, A., & Bradshaw, S., 2011, "Confined particle bed breakage of microwave treated and untreated ores". Minerals Engineering, 24(14), 1625-1630. doi:10.1016/j.mineng.2011.08.020

Alves, Vladmir Kronemberger, 2015, Claudio Luiz Schneider, Thaís Brasil Duque, Douglas B. Mazzinghy, and Antônio E.c. Peres. "Sample Requirements for HPGR Testing Procedure." Minerals Engineering 73: 31-38. doi:10.1016/j.mineng.2014.12.007.

Athayde, Maycon, Mauricio Cota, and Maurício Covcevich., 2018, "Iron Ore Pellet Drying Assisted by Microwave: A Kinetic Evaluation." Mineral Processing and Extractive Metallurgy Review, 1-10. doi:10.1080/08827508.2017.1423295.

Barrios, Gabriel K.p., and Luís Marcelo Tavares., 2016, "A Preliminary Model of High Pressure Roll Grinding Using the Discrete Element Method and Multi-body Dynamics

Coupling." International Journal of Mineral Processing 156: 32-42. doi:10.1016/j.minpro.2016.06.009.

Charikinya, E., S. Bradshaw, and M. Becker., 2015, "Characterising and Quantifying Microwave Induced Damage in Coarse Sphalerite Ore Particles." Minerals Engineering 82 14-24. doi:10.1016/j.mineng.2015.07.020.

Forsmo, S., Apelqvist, A., Björkman, B., & Samskog, P., 2006, "Binding mechanisms in wet iron ore green pellets with a bentonite binder". Powder Technology, 169(3), 147-158. doi:10.1016/j.powtec.2006.08.008

Forsmo, S.p.e., P.-O. Samskog, and B.m.t. Björkman., 2008, "A Study on Plasticity and Compression Strength in Wet Iron Ore Green Pellets Related to Real Process Variations in Raw Material Fineness." Powder Technology 181, no. 3: 321-30. doi:10.1016/j.powtec.2007.05.023.

Sportel H. and Droog J., 1997, "Influence of pore saturation on compressive strength of green iron-ore pellets", Ironmaking & steelmaking, 24(3), pp. 221-223.

Haque, K. E., 1999, "Microwave energy for mineral treatment processes—a brief review". International Journal of Mineral Processing, 57(1), 1-24. doi:10.1016/s0301-7516(99)00009-5

He, C. L., Ma, S. J., Su, X. J., Mo, Q. H., & Yang, J. L., 2015, "Comparison of the Microwave Absorption Characteristics of Hematite, Magnetite and Pyrite. Journal of Microwave Power and Electromagnetic Energy, 49(3), 131-146. doi:10.1080/08327823.2015.11689903

Kapur, P., & Runkana, V., 2003, "Balling and granulation kinetics revisited". International Journal of Mineral Processing, 72(1-4), 417-427. doi:10.1016/s0301-7516(03)00116-9

Kawatra, S., & Ripke, S., 2001, "Developing and understanding the bentonite fiber bonding mechanism". Minerals Engineering, 14(6), 647-659. doi:10.1016/s0892-6875(01)00056-5

Kingman, S., Jackson, K., Bradshaw, S., Rowson, N., & Greenwood, R., 2004, "An investigation into the influence of microwave treatment on mineral ore comminution". Powder Technology, 146(3), 176-184. doi:10.1016/j.powtec.2004.08.006

Kingman, S., & Rowson, N., 1998, Microwave treatment of minerals-a review. Minerals Engineering, 11(11), 1081-1087. doi:10.1016/s0892-6875(98)00094-6

Kumar, P., Sahoo, B., De, S., Kar, D., Chakraborty, S., & Meikap, B., 2010, Iron ore grindability improvement by microwave pre-treatment. Journal of Industrial and Engineering Chemistry, 16(5), 805-812. doi:10.1016/j.jiec.2010.05.008

Leonel, C. M. L.; Peres, A.E.C., 2013, "Calcination as additional unit operation in the pelletizing of iron ores presenting high contents of loss on ignition". Ingeniería. Universidad de Atacama, Vol. 29, p. 1-12,

Nunes S. F, Viera C. B., Goulart L. C., Fonseca M. C., 2014, "Influência da Carga Circulante do Pelotamento na Qualidade Física das Pelotas", 2o Simpósio Brasileiro de Aglomeração de Minério de Ferro, Belo Horizonte, MG, Brasil.

Ribeiro, F. S., Russo, J. F., & Costa, T., 2010, "Aplicação de prensas de rolos em minério de ferro". Rem: Revista Escola De Minas, 63(2), 399-404. doi:10.1590/s0370-44672010000200027

Rizmanoski, V., 2011, "The effect of microwave pretreatment on impact breakage of copper ore". Minerals Engineering, 24(14), 1609-1618. doi:10.1016/j.mineng.2011.08.017

Sahoo, B. K., De, S., Carsky, M., & Meikap, B. C., 2010, "Enhancement of Rheological Behavior of Indian High Ash Coal−Water Suspension by Using Microwave Pretreatment". Industrial & Engineering Chemistry Research, 49(6), 3015-3021. doi:10.1021/ie901770d

Saramak, D., & Kleiv, R. A., 2013, "The effect of feed moisture on the comminution efficiency of HPGR circuits". Minerals Engineering, 43-44, 105-111. doi:10.1016/j.mineng.2012.09.014.

Shaoxian Song A.B., Campos-Toro E.F., Valdivieso A.L., 2013, "Formation of micro-fractures on an oolitic iron ore under microwave treatment and its effect on selective fragmentation", Powder Technology 243 ,155–160.

Meer, F. P., 2015, "Pellet feed grinding by HPGR". Minerals Engineering, 73, 21-30. doi:10.1016/j.mineng.2014.12.018

Zhu, D., Pan, J., Qiu, G., Clout, J., Wang, C., Guo, Y., & Hu, C., 2004, "Mechano-chemical Activation of Magnetite Concentrate for Improving Its Pelletability by High Pressure Roll Grinding. ISIJ International, 44(2), 310-315. doi:10.2355/isijinternational.44.310

CAPÍTULO 7. Considerações Finais

Neste trabalho foi avaliado o controle da umidade para o processo de pelotização de minério de ferro através do uso de micro-ondas. Foi investigado o prensamento de minérios por cominuição em prensa piloto e a secagem de pelotas em bancada e em planta piloto. Ainda, foram investigados os fenômenos que influenciam a operação de uma planta industrial de pelotização.

O processamento por micro-ondas apresentou características singulares em relação ao processo convectivo de aquecimento, representado pelo processo industrial no Artigo B. A rápida concentração de energia e consequente propagação através do sólido mostraram-se características essenciais para retirada da umidade das pelotas. Através dos testes em bancada apresentados no Artigo C, ficou evidente que o diâmetro não é significativo para variação na taxa de secagem das pelotas, como ocorre no aquecimento convectivo. No entanto, a taxas de secagem das pelotas reduz significativamente, após poucos minutos, com a redução da umidade durante o processo, pois a resistência à rotação dos dipolos da molécula de água, sob influência do campo eletromagnético gerado pelas micro-ondas, é o principal mecanismo de aumento da temperatura na pelota. A taxa de secagem no processo realizado por micro-ondas apresentou um estágio de intenso aquecimento (devido ao alto teor de umidade nas pelotas) seguido por um período de queda exponencial da taxa, devido à rápida redução da umidade no núcleo da pelota. O processo ocorre com a redução exponencial da difusividade efetiva da umidade com aumento da temperatura. A energia de ativação equivale à metade da observada no processo convectivo, favorecendo a cinética da secagem por micro-ondas.

Neste contexto a hipótese do aquecimento heterogêneo para o novo processo, combinando micro-ondas e fluxo de ar em leito de pelotas, foi avaliada nos experimentos do Artigo D. Também foi proposto no mesmo artigo um modelo do mecanismo de secagem em leito de

pelotas, simulando uma operação industrial. A complexa distribuição de temperatura, oriunda do campo elétrico gerado, no leito de pelotas, gerou regiões com temperaturas mais elevadas devido ao leito estático. No entanto, apesar da heterogeneidade de temperatura na superfície do leito de pelotas, ao longo da altura foi observado um considerável aumento de temperatura, favorecendo o processo com uso de micro-ondas. Não foi verificado formação da camada de umidade condensada nas camadas intermediárias durante o fluxo gasoso ascendente.

Com base na observação dos experimentos apresentados no Artigo C, o trabalho demostrou a geração de micro trincas nas partículas expostas as micro-ondas, portanto foi proposta a hipótese de menor demanda energética para prensamento do concentrado, a qual foi verificada no capítulo 6 (Artigo E). A geração de finos (% < 10 μm) aumentou de 25 % para 34 %, contribuindo para um sensível aumento da superfície específica do material. No entanto, a condução iônica impulsionada pelo campo magnético, através dos minerais, mostrou-se limitador para o aumento do tempo de exposição, pela queima localizada do minério conhecido como “efeito runaway” (Artigo D). Uma potencial aplicação industrial fomentará a redução da cominuição adicional na etapa de concentração (típica para geração de superfície específica para o processo de aglomeração), gerando um material mais grosseiro para a etapa de filtragem a vácuo e consequentemente redução da umidade. No processo de aglomeração industrial tradicional, o prensamento do concentrado realiza a adequação final da granulometria do material para aumentar a tensão nos capilares e portando permitir a aglomeração.

A possibilidade de elevação em até 40% na geração de superfície específica, através da utilização da micro-ondas, aumenta a eficiência global da unidade de aglomeração (filtragem, pelotamento e queima).

A análise detalhada do atual do processo de pelotização no estado-da-arte (artigo B) apresentou a necessidade crítica de controle granulométrico das pelotas na faixa de menor tamanho (entre +9-12,5 mm). Portanto, garantindo a retirada de umidade da pelota e o correto processo térmico resultando na qualidade física e metalúrgica das pelotas. A hipótese principal do estudo foi evidenciada, demostrando que a técnica de micro-ondas pode contribuir para o processo de secagem.

De maneira geral, o controle de umidade do forno de pelotização foi realizado de forma mais precisa pela exposição do concentrado às micro-ondas na entrada do HPRG, reduzindo a umidade a valores dentro da expectativa das unidades de aglomeração (e adicionalmente micro trincando os minerais) e sequencialmente na zona de secagem dos fornos de pelotas pelos processos combinados (dielétrico e convectivo) em uma futura aplicação industrial.

Capítulo 8. Perspectivas Futuras

- Em uma futura aplicação industrial, a tecnologia de geração de micro-ondas deve ser avaliada, no entanto, existe a necessidade de avaliar magnetrons de alta intensidade (>100kW) e ainda diferentes frequências de micro-ondas de forma a aumentar o rendimento energético.
- A condução das micro-ondas até o forno ou até o HPGR deve ser estudada do ponto de vista de uma aplicação industrial (viabilidade econômica), visto que esta afeta a homogeneidade do processo e o risco de vazamento para o ambiente, mantendo o ambiente seguro para pessoas.
- Variações de formulações de minérios e insumos devem ser estudadas, já que outros insumos e minério apresentam comportamentos específicos quanto à reação a micro-ondas.
- Consequências secundárias para o estado atual da tecnologia de aglomeração será a alteração do padrão de emissões de gases de efeito estufa gerados pela queima de combustível sólido, onde este poderá ser substituido parcialemente por energia elétrica de origem renovável.